Master Thesis in Reservoir Physics

Investigation of Low Salinity Polymer and Surfactant Flooding in Carbonate Reservoir at Reservoir Conditions

Mohamed El-khatib

Center for Integrated Petroleum Research

Department of Physics and Technology

University of Bergen

February 2018

Acknowledgement

The experimental work presented in this study has been carried out at the Centre of Integrated Petroleum Research (UNI Research CIPR) at the University of Bergen, during the period February 2017 to February 2018. I want to thank UNI Research CIPR for providing both research facilities and knowledge sharing from employees.

Additionally, I would like to express my gratitude towards my supervisor, Professor Arne Skauge, for his guidance and support during my work on this thesis.

Special thanks to my co-supervisor, Behruz Shaker Shiran. Your guidance and patience during the experiments and throughout the writing process has been exceptional.

Moreover, I would like to thank Jonas Solbakken for the useful discussions and guidance during the experiments. I would also like to express my gratitude towards my fellow students.

Finally, I would like to thank my family and friends for their motivation and encouragement during my years as a student. Special recognition goes to my mother for her outstanding support, and motivation through my whole life. Tarek, my best friend, thank you for making this possible, and Steinar Thomsen for his support all these years.

Bergen, February 2018

Mohamed El-khatib

Abstract

It is estimated that 40-60% of the world's total hydrocarbon production is from carbonate rocks [1]. Carbonate rocks contain the world`s largest fields in the Middle East (i.e., Ghawar Field, Saudi Arabia).

Waterflooding is a low-cost oil recovery process and is by far the most commonly applied method for improving the oil recovery and maintain pressure support to the reservoir. The composition of water was not considered as an important factor influencing the amount of oil recovered. However, during the last decade, the low salinity water injection techniques have become one of the most important studies in the oil industry because of their possible benefits for improving oil recovery compared to conventional seawater injection. Thus, extensive studies have been developed in the composition of the injected water to an emerging Enhanced Oil Recovery (EOR) technology in carbonate and sandstone reservoirs. This increased investigations on the effect of low salinity water on oil recovery [2]. However, the mechanisms for EOR in carbonates are still poorly understood.

The thesis concerns experimental studies of waterflooding performance in outcrop carbonate rock material. The wettability preference of the rock was changed by aging with crude oil at elevated temperature. The thesis compares the effects and benefits of low salinity brine injection in the tertiary mode, and when combined with a surfactant and a polymer to enhance oil recovery. Also, investigation of how aging time affects oil recovery/production in spontaneous imbibition tests.

During secondary mode injection of high salinity brine, the cores resulted in recovery factors of 43-79% OOIP. In the tertiary mode, varying in production was observed, which gave an incremental oil recovery of 1-11% OOIP. It was observed that the unaged cores gave the highest oil recovery compared to aged cores.

Combination of low salinity and polymer injection resulted in significant increase in oil recovery (additional 7-11% OOIP). The second low salinity injection after polymer flooding resulted in an incremental oil recovery of 2-2.4 %OOIP in aged cores. Hence low salinity seems to have a good potential in Indiana Limestone outcrop.

Nomenclature

Variables

A	Area	[m^2]
B	Atmospheric Pressure	[Pa]
C, c	Concentration	[kg/m^3]
dP	Differential pressure	[mbar]
E_A	Area sweep efficiency	dimensionless
E_D	Microscopic displacement efficiency	dimensionless
E_R	Recovery factor	dimensionless
E_V	Vertical sweep efficiency	dimensionless
E_{Vol}	Volumetric displacement efficiency	dimensionless
h	Height	[m]
I	Ion Strength	[mol/L]
K	Absolute permeability	[m^2] (1 D = $0.98692 \cdot 10^{-12} m^2$])
$k_{eff,i}$	Effective permeability of phase i	[m^2] (1 D = $0.98692 \cdot 10^{-12} m^2$])
$k_{end,i}$	End point permeability of phase i	[m^2] (1 D = $0.98692 \cdot 10^{-12} m^2$])
k_{ri}	Relative permeability of phase i	dimensionless
L	Length	[m]
M	Mobility ratio	dimensionless
M^0	End point mobility ratio	dimensionless
m	mass	[kg]
N	Total reserves originally in place	[m^3]
N_s	Surfactant parameter	dimensionless
N_p	Produced reserves	[m^3]
N_{vc}	Capillary number	dimensionless
P	Pressure	[Pa] (1 mmHg = 133.322 Pa)
PV	Pore volume	dimensionless
Q	Flow rate	[m^3/s]
R, r	Radius	[m]
S	Saturation	dimensionless
T	Temperature	[K] (0°C = 273.13 K)
t	Time	[s]
u	Darcy velocity	[m/s]
V	Volume	[m^3]
WC	Water cut	dimensionless
Δ	Difference	dimensionless
γ	Shear rate	[s^{-1}]
η	Viscosity (depended on shear rate)	[Pa·s] (1 Pa·s = 103 Cp)
θ	Contact angle	[°]
λ	Mobility	[m^2/Pa·s]
λ_0	End point mobility	[m^2/Pa·s]
μ	Viscosity	[Pa·s] (1 Pa·s = 103 Cp)
ρ	Density	[kg/m^3]
σ	Interfacial tension	[N·m^2]

τ	Shear stress	[Pa]
ϕ	Porosity	dimensionless

Subscripts

A	area
abs	absolute
B	bulk
c	capillary
c	core channel
D	microscopic
diff	differential
eff	effective
g	gas
i	component (phase)
i	initial
i	irreducible
ineff	ineffective
inj	injected
max	maximum
o	oil
pol	polymer
p	pore
p	produced
r	relative
r	residual
R	recovery
tot	total
V	vertical
vol	volumetric
w	water

Abbreviations

CDC	Capillary desaturation curve
CMC	Critical micelle concentration
COBR	Crude oil/brine/rock system
Ca^{2+}	Calcium ion
CIPR	Centre for Integrated Petroleum Research
CP	Cone & plate
DG	Double gap
EOR	Enhanced oil recovery
FW	Formation water
FW	Fractionally wet
IOR	Improved oil recovery
IFT	Interfacial tension
HC	Hydrocarbon
HPAM	Hydrolyzed polyacrylamide
HS	High salinity brine
LS	Low salinity brine
LSP	Low salinity polymer
LSS	Low salinity surfactant
MIE	Multicomponent ionic exchange
Mg^{2+}	Magnesium ion
MWL	Mixed wet large
MWS	Mixed wet small
OOIP	Original Oil in Place
ppm	Parts per million
RF	Recovery factor
ROIP	Residual oil in place
SCAL	Special Core Analysis
SO_4^{2-}	Sulfate
TDS	Total dissolved solids
WBT	Water breakthrough
WOR	Water Oil Ratio

Table of Contents

List Of Figures

List Of Tables

1. Introduction

A considerable amount of the world's hydrocarbons exists in carbonate reservoirs. However, carbonate pore structures are often heterogeneous and complex [3]. Many carbonate reservoirs are believed to be in oil-wet to mixed-wet conditions [4, 5]. The wettability of the carbonate rocks and the low porosity/fractured zones, usually result in lower oil recovery compared to sandstones [1]. The injected fluids will possibly flow through the fracture network and bypass the oil in the rock matrix, which results in early water breakthrough.

The reservoir connate-water composition differs significantly from the composition of water for injection [2]. Conventional waterflood brines are seawater and aquifer water. The salinity of these fluids are high, ranging from 35 000 to 300 000 ppm, respectively [6]. Low salinity in waterflooding brine is regarded as low salinity water (LSW) if it is below 6000 ppm according to Alotaibi et al.(2010) [7]. Usually, the (LSW) studies are conducted between 500 to 5000 ppm. The low salinity effect (LSE) and its influence on recovery are discussed further in Chapter 3.4. Wettability alteration appears to be the central mechanism on oil recovery by low salinity waterflooding in carbonate reservoirs.

Benefits of combining low salinity with chemical additives such as surfactants and polymers is seen as an extension of the potential of LSW. The effectiveness of many chemical additives is dependent on the brine concentration and are found to be more stable at low salt concentrations. Also, surfactants that yield low interfacial tension (IFT) at low salinity are more readily available and less expensive compared to those, which are constructed to endure high salinity conditions. The combination of LSW with surfactant and polymers is discussed in Chapter 3.9 and 3.12.

A range of techniques has been developed and applied to improve oil recovery to meet the increasing demands in energy resources as illustrated in Figure 1.1. According to an international EOR project of 1507 projects, gas injection (continues or in a WAG mode) is the most common EOR method in carbonate formation [8]. As illustrated in Figure 1.1, EOR

thermal methods have a small contribution in oil production from carbonate, while chemical methods have more contribution in enhanced oil recovery in carbonate, especially polymer flooding. Other chemical methods that may enhance oil recovery from carbonate is surfactant flooding [9, 10]. A surfactant may alter the wettability of the carbonate rocks and reduce the interfacial tension (IFT) between oil and water.

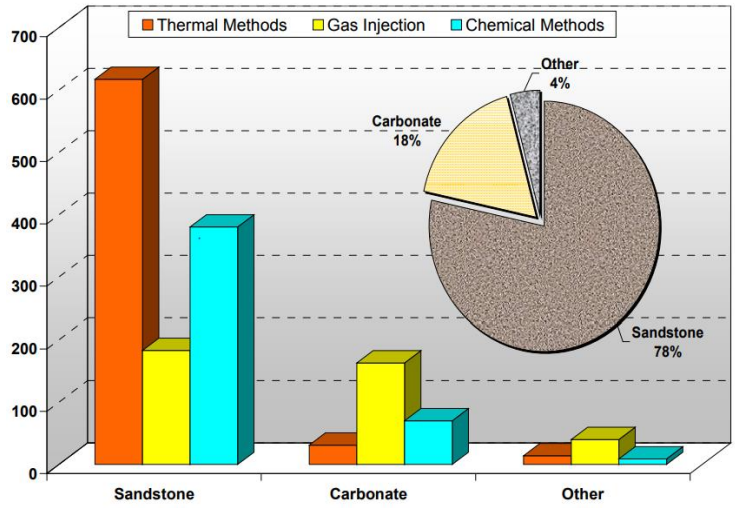

Figure 1.1: Enhanced oil recovery filed projects by lithology [8]

The present study compares the effect of high salinity and low salinity brine in a secondary and tertiary mode in four Indiana Limestone cores. Following tertiary mode, LS brine injection, low salinity surfactant (LSS) and low salinity polymer (LSP) floods were conducted. All experiments were executed at 90°C. Also, investigation of how aging time affects oil recovery/production in spontaneous imbibition tests during high salinity brine and low salinity brine. Other measurements were conducted in this work are, dispersion test, in-situ x-ray saturation monitoring and viscosity measurements.

The work presented in this thesis consist of nine chapters.

- **Chapter 1**: provides a general introduction to the thesis and objectives.

- **Chapter 2 and 3**: presents a literature relevant to the contents of the thesis, including fundamental principles in reservoir engineering and enhanced oil recovery (EOR). These chapters also include a review of low salinity effect with a combination of surfactant/polymers and the proposed mechanism for the increased oil recovery.
- **Chapter 4**: describes the experimental procedures and experimental setup used during the experimental work in this thesis.
- **Chapter 5**: presents the result and discussion obtained in this study, starting with important fluid and rock properties followed up by spontaneous imbibition tests and waterflood experimental data.
- **Chapter 6 and 7**: provides the overall conclusions and recommendations for future work.
- **Chapter 9 (Appendix)**: All data gathered during the experiments are summarized at the end of the thesis.

2. Fundamental Principles in Reservoir Physics

2.1. Porosity

Porosity, ϕ, is the ability of a rock to storage fluids within the void space of the rock. Porosity can be divided into primary and secondary porosity, which depends on the time of formation. Primary porosity is created during deposition, and depends on rock type, grain size, grain orientation and packing[11]. Secondary porosity is re-depositional alteration to the porosity resulting from continues burial of the rock, dissolution of grains or fracturing, and depends on clay, cementation, and chemical reactions [11]. The experiments performed in this thesis have been conducted on Indiana Limestone, the porosity is mainly results of changes that took place after deposition (secondary porosity).

The absolute porosity is a dimensionless parameter and, it is defined as the ratio between pore volume and bulk volume:

$$\phi = \frac{V_p}{V_B} \tag{2.1}$$

Where V_p is the pore volume, constituting the volume of void space and V_B is the bulk volume of the core, the constituting overall volume of voids and grains.

Total porosity ϕ_{tot} which depending on the pores interconnectivity, includes both the effective and ineffective porosity.

$$\phi_{tot} = \phi_{eff} + \phi_{ineff} \tag{2.2}$$

Where the pores connected to the primary pore network is called *effective porosity* ϕ_{eff}, and the pores which are not connected to the pore network is called *ineffective porosity* ϕ_{ineff}. The distinction between ϕ_{eff} and ϕ_{ineff} is illustrated in Figure 2.1:

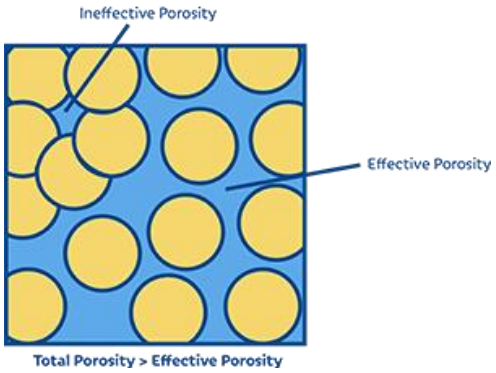

Figure 2.1: The distinction between ϕ_{eff} and ϕ_{ineff} [12]

The ineffective porosity will not influence the flow of fluids during flooding applications, and can therefore, be neglected from equation (2.2) which reduces this equation to:

$$\phi_{eff} = \frac{V_{p,eff}}{V_B} \tag{2.3}$$

Where $V_{p,eff}$, is the effective pore volume. The effective porosity depends on several factors such as rock type , grain size, cementation, orientation, packing, weathering, leaching and type, content and hydration of clay minerals [11]. Effective porosity is of the concern to the Enhanced Oil Recovery (EOR, will be discussed in detail in chapter 3) process, and the rest of the thesis will use porosity as the effective porosity.

Connected pores are not necessarily very efficient at transmitting fluids through formation [13]. Vugs/voids are defined as a large open pore feature in a porous medium. If such vugs are interconnected by remnant primary pores, an excellent reservoir rock may result and hence give efficient transmitting fluids through the formation. On the other hand, the connecting pore throats may be so small that flow from or through the vugs will be complicated.

Sandstone and carbonate represent the two major rock types; which porosity is typically found in the region of 15 to 40%[14]. For must naturally occurring media, the porosity is between 10 to 40% according to Lake (2010) [15].

The flooding experiments performed in this thesis have been conducted on carbonate rocks (Indiana Limestone) which usually have a porosity of 12 to 22% [16, 17].

2.2. Permeability

Permeability is the capability of a porous medium to transmit fluids through its network of interconnected pores under the application of a pressure gradient. Darcy`s law expresses permeability:

$$u = \frac{Q}{A} = -\frac{K}{\mu} \cdot \frac{\Delta P}{L} \tag{2.4}$$

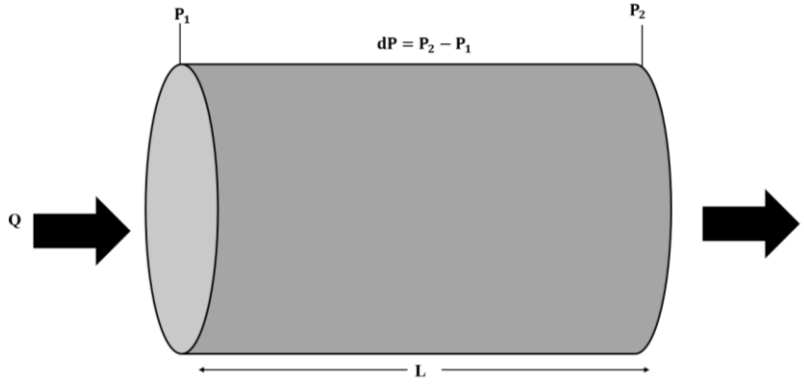

Figure 2.2: Fluid flow in a porous medium

Where u is the Darcy velocity, Q is the flow rate, K is the absolute permeability, ΔP is the pressure drop across the core plug, μ is the fluid viscosity, L is the length of the core plug, and A is the cross-sectional area of the core plug. The minus sign accounts for flow in the direction of decreasing pressure.

Equation (2.4) is only valid when the core plug is [11]:

- Saturated with one single fluid
- Incompressible fluid
- Stationary or laminar flow
- No chemical reactions between the fluid and rock solids
- The core placed in a horizontal position (absence of force of gravity)

The quantitative definition of permeability, as a physical unit, can be derived by rearranging equation (2.4):

$$K = \frac{\mu \cdot \mathrm{L} \cdot Q}{A \cdot \Delta \mathrm{P}} \tag{2.5}$$

Permeability is commonly given in Darcy units, which is equivalent to;

$$1\mathrm{Darcy} = \frac{\frac{1\mathrm{cm}^3}{\mathrm{s}} \cdot 10^{-8}\mathrm{Pa} \cdot \mathrm{s}}{1\mathrm{cm}^2 \cdot 1.01325 \cdot 10^5 \mathrm{Pa/cm}} = 0.98792 \cdot 10^{-8}\mathrm{cm}^2$$

in SI-units.

Permeability is a constant property of porous medium only if there's single fluid flowing through the medium; this is referred as the *absolute permeability.* Permeability is affected by porosity, tortuosity, grain size, grain shape and packing [11].

Sandstones larger pores will usually have higher permeability, and limestones smaller pores have lower permeability. However, fractures, as can be found in limestone, may increase the permeability even if the porosity is low [18].

When the porous medium contains more than one fluid, we refer to the permeability as *effective permeability.* Effective permeability is the ability of a fluid to flow in a porous medium when several immiscible fluid phases are present. The rock has different permeability for different fluid phases. The effective permeability can be found using Darcy`s law for the specific fluid as follows:

$$u_i = \frac{Q_i}{A} = -\frac{K_i}{\mu_i} \cdot \frac{\Delta \mathrm{P}}{L} \tag{2.6}$$

Where *i* denotes the fluid phase. The effective permeability is a function of the fluid saturation, rock properties, absolute permeability, fluid properties, and pressure/temperature conditions[11].

Relative permeability describes the flow in a multiphase system and is defined as the ratio between the effective permeability of a fluid to the absolute permeability of the porous medium:

$$k_{r,i} = \frac{K_{eff,i}}{K} \tag{2.7}$$

Relative permeability is a direct measurement of the ability of the porous medium to conduct one fluid when one or more fluid is present, and it is a function of wettability, pore geometry, fluid distribution, saturation, saturation history and connectivity [19, 20].

2.3. Saturation

In a reservoir rock, the pores can be filled with multiple fluids, such as oil, gas, and water at the same time. The pore volume can be written as volume for each of the phases:

$$V_p = V_o + V_g + V_w \tag{2.8}$$

Which leads to the definition of *saturation*, *S*. S is defined as the pore volume occupied by the volume of fluid *i*:

$$S_i = \frac{V_i}{V_p} \tag{2.9}$$

Where S_i is the saturation of fluid *i*, V_i is the volume of fluid *i*. For a porous medium the saturation will be as follow:

$$S = S_o + S_g + S_w = 1 \tag{2.10}$$

2.4. Wettability

The *wettability* of the rock sample is defined as the tendency of one fluid to spread on or adhere to the rock surface in the presence of another immiscible fluid. In a rock/brine/oil system, the wettability indicates the preference of the rock to oil or water. When the system is in equilibrium, the wetting fluid will fully occupy the smallest pores and be in contact with most of the rock surface. The non-wetting fluid will occupy the center of the larger pores and form

globules that extend over several pores. It is essential to understand that wettability means the wetting preference and does not necessarily refer to the fluid in contact with the rock at any given time [21].

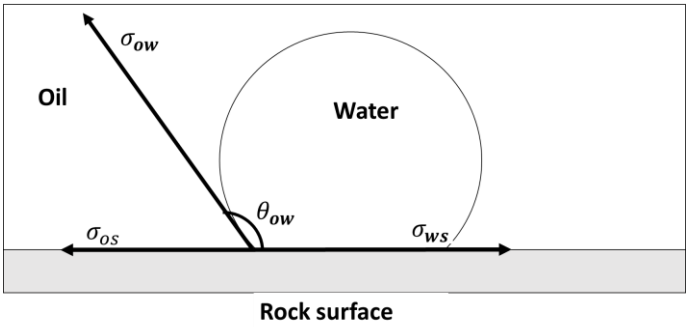

Figure 2.3: Schematic figure of oil, water, rock system at thermodynamic equilibrium state

When oil and water are in contact with rock surface as illustrated in Figure 2.3, there will be solid/fluid and fluid/fluid interactions which represented by Young's equation [22]:

$$cos\theta = \frac{\sigma_{os}-\sigma_{ws}}{\sigma_{ow}} \tag{2.11}$$

Where θ is the contact angle between the two immiscible fluids, which is measured trough the denser phase, and σ_{os}, σ_{ws} , σ_{ow} is the interfacial tension between oil/solid, water/solid and oil/water respectively.

Wettability can be determined by the contact angle between the fluid and solid surface. The contact angle varies between 0-180˚ [11]. Where θ= 0˚ corresponds to water is the spreading fluid, and the solid surface is strongly water-wet. When θ= 90˚, the solid surface has no preference for any of the fluids, and the solid surface either neutral or intermediate-wet. For the contact angle θ = 180˚, oil spread on the solid surface, and the surface is strongly oil-wet. At contact angles between (0˚ < θ < 90˚) the system representing a partially water-wet system, and (90˚ < θ <180˚) representing a partially oil-wet system.

Table 2.1: Wettability classes for a water-oil system, distinguished from the contact angle[11]

Contact angle [°]	**Wettability preference**
0-30	Strongly water-wet
30-90	Preferentially water-wet
90	Neutral wettability
90-150	Preferentially oil-wet
150-180	Strongly oil-wet

In addition to these five classifications of wettability, Anderson (1986) [21] did a classification of wettability based on contact angle where the rock is considered to be water-wet if the contact angle- is from 0° to 75°, intermediate/neutral wet 75°-105° and oil-wet 105° to 180°. Depending on the rock preferences to the fluid, the wettability of a porous media can range from strongly water-wet to strongly oil-wet. If the rock has no strong preference to be in contact with neither oil or water, the rock maintain intermediate or neutral wettability [21]. Anderson (1986), also introduced the fractional wettability, where different areas of the porous media have different wetting preferences, such as the rock have a strong preference to be in contact with water in particular surfaces and strong preference to oil in other surfaces.

The intermediate wettability can also be subdivided into three different classes according to Skauge et al. (2007) [23]. Skauge et al. proposed three different intermediate wettability classes as shown in Figure 2.4:

- Mixed-wet small (MWS)
- Fractionally-wet (FW)
- Mixed-wet large (MWL)

Skauge et al. explained that there are three possible reasons for the origin of oil-wet sites in a porous medium; due to the mineralogy of the rock and surface charges, which may have little affinity for water. Secondary, polar components which can be adsorbed from oil to the solid surface and the third reason is due to rupture of the water film that overlies the rock surface. The latter is due to the relationship between the shape of the pores and disjoining pressure,

which will develop different wetting classes. Disjoining pressure will be explained in (3.4 Wettability Alteration)

In the MWS system, the small pores are oil-wet, and the bigger pores are water-wet. The water-wet pores may not have been in contact with oil and have not developed an affinity for oil. For FW case, the wettability is uncorrelated to the shape of the pores. In MWL system, the large pores are oil-wet, while the small pores are water-wet.

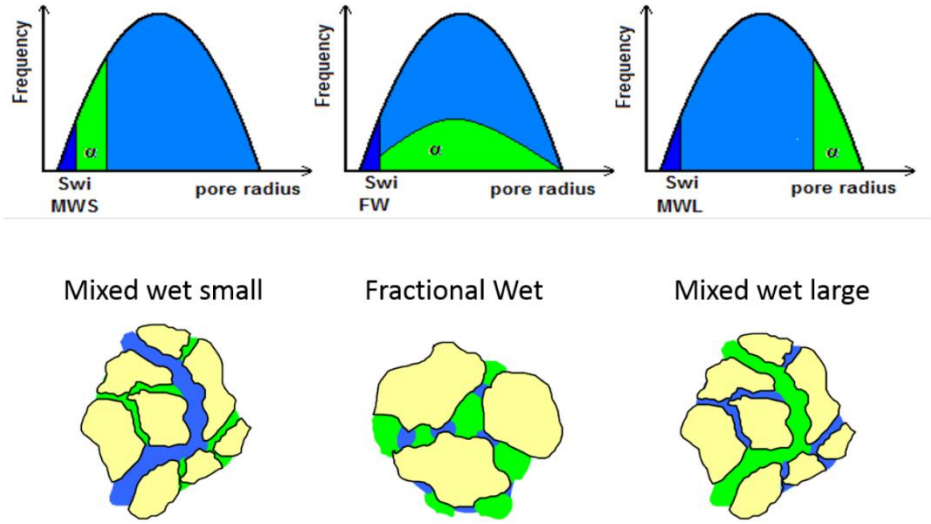

Figure 2.4: Different intermediate wettability classes: MWS (left), FW (middle) and MWL(right), α is the fractional of oil-wet pores[23, 24]

Mixed wettability condition will provide a path for oil to flow even at very low saturation. The small pore rock surface would be preferentially water-wet, and the surface of the larger pores would be strongly oil-wet. If the oil-wet pathways were continuities throughout the rock, water could displace oil from the larger pores, and little or no oil would be held by capillary forces in the small pores. This type of wettability can give very low residual oil saturation which is observed in East Texas filed [25].

The majority of oil reservoirs is believed to be water-wet or initially, was in water-wet conditions. However, as debated the wettability may change to oil-wet or mixed wet when the water films on the rock surface are destroyed, which depends on the shape of the pores [23].

2.5. Capillary Pressure (P_c)

When two immiscible fluids are in contact with each other, an electrostatic force will act upon the two fluids. *Capillary pressure* is the molecular pressure difference across the interface of the two fluids, the wetting fluid and non-wetting fluid [11]. The Laplace equation can express capillary pressure:

$$P_{c,ow} = P_{non-wetting} - P_{wetting} = p_o - p_w = \sigma_{ow}\left(\frac{1}{R_1} - \frac{1}{R_2}\right) \quad (2.12)$$

Where R1 and R2 are the principal radii of the interface curvature and σ is the interfacial tension.

Assuming that the rock pores are cylindrical tubes with oil non-wetting phase and water-wetting phase, Young- Laplace equation can be rewritten as:

$$P_c = p_o - p_w = \frac{2\sigma_{ow}cos\theta_c}{r_c} \quad (2.13)$$

Where θ is the wetting angle, rc is the pore channel radius.

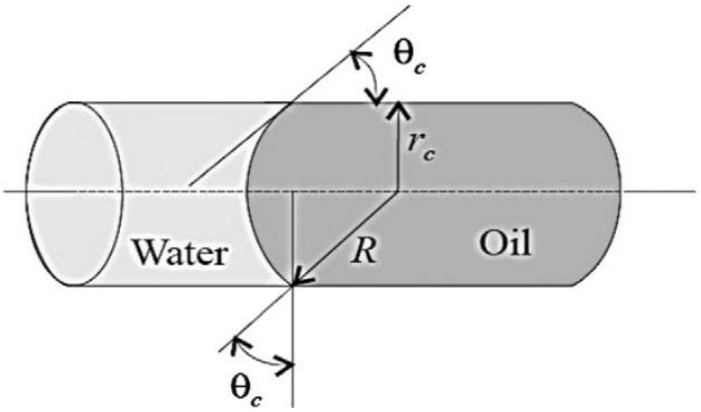

Figure 2.5: Rock pore as a cylindrical tube to derive capillary pressure [26]

Laboratory experiments [11] shows that Pc is a function of:

- Interfacial tension
- Saturation
- Wetting angle
- Pore size distribution
- Saturation history due to hysteresis

2.6. Fluid Mobility and Mobility Ratio

The *mobility* (λ) concept is another important parameter in the fluid displacement. The mobility to a fluid is defined as its relative permeably divided by its viscosity:

$$\lambda_i = \frac{k_{ri}}{\mu_i} \tag{2.14}$$

Where *i* denoted the fluid phase; oil, water or gas. k_r is the relative permeability, and μ is the viscosity of the fluid.

The mobility ratio can be described as follows:

$$M = \frac{\lambda_{displacing\ fluid}}{\lambda_{displaced\ fluid}} \tag{2.15}$$

For the case when the water displaces oil, the mobility ratio is given as:

$$M_{wo} = \frac{k_{rw}}{k_{ro}} \frac{\mu_o}{\mu_w} \tag{2.16}$$

Mobility ratio is an essential parameter for displacement processes and production behavior [15]. To calculate the stability of a waterflood, the endpoint mobility ratio is used denoted by M°_{wo}, where $^{\circ}$ indicates the measurements done at the endpoint *Sor* and *Swi*. Equation 2.16 can be rewritten as:

$$M^{\circ}_{wo} = \frac{k^{\circ}_{rw}}{k^{\circ}_{ro}} \frac{\mu_o}{\mu_w} \tag{2.17}$$

The impact of the mobility ratio on a displacement process of oil by water is shown schematically in Figure 2.6. The curves in Figure 2.6, illustrate the displacement front as a function of different residence times, denoted by *t*, whereas *Sor* and *Swi* denote irreducible oil and water saturation respectively. t_{bt} denotes the time of water breakthrough.

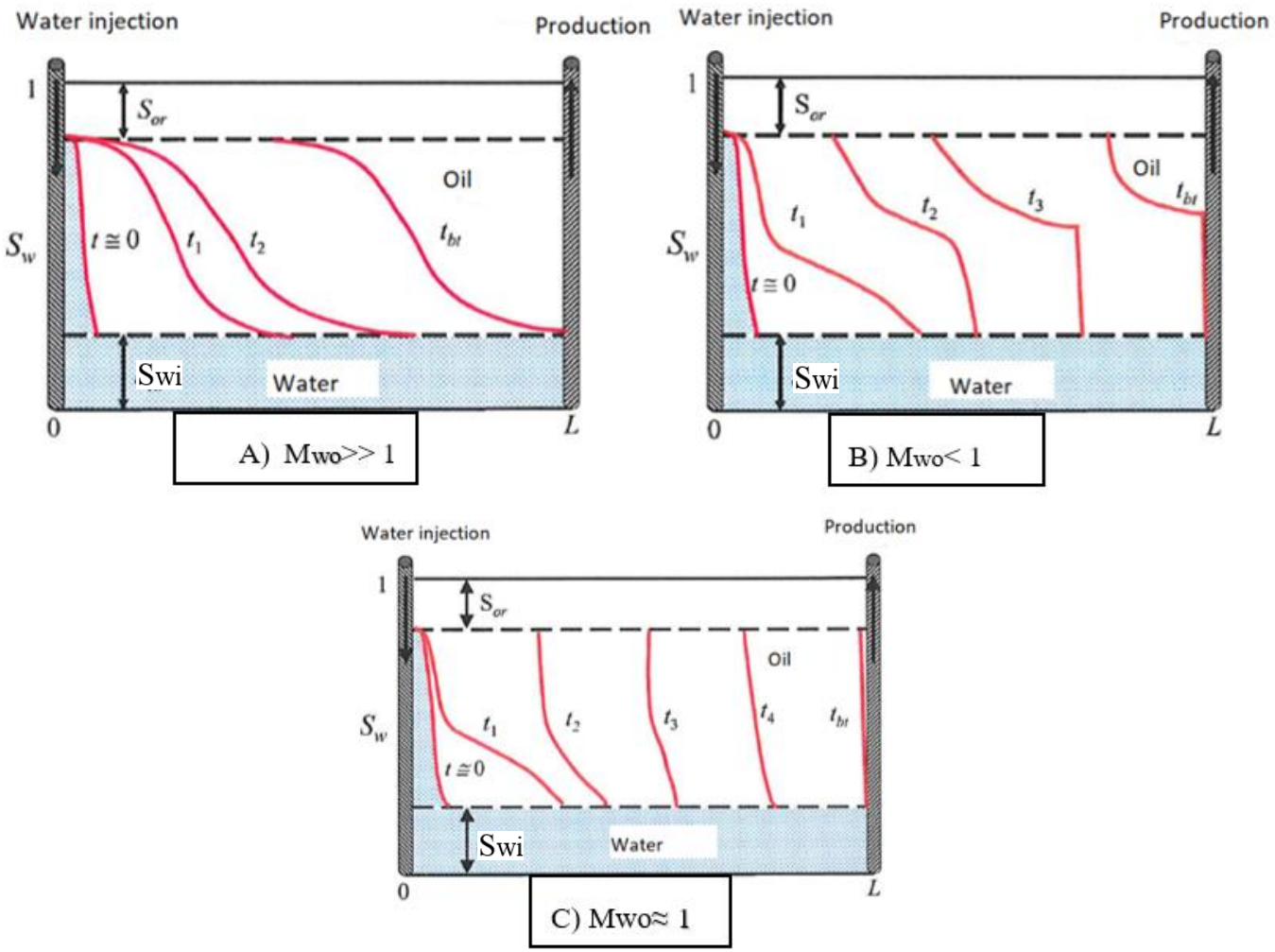

Figure 2.6: Illustration of mobility ratio impact during waterflooding of oil A) Mwo>>1, B) Mwo <1, and C) Mwo ≈ 1 (modified from Lien (2010) [27]

A. The Oil viscosity is much larger than the displacing water ($\mu_o >> \mu_w$). Water is more mobile than oil and gives an unfavorable mobility ratio conditions; $M_{wo} >> 1$. Thus water travels faster towards the production wells. At water breakthrough at the producing well, at time t_{bt}, large quantities of oil remain within the reservoir corresponding to the area over the last curve.

B. Illustrates an opposite scenario where the mobility ratio $M_{wo} < 1$. The water is less mobile than the displaced oil promoting a piston-shaped displacement which results in less oil remaining in the reservoir at water breakthrough at the producing well. The recovery of oil is therefore significantly improved over the recovery illustrated for case A.

C. Illustrates an ideal mobility ratio $M_{wo} \approx 1$ in which displacing water and displaced oil flow through the porous medium at comparable mobilities. The water drives the oil in front of it, and only residual oil remains within the reservoir at breakthrough [22].

Therefore, stable displacement processes occur in the reservoir when the mobility ratio is close to or less than 1 ($M_{wo} \leq 1$). Higher mobility ratios, however, promote early water breakthrough at producing wells and a long tail production of oil [14].

2.7. Drainage/ Imbibition

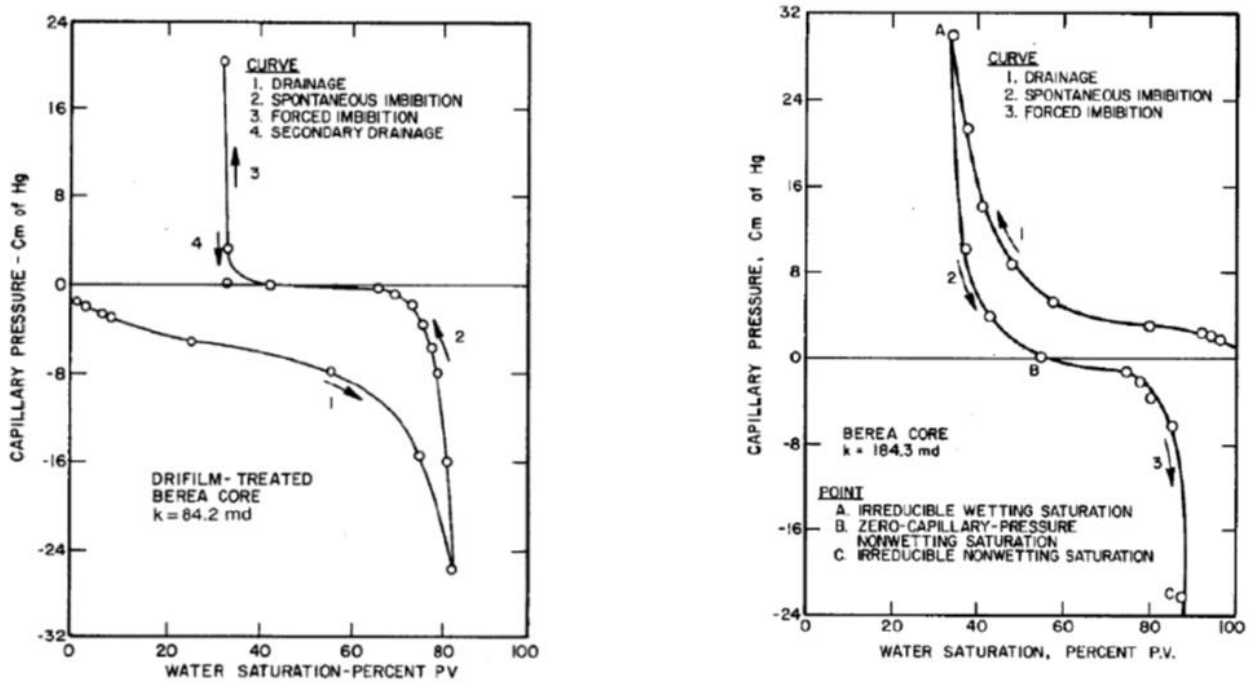

Figure 2.7: Illustration of oil/water capillary pressure curves for an oil-wet core (left) and a water-wet core (right)) [28]

Capillary pressure curves consist of *drainage* and *imbibition* processes. In a drainage process, the wetting fluid is displaced by the non-wetting fluid, while the opposite occurs in an imbibition process. As illustrated in Figure 2.7, in a water-wet case (right, curve 1) the oil pressure (entry pressure) must be higher than the water pressure, for oil to enter the water-filled

pores. This will reduce the saturation of the wetting fluid, which is water in a water-wet medium. When the water saturation decreases, parts of the wetting phase will be disconnected from the bulk wetting phase, and when the capillary pressure is high enough, the rest of the wetting phase in the porous medium will disconnect, resulting in an almost vertical capillary pressure curve (point A in the curve to the right). At this point, the remaining water saturation will be irreducible. Primary drainage is when the porous medium is drained for the first time (curve 1 in Figure 2.7), for instance when oil is displacing water in a 100% water saturated core plug.

During spontaneous imbibition, the saturation of the wetting fluid increase (curve 2 in Figure 2.7, right). Spontaneous imbibition occurs after a drainage process, where the capillary pressure is positive, and the wetting phase imbibes in the smallest pores. Forced imbibition is when the capillary pressure is decreased to a large negative value [28].

Primary drainage is an irreversible process, such as when water is displacing the oil (imbibition), the water starts to fill the smallest pores first, and the capillary pressure will decrease. The imbibition curve will not follow the same path as the primary drainage curve. When the capillary pressure develops towards zero, the oil saturation will go towards residual oil saturation. This phenomenon is called hysteresis [22]. The capillary pressure curves for imbibition and drainage are not the same, due to hysteresis, since the saturation varies, snap-off (described in the next chapter) phenomenon occurs for each filling sequence.

2.8. Residual Oil Saturation (S_{or})

After a water injection, the oil may be trapped in the porous medium, due to the capillary trapping, caused by the interfacial tension between non-miscible phases. The crude oil in a porous medium can be trapped due to two primary mechanisms as illustrated in Figure 2.8 and Figure 2.9:

- Pore doublet model
- Snap-off model

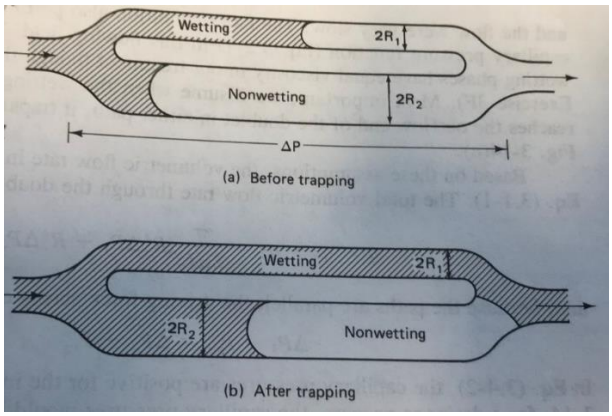

Figure 2.8: Illustration of the pore doublet model, where R1 and R2 are the pore radius, and ΔP is the differential pressure along the pore [15]

Figure 2.9: Illustration of the snap-off model [29]

The pore doublet model shows how oil is trapped by bypassing water in a pore doublet as illustrated in Figure 2.8. A pore channel that splits into two channels, one with radius R1 and one with R2. Since R1 is smaller, R1<<R2, the wetting fluid will bypass this channel quicker than R2, which leads to trapping of oil in the bigger channel.

The snap-off model represents how oil phase snaps off into globules that are localized in the pore bodies of the flow path. In such system there will be a local capillary pressure which varies with the position of the flow path; it is large where the path is narrow, and small where the path is wide as illustrated in Figure 2.9. As the displacing water film becomes thicker (collar of water) in the pore, the oil film becomes thinner, and snaps off and resides in the middle of the pore. The oil is not continues and trapped by capillary forces [19].

2.9. Capillary Number (N_{vc}) and Capillary Desaturation Curve (CDC)

The *capillary number* (N_{vc}) expresses the ratio between the viscous forces, *VF*, to capillary forces, *CF*, and can be defined as:

$$N_{vc} = \frac{VF}{CF} \tag{2.18}$$

Alternatively, expressed through Darcy`s law

$$N_{vc} = \frac{u_w \cdot \mu_w}{\sigma_{o/w}} \tag{2.19}$$

Where u_w is the Darcy velocity of water, μ_w is the viscosity of water and, $\sigma_{o/w}$ is the oil/water interfacial tension.

After a waterflooding oil might be trapped as immobile globules distributed through the porous medium (as discussed in chapter 2.8). The two forces acting on the immobile globules (oil) are the capillary forces and viscous forces. Several authors have correlated the ratio between these forces [30-32] and how capillary number impact residual oil saturation. As illustrated in equation (2.19), an increase in the viscous force or reducing in the capillary forces leads to a higher capillary number which will mobilize oil. This relationship is represented in a capillary desaturation curve (CDC), illustrated in Figure 2.10.

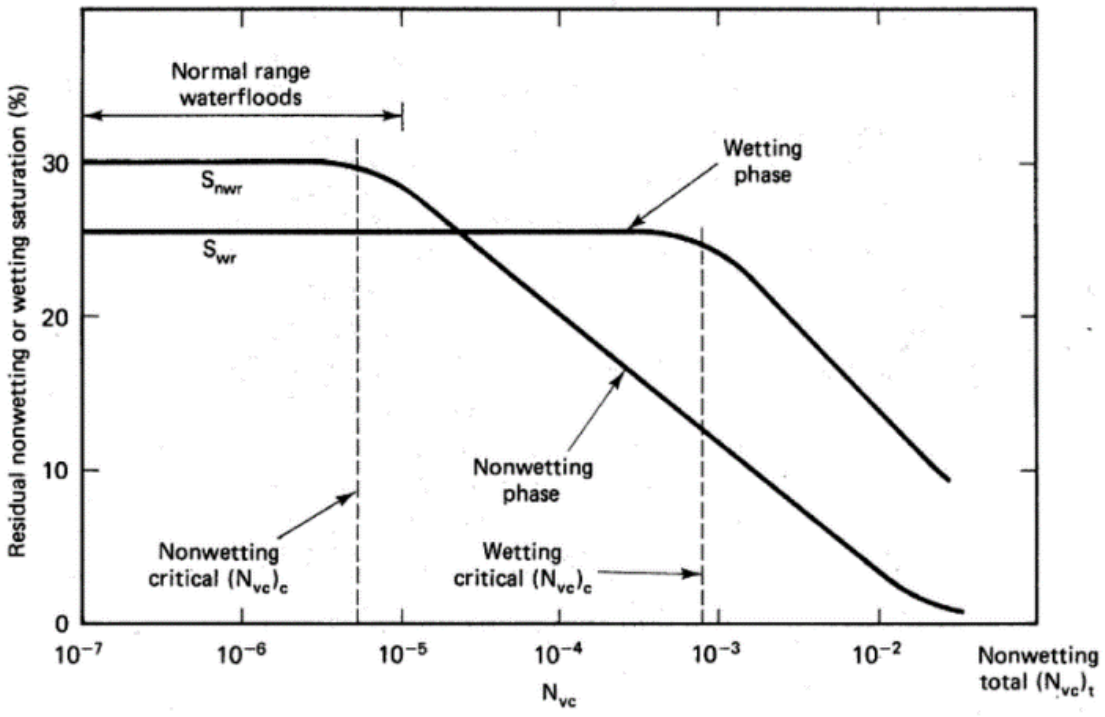

Figure 2.10: Schematic capillary desaturation curve, wetting and non- wetting phase [33]

Observation from Figure 2.10, shows that at low N_{vc}, S_{or} is constant. When the N_{vc} magnitude increase, a knee in the curve (critical capillary number) occurs and, S_{or} begins to decrease. To reduce S_{or} significantly, the N_{vc} must be increased by 2-3 orders of magnitude [34]. The CDC is influenced by wettability preferences and pore size distribution of the porous medium. The critical capillary number is higher for the wetting phase opposed to the non- wetting phase since it requires a higher N_{vc} for a given degree of desaturation for the wetting phase [15]. The knee in the curve will be less pronounced if the pore size distribution is varied [14].

To achieve low residual oil saturation, a higher N_{vc} is required, which can be accomplished through the following processes based on equation (2.19) [14]:

- Increasing the velocity of the water
- Increasing the viscosity of the water
- Decreasing the IFT between oil and water

The velocity of water cannot be increased significantly in the field, due to capacity and pressure limitations of the injection equipment. A polymer can be added to increase the viscosity of the water. However, the reduction in the injectivity limits the range. Interfacial tension can be reduced by adding a surfactant to the injection water, which will lead to increase in N_{vc} and reducing the residual oil.

2.10. Wettability and Its Effect on Waterflood and Residual Oil Saturation

It is essential to know the wettability preference of the reservoir rock. When performing a waterflood for example on a strongly oil-wet core, the efficiency is much lower than a water-wet core [21]. Several authors have shown that wettability affects oil recovery when waterflood is performed [25, 35-37]. Experimental studies has shown that waterflood into water-wet rocks is more efficient than oil-wet rocks [19]. Wettability affects waterflood behavior by controlling the flow and spatial distribution of fluids in the core [19].

During a waterflood of a strong water-wet system, water imbibes into the smaller pores moving the oil into the larger pores. Since the system is water-wet, the water advance along the pore

walls in a uniform front displacing oil in front of it. After the waterfront passes, the oil left is immobile, because of that a little or no production of oil exists after water breakthrough. The remaining oil is capillary trapped as globules in the center of the larger pores, as seen in Figure 2.11, case a, or as larger patches of oil extending over many pores surrounded by water.

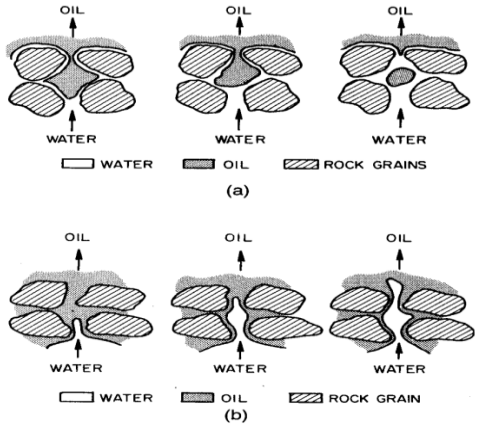

Figure 2.11: Water displacing oil from a pore during a waterflood: a) strongly water-wet rock, b) strongly oil-wet rock [38]

In a strongly oil-wet case, oil will be in the smallest pores and as a thin film at the rock surface. In a waterflood, the water will invade the center of the pores and will form continuous channels or fingers through the centers of the larger pores pushing the oil in front, as illustrated in Figure 2.11, case b. Water breakthrough occurs at an earlier stage than the strongly water-wet case, and the oil is recovered in a tail production. Thus, the oil recovery is less efficient in an oil-wet system compared to strongly water-wet system. The residual oil is found in small pores, continues as films over the rock surface and big pockets of oil surrounded by water.

However, some researchers observed that highest oil recovery was achieved when the porous medium was in intermediate-wet state. Jadhunandan and Morrow (1995) [39] investigated the relationship between wettability and oil recovery by waterflooding. They found that after injection of 20 pore volumes of brine, the maximum oil recovery was achieved for the weakly water-wet state (close to neutral-wet).

Skauge and Ottesen (2002) [40] summarized waterflooding experiments of 350 North Sea reservoirs cores. They concluded that residual oil saturation decreases as the wettability of the core shifts from strongly water-wet or strong oil-wet to an intermediate wetting system as seen in Figure 2.12.

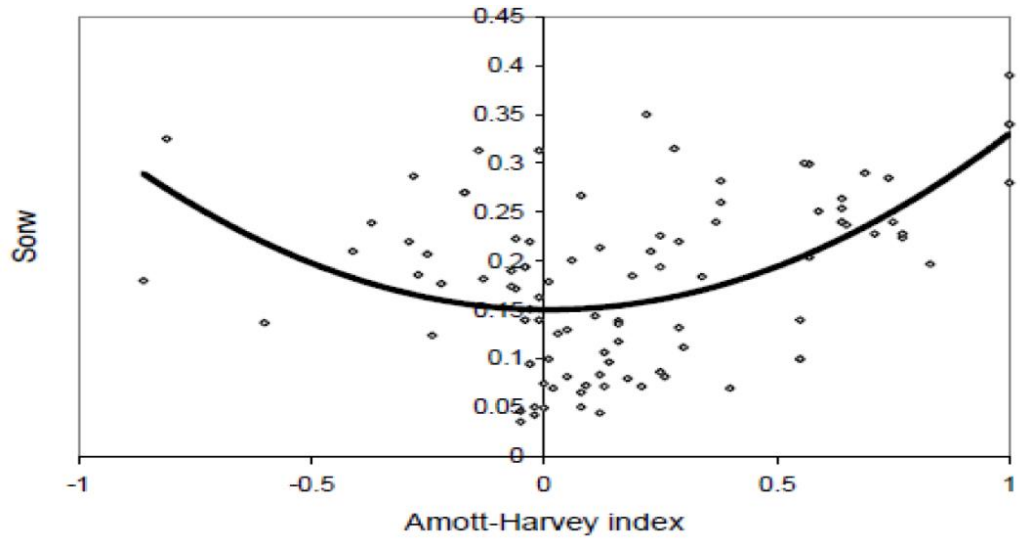

Figure 2.12: Residual oil saturation measurements of 30 North Sea reservoirs [40]

Figure 2.12 shows residual oil saturation after waterflood for the three different intermediate wettability classes. A study made by Skauge et al. (2003) [41] showed that the highest remaining oil saturation was in mixed-wet small rocks. Oil located in the smallest pores in the porous medium which require higher capillary pressure to mobilize the oil from the smallest pores. As seen in the figure below, the lowest residual oil is achieved from the mixed wet large (MWL) pores. Skauge et al. verified this by experimental work in (2007) [23].

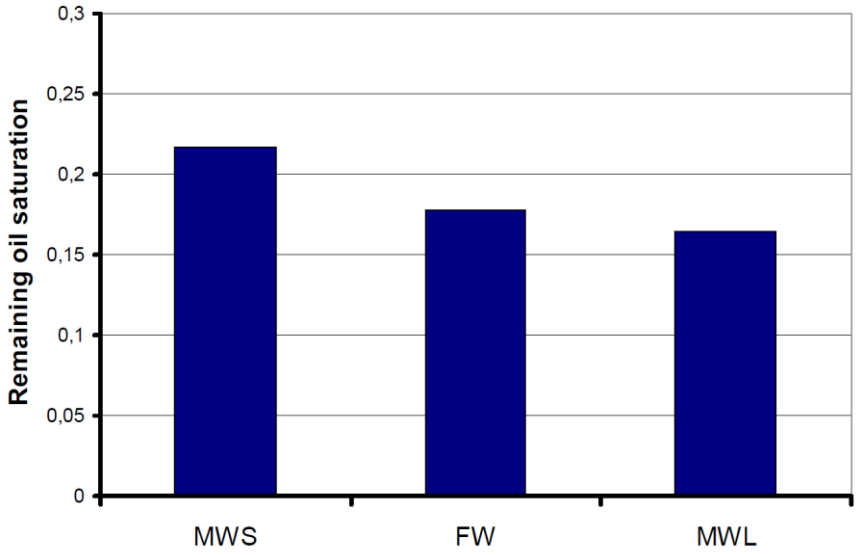

Figure 2.13: Average remaining oil saturation from intermediate wet classes suggested by Skauge et al. (2003)[41]

2.11. Wettability and Its Effect on Relative Permeability

The wettability of a porous medium affects the relative permeability. The relative permeability is affected since the wettability controls the flow location, and the distribution of fluids in a porous medium. Since the wettability affects the saturation distribution in the pores, the wetting fluid will adhere to the pore walls and will occupy the smaller pores while the non-wetting fluid located in the centers of the larger pores. This trapped nonwetting fluid at S_{or} will reduce the flow of the wetting fluid. E.g., water relative permeability will be low for a water-wet system compared to oil-wet system. This is because of the wetting fluid tends to travel through the smaller, less permeable pores while the non-wetting (oil) flows easily through the bigger pores [19]. For the oil-wet case, the process is reversed. As illustrated in the curves in Figure 2.14, water will flow easily in oil-wet rocks compared to water-wet rocks. Thus, the wettability affects the relative permeability curves, as illustrated in Figure 2.14. The end-point relative permeabilities, and where the two curves intersect (where oil and water permeabilities are equal), depends on the wettability. Craig (1971) [33] developed a list for determining the wettability from relative permeability curves as shown in Table 2.2

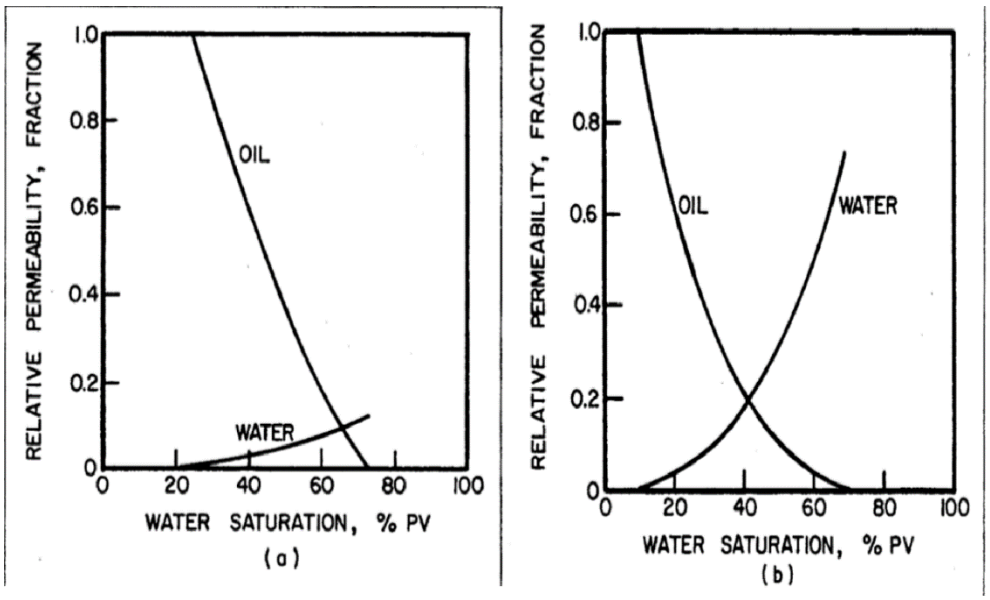

Figure 2.14: Typical relative permeability curves, water saturation increasing. a) Strongly water-wet rock. b) Strongly oil-wet core [19]

Table 2.2: Craig`s rules of thumb for determining wettability

Craig`s rules of thumbs for determining wettability		
	Water-wet	**Oil-wet**
S_{wi}	Greater than 20-25 %	Less than 15 %
$S_{w,intersection}$*	Greater than 50 %	Less than 50 %
$K_{rw,Sor}$	Less than 30 %	Greater than 50 %

*$S_{w,intersection}$: is the saturation at which oil and water permabilties are equal (crossover saturation)

2.12. Carbonate Reservoir

Carbonate reservoirs are estimated to contain 60% of the world oil and 40 % of worlds gas reserves [42]. Carbonates are highly heterogeneous and naturally fractured which can vary enormously in rock properties within a small section of the reservoir; therefore they are difficult to predict. A cross plots of porosity/permeability for sandstone often shows a clear trend, carbonates in the other hand shows a scatter of data due to the wide range of the petrophysical properties.

A study by Freire et al. (2016) [17] on Indiana Limestone, using X-ray fluorescence spectroscopy showed that the mineral composition of the rock is 98.6wt% calcite (CaCO3). They also reported a porosity of (12 ± 2) % and a coordination number of 2.6 ± 0.2. The coordination number represents the number of connection between each pore throat, which indicates the connectivity of the pore space. The coordination number by Freire et al. was close to the results of a study made by Gharbi and Blunt (2012) [20], where they reported a coordination number of 2.97 and a porosity of 13.05%.

Gharbi and Blunt 2012 [20] studied six carbonate rocks to analyze relative permeability with different connectivity and pore structure at five different wettability scenarios, (f =0, f =0.25, f=0.5, f = 0.75 and f = 1). Only three wettability scenarios will be discussed here (f =0, f=0.5 and f = 1); water-wet, fractional-wet and oil-wet as illustrated in Figure 2.15. For a water-wet case (Figure 2.15, left) water remains in the smallest portions of the pore space, resulting very low water relative permeability and significant trapping of oil in the larger pores at the end of waterflooding, primarily caused by snap-off. Since Indiana Limestone is poorly connected carbonate (coordination number of 2.97, there are fewer ways for oil to escape), more oil can be trapped by snap-off in the pore space.

For the neutral-wet case, Figure 2.15 (middle), the pores have an equal mix of water and oil-wet pores. The residual oil saturation is low since the oil remains connected at pores and throats through the network. As shown in Figure 2.15 (middle) the water relative permeability shows a water-wet behavior, where there is a sharp decrease in oil relative permeability and significant trapping.

The oil-wet case, Figure 2.15 (right), the water relative permeability rise to higher values since the water fills the centers of the larger pores, and water is more mobile (low oil relative permeability at residual oil saturation). The residual oil saturation decreases with increasing connectivity, regardless of wettability. The highest water saturation is at the mixed-wet case (f=0.75) for poorly connected pores, this confirms that waterflooding is most effective for mixed-wet carbonates that have a preference to an oil-wet behavior.

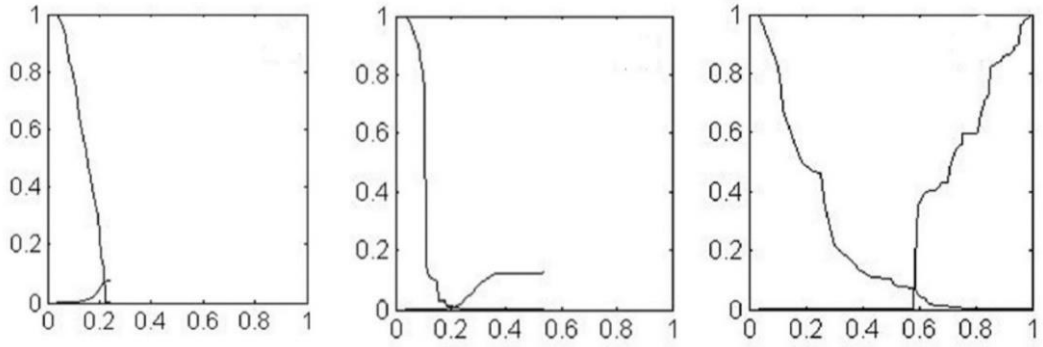

Figure 2.15: Waterflood relative permeability for Indiana Limestone, strongly water-wet case(f = 0) (left), mixed wet case(f = 0.5) (middle), strongly oil-wet case (f = 1) (right).Y-axis is relative permeability and x-axis is water saturation [20]

Carbonate rocks are positively charged at the rock surface [43, 44]. The mineral surface is believed to be naturally water-wet if it has not been contacted by crude oil as reported by Morrow et al. (1986) [45]. Under reservoir conditions, the polar components in crude oil adsorb on the pore surface, which can lead to wettability alteration as oil-wet- or mixed wet state.

In general carbonate reservoirs are classified as either oil or intermediate wet. Chilinager and Yen (1983) [4] analyzed 161 carbonate core samples from different regions of the world. They found that 15% of these rocks were strongly oil-wet (contact angle 160-180°), 65% oil-wet (contact angle 100-160°), 12% intermediated-wet (contact angle 80-100°), and 8% were water-wet (contact angle 0-80°).

A study by Treiber et al.(1972) [5] investigated contact angle tests and flow tests of 55 different reservoirs, conducted at the laboratory. Their study indicated that the wettability spectrum could cover from strongly water-wet to strongly oil-wet. 64% of carbonate rocks were intermediate-wet, 28% oil-wet and 8% were water-wet.

3. Enhanced Oil Recovery (EOR)

During the production of an oil filed, several practices may be implemented to improve the oil recovery. These methods are referred to as improved oil recovery (IOR), and it is defined as all economic practices that are intended to improve the oil recovery factor and/or accelerate reserves [14]. IOR, therefore, includes infill drilling, horizontal wells, reservoir management and enhanced oil recovery (EOR)[46].

The oil recovery mechanisms may be subdivided into three stages:

- Primary Oil Recovery
- Secondary Oil Recovery
- Tertiary Oil Recovery

3.1. Primary Oil Recovery

The efficiency of oil displacement in primary oil recovery process depends on the natural pressure of the reservoir. The natural pressure drive of the reservoir may result from rock and fluid expansion drive, solution gas drive, gas cap drive, gravitational force, water drive (aquifer drive) [14].

3.2. Secondary Oil Recovery

When oil production declines after primary oil recovery, the secondary oil recovery methods are applied to increase the pressure required to drive the oil to production wells. The conventional processes used to maintain the pressure in the reservoir are to inject gas or water. The injected fluid will displace the oil. The secondary mode injection of water often referred to as waterflooding.

Waterflooding improves oil recovery by two mechanisms [18]:

- It provides the pressure energy to overcome the capillary forces that entrap the oil
- Improves mobility ratio as compared to the solution gas drive if the reservoir was subjected to during primary depletion.

3.3. Tertiary Oil Recovery

The oil recovery performance of waterfloods can be improved by methods that increase the oil displacement efficiency, the volumetric sweep efficiency, or both. These improved methods, which involve the addition of gas, chemical, solvent or heat [15]. EOR is sometimes referred to as tertiary recovery [46]. EOR is defined as “oil recovery by injection of materials not normally present in the reservoir such as e.g., surfactants and polymers [14]. When production from the reservoir is no more economical with conventional methods, EOR methods may be used to extract more of the oil in an economical manner. EOR can be divided into three major categories [18]:

- Thermal process
- Chemical process
- Miscible process

Thermal methods have been used for the recovery of heavy oil while chemical and miscible for the light oils[18]. Thermal methods include, in situ combustion and steam injection. Chemical flooding processes such as surfactants, polymers, and low salinity water. Miscible flooding processes is an injection of a solvent such as alcohol, condensed hydrocarbon gases or carbon dioxide [14]. All these methods are used to increase the oil recovery.

Oil recovery is defined as the ratio between produced oil and oil initially in place and can be written as:

$$E_R = \frac{N_p}{N} = E_D x E_{vol} \tag{3.1}$$

Where

- E_R is the recovery factor
- N_p is the produced oil volume
- N is the total volume originally in place
- E_D is the microscopic displacement efficiency
- E_{vol} is the volumetric displacement efficiency (Areal x Vertical sweep efficiency)

EOR methods should target the microscopic and volumetric displacement efficiency, where Evol and ED can be rewritten as:

$$E_D = \frac{Volume\ oil\ displaced}{Volume\ oil\ contaced} \tag{3.2}$$

$$E_{vol} = \frac{Volume\ oil\ contacted}{Total\ oil\ in\ place} \tag{3.3}$$

A surfactant may be used to increase the microscopic displacement efficiency, by influencing the interfacial tension between the oil and the water. Hence it mobilizes the oil that is capillary trapped in the pores. Moreover, more oil can be contacted with a surfactant and may increase the recovery factor.

Adding polymer to the injected fluid, e.g., water will increase the viscosity of the water. By injection of more viscous fluid, the displacement front will be stabilized, and the sweep efficiency becomes higher in the reservoir. Polymer injection can increase the recovery factor by increasing the volumetric displacement efficiency.

3.4. Wettability Alteration

Wettability alterations towards more water-wet state or oil-wet state have been proposed to be the cause of increased oil recovery with low salinity waterflooding. The degree of wettability alteration is strongly dependent on the stability of the water film between the mineral surface and the oil phase. The stability of the water film is dependent on the disjoining pressure.

Disjoining pressure (Π) is the force acting between two interfaces separated by a thin film. The disjoining pressure is a result of three different forces; electrostatic interactions, van der Waals interactions, and hydration forces. The disjoining pressure quantifies the driving force for spontaneous thickening. If the value of the disjoining pressure is positive (repulsive), the two interfaces will repel each other, and the wetting film is stable, and the mineral surface will remain water-wet. However, if the disjoining pressure is negative (attractive forces) the interfaces will attract each other, and the wetting film is unstable. This will allow non-wetting phase (e.g., crude oil) to be in contact with the mineral surface and possibly promote a wettability alteration towards less water-wet state [23].

The fact that many sedimentary rocks were deposited in aqueous environments, and almost all clean sedimentary rocks are strongly water-wet, it was believed that all petroleum reservoirs are strongly water-wet. When oil migrates into the reservoir, wettability shifts may occur toward more oil-wet state.

Skauge et al. (2007) [23] investigated how water films separating crude oil from the mineral surface can be destabilized The stability of water films is governed by disjoining pressure, which depends on pore shape, the composition of crude oil/brine/rock (COBR) and the applied capillary pressure. Therefore, to destroy the water films, disjoining pressure must be overcome.

Several mechanisms have been proposed in the literature for the wettability alteration of a rock surface to destabilize the water film during COBR interactions. Buckley et al.(1998) [47] investigated mechanisms affecting wettability alteration by crude oil. These are mechanisms are:

- **Polar interactions:** This mechanism occurs in the absence of water film between oil and mineral surface. Direct contact between a polar component such as asphaltenes in crude oil and polar components on the solid surface, which can be adsorbed to the mineral surface, leads to wettability alteration. Clay content, type of cations, nitrogen content in the oil and the solvent that dissolves the polar compounds will influence the degree of wettability alteration (Figure 3.1a)
- **Surface precipitation:** Depends on crude oil solvent properties concerning the asphaltenes. If the crude oil is not a suitable solvent for its asphaltenes compounds, the tendency of wettability alteration is enhanced. (Figure 3.1b)
- **Acid/ base interaction:** Controls surface charge at oil/water and solid/ water interfaces. In the presence of water, both the solid and oil interfaces become charged. Polar functional groups on both the mineral and the oil can act as acids (losing a proton and becoming negatively charged) and bases (gaining a proton and becoming positively charged). The stability of the water film may be destabilized at the rock surface, leading to wettability alteration (Figure 3.1 c)
- **Ion binding:** Divalent cations such as $Ca^{2+}$and Mg^{2+} and multivalent ions can bind at both oil and solid/ water interfaces and/ or bridge between them. When Ca^{2+} is present, several interactions can occur:
    - Oil-Ca^{2+}- Oil
    - Mineral- Ca^{2+}-Mineral
    - Mineral- Ca^{2+}- Oil, (Figure 3.1d)

The first two can limit wettability alteration, whereas the third can promote it. These mechanisms are believed to be the main reason for wettability alteration in sandstone reservoirs contain acidic oil leading to a more oil-wet state.

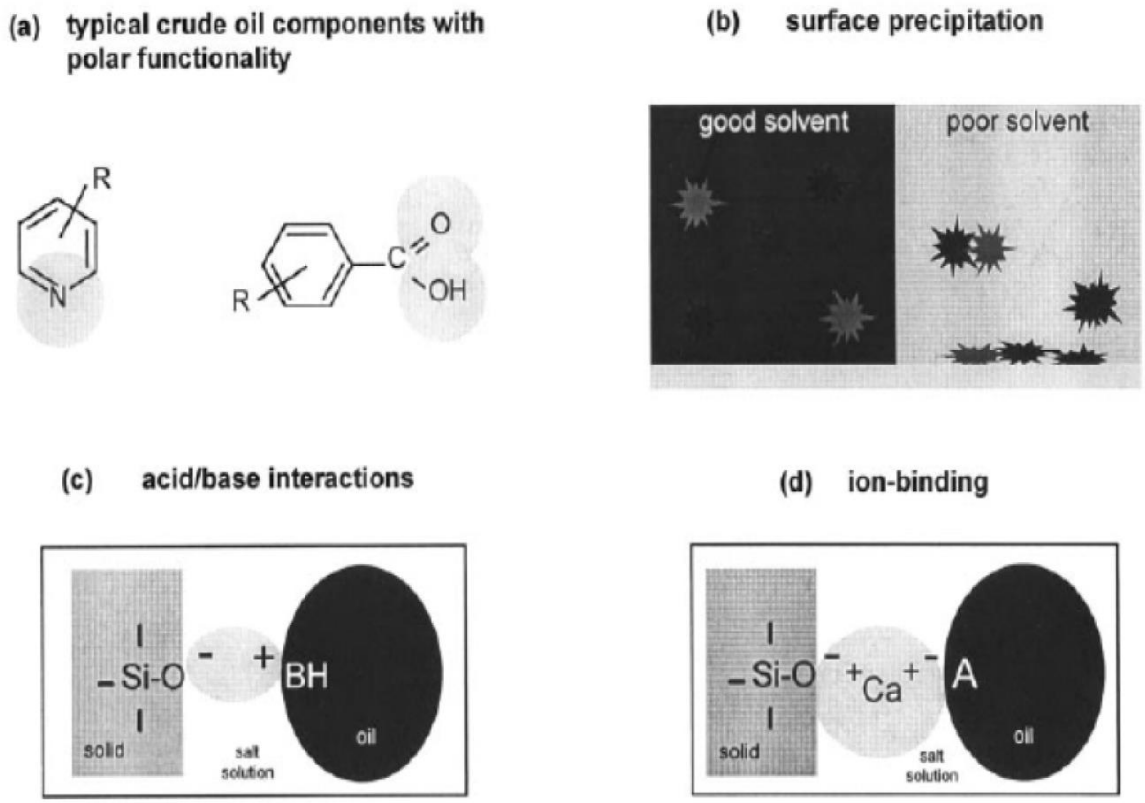

Figure 3.1: Mechanisms of COBR leading to wettability alteration [47]

3.5. Low Salinity Waterflooding

Waterflooding process has been widely applied as a secondary oil recovery method during the past decades. In the recent years, many types of research have been developed using low salinity water injection in a favorable way to improve oil recovery in sandstones and carbonates. Low salinity as a "smart water" with the correct composition can act as a tertiary recovery method and can impact oil recovery depending on the rock mineralogy [48, 49].

There are several mechanisms that have been proposed, for low salinity effect (LSE) with experimental evidence supporting or opposing to the proposed mechanisms. This is due to the complex nature of the interaction between crude oil, brine, and rock. The main mechanisms that are debated among researchers for sandstones are [50, 51]:

- **Wettability alteration**
- **Electrical double layer (EDL) expansion**
- **Migration of fines (sandstone):** where fines detach from the pore walls under certain brine salinity. Oil attached to fines might also be detached along with fines, which will improve water-wetness and oil recovery [52]
- **Increase in pH:** may lead to in- situ surfactant generation which may decrease the interfacial tension between water and oil and lead to increase in capillary number, hence lowering residual oil saturation [53]
- **Multi-ion Exchange (MIE):** was suggested by Lager et al. (2008) [54] where divalent cations (Mg^{2+} and Ca^{2+}) adsorbed on the solid surface are exchanged with monovalent cations in the low salinity brine
- **Salting-in Mechanism**

The main mechanism is still uncertain, especially for carbonate rocks. Some of the uncertainty can be related to the absence of clay in carbonates (fines migration), which can be difficult to relate to wettability- alteration mechanism in carbonates [55]. As mentioned earlier carbonates are heterogeneous rocks which may have complicated chemical interaction between rock/oil/brine, and therefore can be difficult to predict oil recovery by low salinity.

Several research studies have been published in the literature investigating the impact of salinity and ionic strength on oil recovery in carbonates. Published studies show a positive, small or negligible effect of low salinity [49, 50, 56-59]. Several mechanisms have been proposed as the main reason for the enhanced oil recovery using low salinity in carbonates:

- Adsorption of sulfate ions associated with co-adsorption of divalent cations (Ca^{2+} and Mg^{2+})
- Change in the rock surface charge
- Microscopic dissolution of anhydrite [48] or calcite [49, 60]

The wettability alteration is related to a synergistic interaction between the potential determining ions Ca^{2+}, Mg^{2+} and SO_4^{2-} and adsorbed carboxylic material on the carbonate

surface. Higher oil recovery is due to the concentration of these ions in the EDL, which is improved in higher temperatures above 70°C. [49, 59, 61]

Several mechanisms have been suggested for increased oil recovery in carbonates, but the majority of researchers believe that the wettability alteration is the main reason [48, 49, 57, 59, 62]. The mechanism causing wettability alteration may be the dissolution of anhydrite, surface charge alteration, in- situ surfactant generation, or combination of these mechanisms [63].

3.6. Low Salinity Effect in Sandstones

Tang and Morrow (1997) [55] studied the impact of salinity on oil recovery for both connate and invading brines trough imbibition and waterflooding experiments in sandstone cores. They found that the connate and invading brines have a significant effect on wettability and oil recovery at reservoir temperatures. Decreasing salinity of injection water of the same composition as the connate water or one of them caused increases in oil recovery. The oil recovery was highest at high temperatures, which explained by increase in water-wetness of the cores resulting in higher oil recovery.

Zhang et al. (2007a) [64] investigated low salinity effect in Berea sandstone during secondary and tertiary oil recovery processes. They reported oil recovery of 16% OIIP by injection of 1500ppm low salinity brine

Agbalaka et al. (2009) [65] performed waterflooding testes on Berea sandstone and shale-sandstone. They observed additional oil recovery in both secondary and tertiary modes when the concentration of the injected brine varied from 4wt% NaCl to 1wt% NaCl. The oil recovery increased at higher temperatures compared to ambient temperatures. Studying the Amott-Harvey index showed an increase in water-wetness with a decrease in salinity.

3.7. Low Salinity Effect in Carbonates

The effect of LSW in carbonates is still not covered well compared to sandstones. This section will highlight the studies to determine the mechanism of oil recovery from carbonate rocks; the experimental studies, and some field applications.

Hognesen et al. (2005) [66] performed spontaneous imbibition experiments on chalk and limestone cores to investigate the effect of sulfate ion concentration as a wettability modifying agent. They found that increasing the temperatures; sulfate ion acts as wettability modifier which reacts with the rock surface, shifting the wettability from mixed-wet state to water-wet state, and thus increases the oil recovery.

Webb et al. (2005) [67] performed reservoir conditions spontaneous imbibition study on cores from the North Sea carbonate field (Valhall). They found that seawater could alter wettability of the carbonates to a more water-wet state compared to sulfate free water. They found from the change in the capillary pressure curves that the effect of seawater on carbonates is more favorable compared to formation water injection. 40% of OOIP was recovered from the core spontaneously using seawater compared to formation water. When forced seawater injection was performed the oil recovery increased from 40% to 60% OOIP.

Zhang et al. (2006a) [68] studied the symbiotic effect of calcium and sulfate ions when using seawater as an imbibing wettability modifier on outcrop chalk from Stevens Klint (SK). The acid number (AN) of the oil was 2.07 mg of KOH/g, and the brine was synthetic seawater, SW, and modified SW (various calcium and constant sulfate concentrations) with the same ionic strength by modifying NaCl. They performed imbibition tests at various temperatures (70-130°C). They concluded that oil recovery increased when Ca^{2+} concentration increased in both the injection fluid and the initial brine. They related the incremental oil recovery to wettability alteration and temperature increase.

Zhang et al.(2007b) [69] studied the effects of the divalent cations ($Ca^{2+}$and Mg^{2+}) in the presence of sulfate, using seawater as an imbibing wettability modifier on chalk from Stevens

Klint (SK). The acid number (AN) of the oil was 2.07 mg of KOH/g. The imbibition at 70˚C was performed using modified seawater without Calcium and Magnesium but with different amounts of Sulfate, where the concentration of sulfate − varied from zero to four times the concentration present in seawater, and the ionic strength was constant and similar to seawater by adjusting with NaCl. They concluded that wettability alteration occurs if the imbibing water contains either Ca^{2+} and sulfate or Mg^{2+} and sulfate, and they found that the efficiency increased as temperature increased, as illustrated in Figure 3.2.

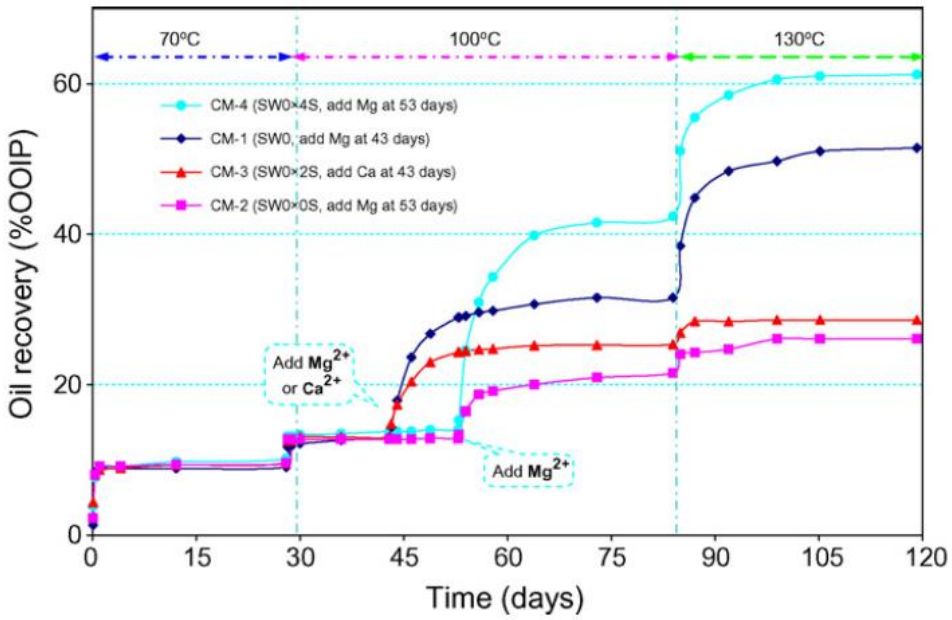

Figure 3.2: Spontaneous imbibition test conducted at 70˚C, 100˚C and 130˚C. CM is the core ID [69]

Strand et al. (2008) [70] performed a study in fractured limestone from the Middle East with seawater injection. The aim was to test if the results from chalk are also obtained from limestone. Chalk is a pure, biogenic material, and has much larger surface area compared to limestone. Thus, the reactivity of chalk surface toward potential determining ions is higher than limestone. The oil components adsorbed onto the surface, carboxylic material, which could modify wettability of limestone in the same way as for chalk using seawater. The study showed 15% OOIP increase in oil recovery from limestone when seawater contained sulfate, rather than water free sulfate at 120˚C. The study also confirmed that wettability alteration and sulfate

adsorption is almost the same for both limestone and chalk, using chromatographic wettability tests.

Hiorth et al.(2010) [60] studied the influence of water chemistry on the surface charges and rock dissolution of pure calcium carbonates similar to the Stevens Klint chalk by constructing and applying a chemical model that couples bulk aqueous and surface chemistry to address mineral precipitation and dissolution. The chemical model was made by using spontaneous imbibition and zeta potential experiment data by previous work by Austad [56, 71]. The model predicted the surface potential of calcite and adsorption of sulfate ion from the pore water. The study concluded that mineral dissolution is the controlling factor that increased oil recovery in the spontaneous imbibition tests and that the dissolution of calcite is strongly dependent on temperature.

3.7.1. Coreflooding Experiments

Bagci et al. (2001) [72] studied waterflooding in a packed 1D unconsolidated limestone. The aim of the study was to investigate the effect of different brine composition on oil recovery. They studied NaCl, $CaCl_2$, KCl and binary mixtures of these salts at two different concentrations of 2 and 5wt%. They reported high oil recovery ranged from 18.3-35.5% OOIP, where the highest recovery (35.5% OOIP) was obtained by 2wt% KCl. The oil recovery increased with decrease in salinity of the injection brine. They also reported that low salinity brine injection gave high pH in the effluent brine, due to ions exchange reactions with the clay present in the rock. The reason for the increased oil recovery was believed to be wettability alteration, but no mechanism was explained in detail.

Yousef et al.(2011) [49] studied composite cores from one of the Saudi Arabian carbonate reservoirs, where they investigated the impact of altering salinity and ionic composition of the injected seawater (57.670 ppm) on oil/brine/rock interactions and recovery mechanism. They performed wettability tests on the limestone, including nuclear magnetic resonance (NMR) and contact angle measurements. They started with seawater and diluted the seawater ending with 100 times diluted seawater. They observed that the additional oil recovery was approximately

7-8.5 % with twice diluted seawater, 9-10 % with ten times diluted seawater, and 1-1.6% with 20 times diluted seawater, and no oil recovery with 100 times diluted seawater, all regarding OOIP (Figure 3.3).

The driving mechanism behind the increase in oil recovery was proposed as wettability alteration toward more water-wet state. Contact angle measurements highlighted that injection of seawater was capable of changing the rock wettability towards water-wet state. They concluded that wettability alteration was a result of anhydrite dissolution and change in surface charge as illustrated in Figure 3.4 by Al- Shalabi et al. (2016)[73].

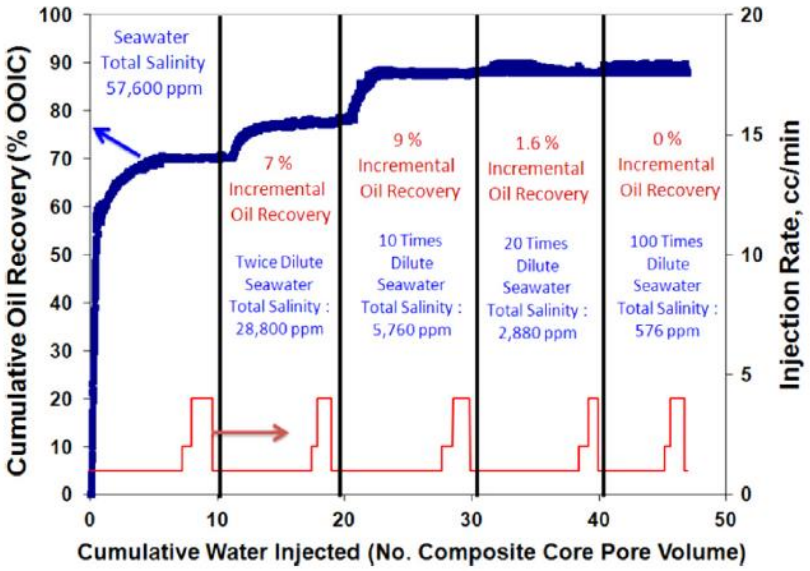

Figure 3.3: Oil recovery curve from(one of the experiment) by Yousef et al. (2011)[49] (modified by Al-Shalabi (2016) [73])

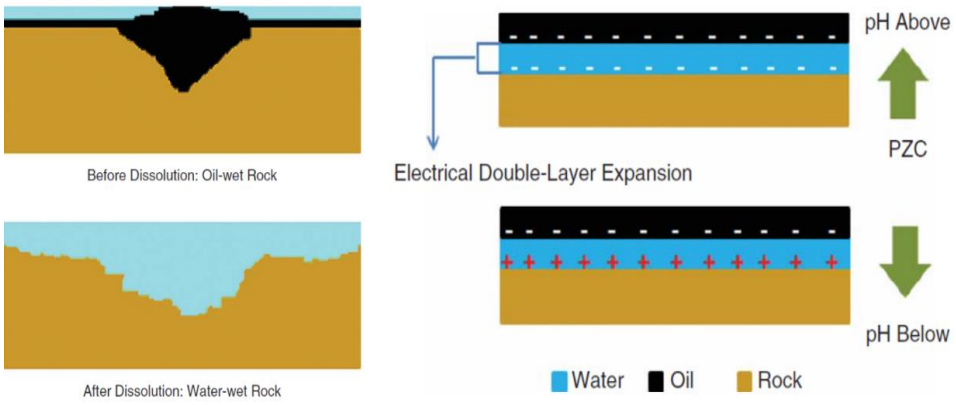

Figure 3.4: Wettability alteration by a) dissolution (left) and b) change in surface charge (right) [73].

Al- Shalabi et al. (2015) [63] analyzed Yousef et al. coreflood experiment by comparison between two geochemical simulators UTCHEM and PHREEQC through modeling fluid and solid species concentrations. They also investigated that if anhydrite dissolution is more effective in wettability alteration, or if it is the change in surface charge that is more dominant in wettability alteration. Al- Shalabi et al. concluded that the wettability change during Yousef et al. could be explained as wettability alteration due to change in surface charge rather than anhydrite dissolution. The mechanism was explained as the pH of the solution exceeds the point of zero charge (PZC), which changes the rock surface charge; the electrical double layer (EDL) expands, and may alter the rock wettability, hence increase the oil recovery as shown in Figure 3.4.

Zahid et al. (2012) [74] investigated the potential of using low salinity waterflooding to increase oil recovery in three reservoir carbonate materials and three Aalborg outcrop chalk. They used seawater of (57.670 ppm), and diluted seawater (twice, ten times and twenty times diluted seawater). Aalborg chalk cores did not increase oil recovery during low salinity waterflood, neither at room temperature nor higher temperatures. No low salinity (diluted seawater) effect was observed during the waterflood experiments using reservoir carbonate core plugs at room temperature. However, increase in oil recovery was observed when the carbonate reservoir rock was at an elevated temperature of 90°C. They also observed higher differential pressure during injection of diluted seawater in carbonate material, which was explained as a sign of either dissolution or fines migration. One of the core plugs (carbonate reservoir) was damaged in the experiment. They believed that the combined fine migration and dissolution effects were the reason for increased oil recovery.

Mohanty and Chandrasekhar (2013) [57] conducted series of high temperature (120°C) tests on limestone rocks, including contact angle, imbibition tests, core flood experiments and ion analysis to find the brines that improve oil recovery. Contact angle measurement showed that modified seawater containing magnesium and sulfate and diluted seawater changed aged oil-wet calcite plates to more water-wet state. Presence of calcium without magnesium or sulfate was unsuccessful in changing calcite wettability, and therefore no significant contribution of calcium ion to incremental oil recovery by low salinity injection was observed. Modified seawater containing high SO_4^{2-}(43.419 ppm) and diluted seawater (872 ppm) improved oil

recovery from 40% OOIP (for formation brine waterflood) to about 80% OOIP in both secondary and tertiary modes with seawater and diluted seawater. They believed that the mechanism responsible for the additional oil recovery is a multi-ion exchange and mineral dissolution responsible for desorption of organic acid groups which lead to more water-wet conditions.

Most of the research on low salinity effect suggest that low salinity brine shifts the wettability from oil-wet to more water-wet state. However, there are studies which report wettability shifts to less water-wet state. Al- Attar et al.(2013) [62] found that low salinity water shifted wettability from water-wet to an intermediate state in carbonates, thus triggered incremental oil recovery.

Al- Attar et al. (2013) investigated low salinity water injection on carbonates from Bu Hasa filed in Abu Dhabi using seawater and two injection water. They performed core floods, interfacial tension (IFT), pH, and contact angle testes at ambient conditions, where they found that oil recovery increased from 63% OOIP to 84.5% OOIP when salinity in injection water was reduced from 197357 ppm to 5000 ppm. The latter was used to evaluate the impact of changing the sulfate and calcium ion concentrations to examine if there is any optimum concentration of these ions. They found that increasing calcium concentration resulted in decreasing oil recoveries while increasing sulfate to a certain level (46.8 ppm) in the 5000 ppm brine resulted in highest oil recovery. pH and IFT measurements could not justify the incremental oil recovery by low salinity.

Al- Attar et al. tested wettability alteration by contact angle measurements. They reported that contact angle increased with the decrease of the brine concentration. For example, the contact angle increased from 45° in the presence of filed formation water (197 357 ppm) to 70° when salinity was reduced to 1000 ppm.

Another study that supports Al-Attar work is by Sari et al.(2017) [75] who investigated contact angle of aged and unaged carbonate cores. They observed that contact angle for unaged carbonate substrate increased from 30° to 50° with a decrease in salinity formation brine FB (252244 ppm) to ten-time diluted formation brine 10dFB (25224.4 ppm). This indicates

wettability alteration from strongly water-wet to less water-wet conditions. For the aged carbonate sample, the contact angle level was increased from 35° to 105° when salinity level decreased from FB to 10dFB.

Shehata et al. (2014) [76] studied core floods on Indiana Limestone cores at 90°C, where they investigated the impact of salinity of the injected brine on oil recovery during secondary and tertiary recovery modes. Various brines where used, including deionized water, seawater, both diluted seawater and ions free seawater, such as $Na^{+}, Ca^{2+}, Mg^{2+}, SO_4^{2-}$were excluded. Their study aimed at determining the impact on fluid/rock interactions and how it does affect oil recovery by using different brines. Their core flooding results indicated that using deionized water after seawater (and vice versa) can improve oil recovery. No mechanism was explained in detail, but they believed it caused by a sudden change of brine ionic composition.

Awolayo et al.(2014) [77] investigated the impact of sulfate ion on a Middle East carbonate core plugs with an injection of different types of seawater to examine the impact on oil recovery, wettability, and surface charge modifications. They conducted several tests, including core floods, contact angle measurements, zeta potential tests, and ionic analysis. They found that increasing sulfate concentrations (four times of the base brine) were effective on displacement efficiency.

3.7.2. Proposed Mechanisms for Low Salinity Effect On Carbonate Rocks

Wettability alteration

Initially, in a reservoir, the thermodynamic equilibrium has been established between the rock, formation water and oil through million years. This equilibrium can be disturbed concerning wettability of the rocks, especially in carbonate rock surface. Wettability alteration is believed to be the possible reason for the enhanced oil recovery of carbonate rocks by modifying the ionic composition in the injected water. The wettability alteration can occur due to the change

in the surface charge of the rock or dissolution. The change in the surface charge is mostly related to the sulfate adsorption on the rock surface.

Strand et al. (2003) [78] performed different tests to investigate the sulfate concentration on wettability alteration with and without cationic surfactant solution. The tests included spontaneous imbibition at different temperatures in chalk and dolomite, contact angle measurements on different carbonate crystals (calcite, dolomite, and magnesite), and IFT measurements. They concluded that at low temperatures, the spontaneous imbibition decreased as the injected brine salinity increased, which was explained by the effect of temperature on the IFT and critical micelle concentration (CMC) value (Explained in chapter 3.8.Surfactants). Sulfate worked as a catalyst for imbibition rate in the presence of surfactant at 70°C below a concentration of 1.0g/L. Sulfate as a catalyst for improving imbibition rate comes from adherence on the rock surface. This makes rock surface partially negatively charged due to the presence of other positively charged metal ions. They also concluded that both sulfate and cationic surfactant affect wettability alteration, turning carbonate rocks more water-wet at different degrees regarding carbonate rock types (Calcite, Dolomite, and Magnesite). They also concluded that the adsorption of sulfate onto the water-wet zones of the chalk changes the surface charge so that the cationic surfactants could remove adsorbed carboxylic material more efficiently.

Hognesen et al. (2005) [66] investigated spontaneous imbibition on carbonates (chalk and limestone) to study the effect of cationic surfactant and sulfates as a wetting modification using seawater. They concluded that sulfate acts as a surface agent towards carbonate surface to improve water-wetness of carbonate reservoirs. With increasing temperature (90-130°C) the affinity of sulfate towards the carbonate surface increases, and sulfate acts as a catalyst causing an increase in oil recovery by imbibition in the presence of surfactants.

The concentration of sulfate in Hognesen et al. was 2.31g/L in the injected water, which in the study by (Strand et al. 2003 [78]) the concentration of sulfate was 1.0g/L. Higher sulfate concentration resulted in much higher oil recovery due to the increase in sulfate adsorption on the rock surface. The increase in the affinity of sulfate changes the surface charge from positive to negative and causes repulsion of carboxylic group, making the system to become more water-wet. Using sulfates and cationic surfactants result in lowering the IFT besides wettability

alteration. When temperature increases, the carboxylic group will be detached from the rock surface due to increase in the adsorption of sulfates on the rock surface, which increases the water-wetness of the rock. Hognesen et al. also stated that using sulfate as a wettability modifying agent in carbonates has limitations with regard to initial brine salinity (especially the concentration of calcium) and temperature. The ratio between calcium in the connate water and sulfate concentration must be known to avoid a $CaSO_4$ precipitation.

Zhang et al.(2006a) [68] studied the symbiotic effect of Ca^{2+} and sulfate when using seawater as an imbibing wettability modifier on outcrop chalk from Stevens Klint (SK). They concluded that Ca^{2+} is also an active agent in increasing the spontaneous imbibition of water into moderate water-wet chalk. Sulfate present in the injection water will adsorb onto the positively charged chalk surface and lower the positive surface charge. Electrostatic repulsion decreases, and more Ca^{2+} can adsorb onto the chalk surface and, the excess of Ca^{2+} is now closer to the chalk surface. Ca^{2+} can react with adsorbed carboxylic group bonded to the chalk surface and release some of the organic carboxylic materials. The mechanism is illustrated in Figure 3.5. They also concluded that wettability alteration is temperature dependent.

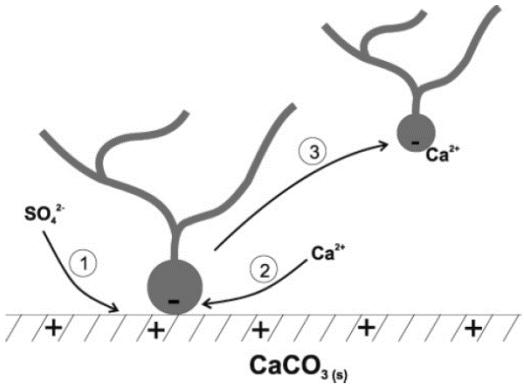

Figure 3.5:Proposed wettability alteration mechanism in chalk [68]

A study by Strand et al. (2006) [56] proposed a wettability alteration mechanism of carbonates that leads to enhanced oil recovery. They explained the mechanism as surface charge alteration; by adsorption of SO_4^{2-} with co-adsorption of Ca^{2+} on chalk- rock surface and substituting of Ca^{2+} on chalk- rock surface by Mg^{2+} because of an increase in ion reactivity at higher temperature. The experiment was performed by spontaneous imbibition of seawater into a chalk

core at higher temperatures. They proposed that sulfate ion will adsorb on a positively charged chalk surface, which will lead to the bond between negative oil component and the rock surface to deteriorate. Consequently, a decrease in the positive surface charge will allow more ions of Ca^{2+} to be able to attach to the rock surface allowing release of negatively charged oil component. At higher temperatures, these ions become more reactive with chalk-rock surface which will induce the substitution of Ca^{2+} on rock surface for Mg^{2+}.

Zhang et al. (2007b) [69] continued investigating wettability change mechanism on chalk by adding SO_4^{2-}, $Ca^{2+}$and Mg^{2+} to the imbibing brine at high temperatures. They found that Mg^{2+} at higher temperatures can substitute $Ca^{2+}$from the chalk surface, and this effect increased with increased temperatures. They reported that in order to increase the oil recovery, SO_4^{2-} must interact either with Ca^{2+}or Mg^{2+}.

Figure 3.6 shows the suggested mechanism (case A and B):

A) At low and high temperatures calcium can react with the adsorbed carboxylic group and release it from the surface
B) At high temperatures, magnesium may displace calcium- carboxylate complex

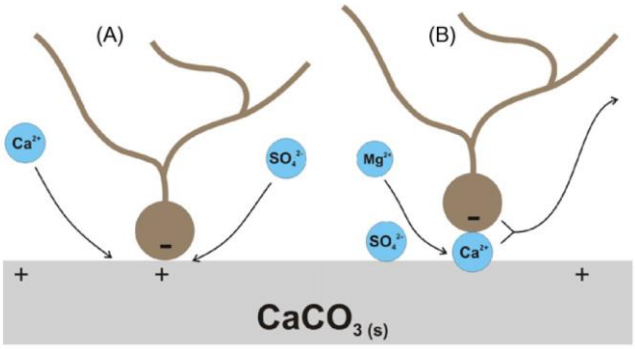

Figure 3.6: The two suggested wettability alteration mechanism in carbonates by using low salinity brine containing either SO_4^{2-} and Ca^{2+} or SO_4^{2-} and Mg^{2+} alternatively, both of them in the presence of high temperatures (>90°C) for obtaining improved water-wetness [50]

The Carboxylic group,$-COO^-$ is a strong hydrophilic group, which can create a water saturation close to the rock surface. Zhang et al. stated that it is difficult to relate this observation to the limestone since the reactivity of biogenic chalk is much higher than for recrystallized limestone.

3.7.3. Wettability Alteration: Microscopic Dissolution of Anhydrite and Calcite

In the case of rock dissolution, brine chemistry could dissolve rock minerals and affect the rock wettability.

Hiorth et al. (2010) [60] studied the influence of water chemistry on the dissolution of pure calcium carbonates to address mineral precipitation and dissolution. A chemical model was constructed that includes both bulk aqueous and surface chemistry to predict the surface potential of calcite and adsorption of sulfate ions from the pore water. In their chemical modeling they found that seawater was in equilibrium with calcite at low temperatures, but when the temperature increases calcium in seawater react with sulfate and anhydrite was precipitated. When anhydrite was formed, the aqueous phase loses calcium and need to be supplied by calcium to maintain equilibrium. The source of calcium ions came from calcite dissolution, if the calcite dissolution occurs at the place where the oil is adsorbed, then the oil can be liberated from the rock surface as illustrated in Figure 3.7, where the water-wetness increases if the process has the right temperature.

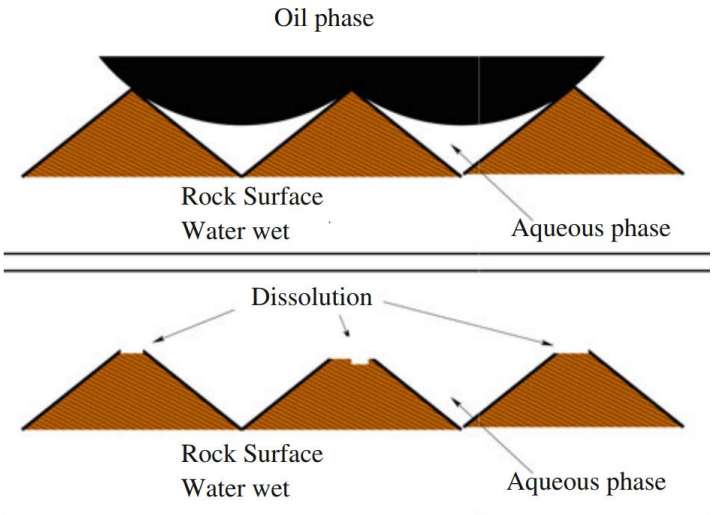

Figure 3.7: Top: Illustration of pore space, the oil is attached to the rock surface, before dissolution reaction. Bottom: Dissolution of the chalk surface occur where the oil was attached, and new water-wet rock surface has been created [60]

It was also concluded that surface potential changes (caused by injection water chemistry) are not able to explain the observed changes in the oil recovery. Chalk dissolution appeared to be the controlling factor which can explain compaction and increase in oil recovery.

Austad et al. (2011) [48] investigated low salinity water effects on carbonate reservoirs at elevated temperature. The oil recovery was tested under forced displacement using different brines. They observed an incremental oil of 1-5% OOIP as the brine ionic strength reduced and anhydrite was flushed out from the sample at the end of the experiment. They concluded that if anhydrite was present in the rock formation, then the core material will respond to low salinity flood. The incremental oil release has been attributed to wettability alteration of carbonate surface by dissolution of anhydrite.

Yousef et al.(2011) [49] studied composite cores from one of the Saudi Arabian carbonate reservoirs, as mentioned earlier. Nuclear Magnetic Resonance (NMR) results indicated that injection of different salinity concentrations were able to cause an alteration in the surface relaxation time of the carbonate rock. Hence it was able to enhance connectivity among pore systems because of rock dissolution. They suggested that the driving mechanism behind the increase in oil recovery was wettability alteration toward more water-wet state. They concluded that wettability alteration was a result of anhydrite dissolution and change in surface charge based on NMR and Zeta potential tests.

Al-Shalabi et al. (2014) [63] performed an extensive numerical work of low salinity water in carbonates including history matching of Yousef et al. (2011) coreflood experiments. They concluded that the incremental oil recovery by low salinity water in carbonates could be explained as wettability alteration caused by both change in surface charge and anhydrite dissolution, Figure 3.4. However, they also concluded that the primary contributor of incremental oil recovery based on their numerical work, was due to change in surface charge rather than anhydrite dissolution, as reported by Yousef et al. (2011).

3.7.4. Wettability Alteration: Surface-Charge change

R.Gomari et al. (2006) [79] conducted zeta potential and contact angle measurements on calcite powder and chunk calcite, to investigate the reason for wettability alteration. Ion composition effects such as sulfate and magnesium on the adsorption of different fatty acids were studied. The zeta potential measurements of chunk calcite showed that the electrical properties of pure calcite surface were changed from positively charged surface to more negatively charged surface in the presence of fatty acids. The contact angle measurements also reflected this, where the wettability increased to more water-wet state in the presence of ions such as sulfate and magnesium. They concluded that magnesium ions convert calcite surface to more water-wet state compared to sulfate, even if magnesium and sulfate ions have an affinity to calcite surface. However, magnesium ions affect the calcite stability, which may explain the higher water-wetness of the calcite surface as stated.

Zhang and Austad (2006) [71] investigated zeta potential of Stevns Clint chalk surface suspended in brine solution by changing the sulfate and calcium concentrations. This work aimed to study if sulfate and calcium ions could modify the surface charge of the chalk particles. They concluded that the zeta potential of chalk surfaces was changed by the presence of calcium and sulfate ions in the equilibrium solution. They observed that when sulfate ions exceeded calcium ions, the zeta potential becomes more negative. Thus the sulfate ions reduce the electrostatic repulsive force as it makes the rock surface more negative. They also concluded that using sulfate as a wettability modifying agent increases water-wetness, due to adsorption of sulfate onto the water-wet sites of the chalk surface, thus surface charge become less positive or negative, which enable desorption of negatively charged carboxylic materials.

Mahani et al. (2015) [80] investigated the zeta potential and contact angle measurements on limestone and dolomite rocks to study the reason for wettability alteration by low salinity water. They reported that a positive effect of low salinity exists without any rock dissolution and, it is mainly driven by the surface-charge change due to electrostatic interactions between crude oil and rock. Low salinity was able to change the wettability of limestone, which was reflected through zeta potential (from positive to more negative) and contact angle measurements (decrease in contact angle).

Sari et al. (2017) [75] investigated the zeta potential at the interfaces of oil/brine and brine/rock in aged and unaged carbonate rocks, including contact angle measurements. They removed sulfate ions from the brine used in the experiment, to study wettability alteration with low salinity brine in the absence of the latter ion. They concluded that the low salinity effect was governed by zeta potential at the interfaces of fluid-fluid and fluid-rock, rather than salinity level. They also observed that the contact angle of unaged cores increased from 30° to 50°, suggesting that the low salinity water shifted the wettability of the rock from strongly water-wet to less water-wet. Moreover, the aged core altered wettability to more oil-wet with low salinity. They observed that polarity of zeta potential shifted from positive to negative, thus as stated the wettability shifted from strongly water-wet to intermediate-wet or slightly oil-wet.

3.8. Surfactants

Surface – active agents or surfactants are composed of monomer, a nonpolar "tail" (lypophile) moiety and a polar "head group" (hydrophile) moiety, and the entire monomer is called amphiphile because of the dual nature. Figure 3.8 illustrates a surfactant molecule.

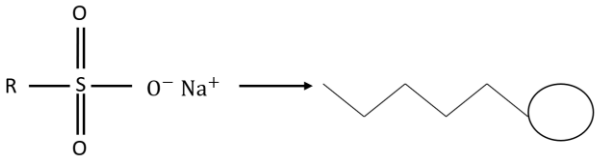

Figure 3.8: Schematic structure of a Surfactant model, molecular formula of sulfonates, where R represents the hydrocarbon group (nonpolar).

Surfactants can be divided into four groups depending on their polar moieties [15]:

- **Anionics** are the most commonly used surfactants in oil recovery since they are soluble in the aqueous phase, have good reservoir properties and low cost.
- **Cationics** are used little due to high adsorption by the anionic surfaces of interstitial clay.
- **Non- ionics** are mainly used as co-surfactants.
- **Amphoterics** have not been used in oil recovery.

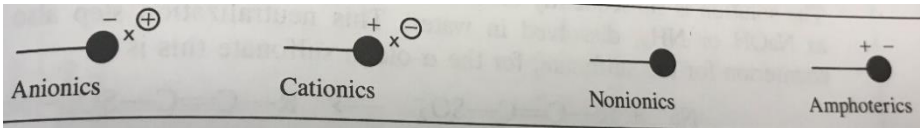

Figure 3.9: Classifications of Surfactants [15]

The primary use of surfactant flooding is to recover the capillary trapped residual oil after waterflooding. By adding a surfactant to a solution, it reduces the interfacial tension (IFT) between two immiscible phases (oil and water), hence strong reduction of IFT can mobilize the trapped oil.

When anionic surfactant is dissolved in aqueous solution, the surfactant disassociates into cation Na^+ moreover, an anionic monomer. If the concentration of surfactant increase, the lyophilic moieties begin to associate among themselves into *micelles*, with lipophilic oriented inward and hydrophilic outward as illustrated in Figure 3.10. A plot of surfactant monomers concentration versus total surfactant concentration (Figure 3.10) is a curve that begins at the origin, increases monotonically, and then levels off at *critical micelle concentration (CMC)*. Above CMC, all further increases in surfactant concentration only increase the micelles concentration and not of monomers.

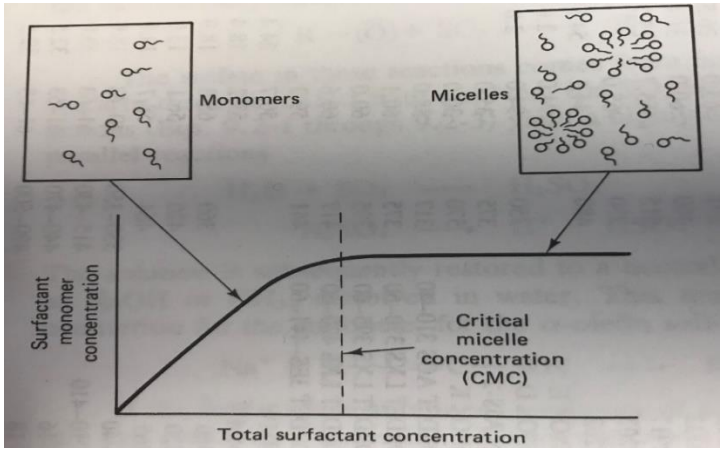

Figure 3.10: Illustration of critical micelle concentration [15]

When surfactants are added to a mixture of oil and water, the monomers will orient themselves at the interface with the lipophilic “tail” placed in the oleic phase and hydrophilic “heads” in

the water phase. Increased concentration of surfactant at the interface results in a reduction of the IFT between two phases. However, this process leads to the alteration of the solubility of the surfactant in bulk oleic and aqueous phases which might affect the interfacial tension [11].

Microemulsion forms when the surfactant mixes with oil and water above the CMC and is a thermodynamically stable liquid phase [15] ; depending on the phase behavior of the mixture, three types of microemulsion forms according to Winsor (1954) [81]. Winsor classified microemulsion containing oil, water, and surfactant as type I, type II and type III.

The salinity of the brine is the most important factor affecting surfactant-oil-brine (SOB) behavior [15]. Depending on the brine salinity, three different phase systems can form [11]:

- **Type II (-) system (Winsor type I)**, at low salinity a typical surfactant exhibits good solubility in the aqueous phase and poor solubility in the oleic phase. Thus, near the SOB, Type II (-) will split into two phases, an excess oil phase and a (water external) microemulsion phase containing brine, surfactant, and some solubilized oil. The solubilized oil is placed inside micelles causing them to swollen as illustrated in Figure 3.11. This phase behavior is called type II (-) system because;
    - Only two phases can form near oil-brine boundary
    - The tie line in the two-phase region have a negative slope
- **Type II (+) system (Winsor type II)**, at high brine salinity electrostatic forces decreases the surfactant solubility in the aqueous phase. At this stage, the SOB near the interface will split into two phases, an excess brine phase and an(oil external) microemulsion phase containing swollen micelles of surfactant with some solubilized Figure 3.11. This phase behavior is called type II (+) system because;
    - Only two phases can form near oil-brine boundary
    - The tie line in the two-phase region has a positive slope
- **Type III system (Winsor type III)**, at intermediate salinities a third microemulsion phase occurs. The overall composition of the three-phase region separates into excess oil and brine phases, and into a microemulsion phase whose composition is represented by the invariant point as illustrated in Figure 3.12. This type has two IFTs; between oil and microemulsion and between brine and microemulsion. Experimental studies have shown that lowest interfacial tensions are obtained at these conditions, which makes phase state the most attractive for oil recovery by surfactant flooding[11].

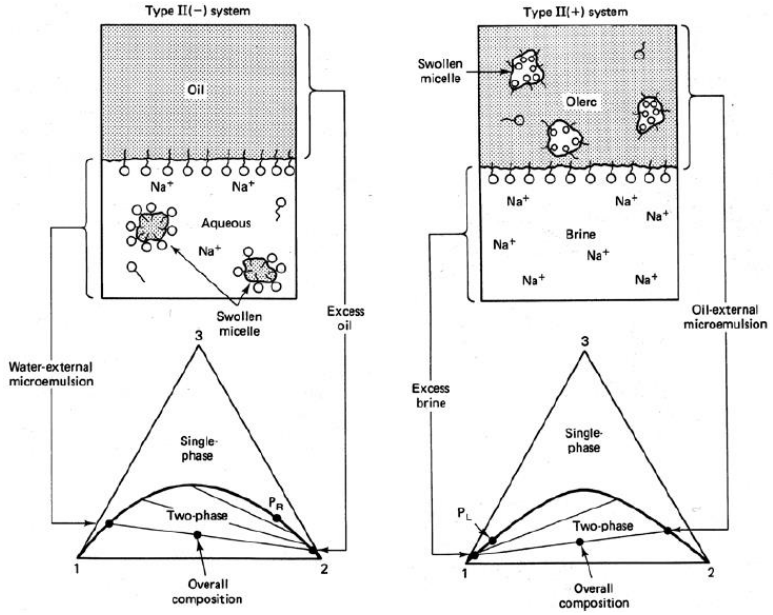

Figure 3.11: Illustration of type II(-) and II(+) [15].The numbers in the corner of the ternary diagram 1, 2 and 3 represent brine, oil and surfactant pseudo component

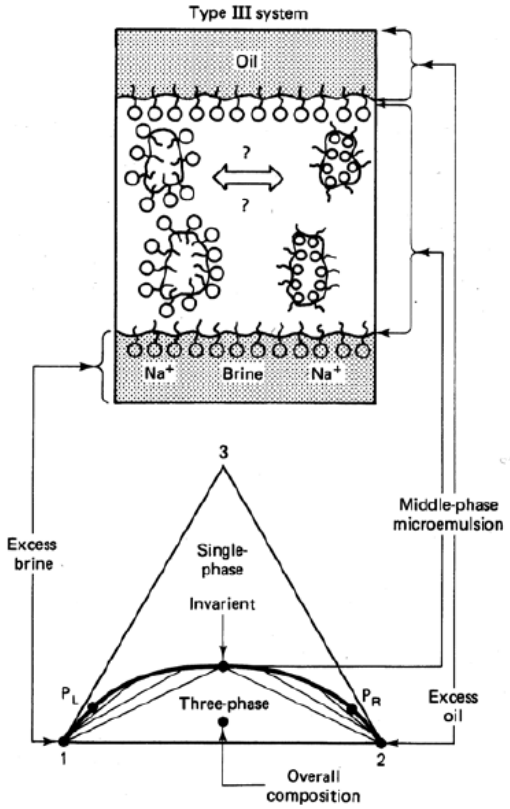

Figure 3.12: Illustration of type III. The numbers in the corner of the ternary diagram 1,2 and 3 represent brine, oil and surfactant pseudo component [15].

Salinity is the main important factor affecting surfactant-oil-brine (SOB) behavior; however as stated by Lake et al. (2010) [15], other parameters can affect the SOB, such as the type of salt, oil properties, temperature, pressure, and ratio between water and the oleic phases.

3.9. Low Salinity Surfactant Flooding

Injection of brine with low salinity is an essential parameter in surfactant flooding. Research has shown that combining surfactant with low salinity brine benefits increased oil recovery.

Alagic and Skauge (2010) [82] conducted coreflood experiments on outcrop sandstone cores, to investigate the effect of low salinity brine injection with surfactant flooding. They observed a recovery of 90% of OOIP when injecting anionic surfactants in a tertiary mode. This behavior was confirmed in three experiments. They also reported that the effect of surfactant injection as a tertiary recovery mechanism was significantly reduced when no prior pre-flush of low salinity brine was done. The increased effect of surfactants was attributed to destabilization of oil layers caused by a change in brine salinity and simultaneous mobilization of residual oil at low IFT. During surfactant flooding the surfactants formed a Winsor type I microemulsion, giving low retention. This in combination with high recoveries promotes this hybrid EOR method as an attractive, economical method.

Tavassoli et al. (2015) [83] introduced a mechanistic model to study the combined effect of low salinity and surfactant flooding. They investigated the combined effect by using UTCHEM-IPHREEQC simulator. The experiment by Alagic and Skauge [82] were used to evaluate oil recovery, effluent ionic composition, and pressure gradient data. An excellent history match was obtained between the simulation data and the experimental data from Alagic and Skauge for low salinity surfactants floods. Moreover, they performed several simulations from which they concluded that the high salinity surfactant flood recovered 100% of OOIP within 2 PV better than the low salinity surfactant flood (92.3% OOIP). They also concluded the importance of surfactant selection and design rather than the benefits of low salinity on a surfactant flood.

Alagic et al. (2011) [84] performed core displacement tests on aged and unaged Berea cores, testing the effect of low salinity surfactant flooding on longer cores to investigate the effect of aging on oil recovery. The studies showed high incremental recoveries for both unaged and aged cores. The highest oil recovery was observed on the aged cores, for low salinity flooding and combined low salinity with surfactant flooding. This indicates that less water-wet cores could have more unstable oil layers with larger degree of continuous oil. They also reported that the high recovery by surfactant was believed to be more of avoiding re-trapping of oil at lower capillary pressure than the classical oil mobilization as an effect of high capillary number.

Spildo et al. (2012) [85] investigated the effect of combining low salinity water (LSW) injection and reduced capillarity by surfactants regarding EOR additional oil recovery and cost efficiency. Berea sandstone cores were used for this experiment, and the brines had TDS of 36494 ppm seawater (SSW) and 3002 ppm (LSW). The cores were first pre-flushed with SSW to establish Sor, followed by an LSW flood to create a low salinity environment. When the cores were injected with LSW in a tertiary mode, a limited production was noticed. To investigate the effect of low salinity surfactant (LSS) injection, the cores were injected with a LSS after LSW. Spildo et al. concluded that surfactant injection of Winsor I phase behavior (lower phase microemulsion) at low salinity yields good recovery and low surfactant retention. Also, intermediate-wet conditions seem to be more favorable compared to water-wet conditions.

Johannessen and Spildo (2013) [86] investigated the effect of combining surfactants with low salinity injection. Their experiment was conducted using aged Berea sandstone cores, and synthetic seawater (SSW), 43% diluted SSW (Optimal salinity surfactant, OSS) and 7% diluted SSW (LS). The LS brine showed insignificant additional oil recovery on Berea sandstone cores compared to SSW alone. Injecting surfactants in tertiary mode gave higher oil recoveries for 7% SSW than what would be predicted by the capillary number relationship. It was also observed that moderate reduction in IFT under low salinity conditions gave the same oil recovery as ultralow IFT gave for higher salinities. Also, it was observed that flooding in low salinity environment had less surfactant retention compared to higher salinities, making it more economically feasible.

Khanamiri et al. (2015) [87]) conducted several corefloods on Berea sandstone cores to study the effect of surfactant injection and surfactant combined with low salinity brine (LS). They concluded that tertiary injection of low salinity surfactant after establishing low salinity environment in a secondary mode is more efficient, compared to high salinity environments.

3.10. Polymer

Polymer flooding is a chemical EOR method where polymer, which is long repetitive (monomers) chains of high molecular weight linked by covalent bonds, is added to the injected water to:

- Increase the viscosity of water
- Reduce relative permeability to water (displacing phase)

Decreasing relative permeability to water will lower the mobility ratio, M, which will increase the volumetric sweep efficiency and achieve increased oil displacement efficiency. Polymer flooding will be favorable in reservoirs where the oil viscosity is high or in heterogeneous reservoirs where the permeability contrast is large.

There are two types of water-soluble viscosity enhancing polymers use for EOR purposes; *synthetic polymers* and *biopolymers*. Biopolymers are biological polymers formed through polymerization of saccharide molecules in fermentation processes. Among biopolymers, Scleroglucan and especially Xanthan polymers are used in EOR applications. Both polymers have a helical, rodlike structure and are extremely pseudoplastic with high viscofying effect and the viscosity is almost insensitive to salinity [11].

The most used polymer in filed applications are synthetic polymers, such as acrylamide-based polymers, *polyacrylamide*, PAM, or *hydrolyzed polyacrylamide*, HPAM, due to their relatively low price and availability from industries. The molecular weight range for HPAM polymers utilized for EOR purposes are commonly in the range from 2-20 x 10^6 Dalton [88].

The name HPAM comes from polyacrylamides that have undergone partial hydrolysis, which causes anionic (negatively charged) carboxyl group ($-COO^-$) to be scattered along the backbone chain. A typical hydrolysis degree is 15- 35% [89] of the acrylamide monomers. Hence the HPAM is negatively charged , which accounts for many of its physical properties, such as water solubility, viscosity and retention [89]. According to Shupe (1981) [90], if hydrolysis degree is too low, the polymer will not be soluble in water. On the other hand, if hydrolysis is too high, its properties will be sensitive to salinity and hardness.

Synthetic polymers are usually highly flexible molecules in which the polymer backbone consists of a relatively chemically stable carbon molecular chain with single and flexible carbon-carbon bonds. The chain water-soluble chemical groups (e.g., amide groups) on the molecule make the polymer molecule soluble in water [91]. Figure 3.13 shows typical molecular structures of unhydrolyzed polyacrylamide (PAM) and hydrolyzed structure (HPAM).

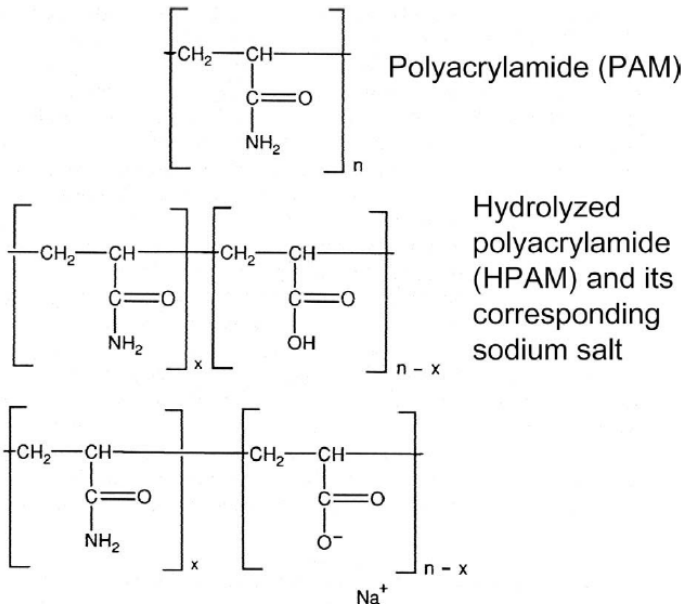

Figure 3.13: Chemical structure of PAM and HPAM polymer molecules [91]

PAM is not a good viscous enhancement agent and is not propagated well through sand reservoirs compared to HPAM when dissolved in a low salinity environment [91]. The reason for this is that PAM is slightly positively charged (cationic) in an acidic or neutral pH environment, which makes PAM adsorb onto reservoir rock surface, especially sandstone surface.

As seen in Figure 3.13, HPAM comes in two molecular forms regarding the carboxylate groups. In low salinity brines, the electrostatic repulsion between the backbone negatively charged carboxyl groups (COO^-) causing the polymer chains to extend in a stiff rodlike molecule which gives a strong viscofying effect. High salinity brines cause the electrostatic field around the carboxylate groups to shrink and allows the HPAM molecule to become more balled-up form because of a high degree of electrostatic repulsion between the negatively charged carboxylate groups on the polymer's backbone as shown in Figure 3.14. Hence, increasing solution salinity and hardness (in particular Mg^{2+} and Ca^{2+}) reduce the backbone repulsions due to shielding of the negative charges. This leads to a flexible coiled conformation, which reduces viscosifying power of HPAM as illustrated in Figure 3.14.

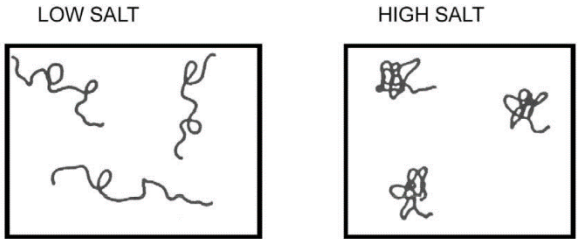

Figure 3.14: Schematic illustration of the effect of salinity on the molecular conformation coil such as HPAM [91]

Polymer flow in porous media is complex and involves several mechanisms as it travels the tortuous pore network of a porous media consisting of variation in both pores and pore throats. Hence the shear rate will depend on the solution velocity and the properties of the porous medium such as porosity and permeability [88]. When dealing with polymer flooding in a porous medium, one has to deal with average values of viscosity, *apparent viscosity*. Since the effective shear rate $\dot{\gamma}$ is proportional to flow rate [92], some models tried to connect $\dot{\gamma}$ to flow rate and the propeties of the porous medium, Chauveteau et al. (1984) [93] defined the active (equivalent) porous medium shear rate, based on a simple capillary bundle model derived from the Hagen- Poiseuille equation for a flow in capillary bundle as :

$$\dot{\gamma} = \alpha \frac{4u}{\sqrt{8\varphi k}} \tag{3.4}$$

Where α is a constant related to pore geometry and type of porous medium, and k is the water permeability, φ is the porosity, and u is the solution velocity. For a bundle of capillaries α=1, for unconsolidated sand α vary from 1.05 to 2.5, and for consolidated sand, α varies from 1.4 to 14.

3.11. Polymer Retention

During flow in porous media, interactions between polymer molecules and the porous medium cause polymers to be retained within the medium [88]. As a consequence, polymer solution viscosity decreases leading to a reduced flooding efficiency. Retention of the polymer may contribute positively to the flooding process due to a lowering of the permeability. However, the decrease in bulk polymer viscosity tends to reduce oil recovery despite the permeability reduction. Polymer retention varies with polymer type, concentration and molecular weight, rock characteristic and composition, and brine properties (salinity, hardness, pH) [15].

Three central polymer retention mechanisms which are proposed in the literature [88] (illustrated in Figure 3.15):

- Adsorption
- Mechanical entrapment
- Hydrodynamic retention

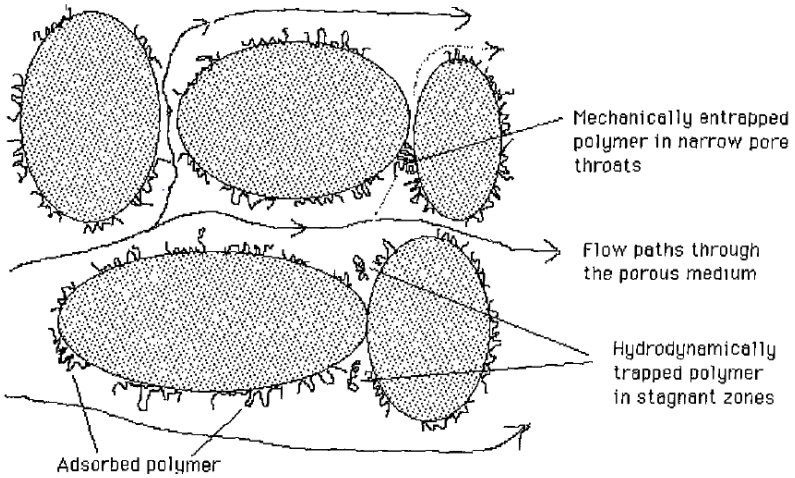

Figure 3.15: Schematic of polymer retention mechanisms [88]

Adsorption of the polymer is the result of interactions between polymer molecules and rock surface causing polymers to be bound to the rock by physical adsorption mechanisms (van der Waal forces and hydrogen bonding). The amount of adsorption depends on surface area; the larger the surface area available, the higher the adsorption levels. Further, polymer adsorption results in decreased rock permeability dependent on initial permeability and thickness of the adsorbed layer. The thickness of the adsorbed layer, in turn, is dependent on the polymer molecular weight (i.e., size of polymer coil) and polymer concentration. Adsorption of polymer on the pore walls will also act to delay the propagation of the polymer solution within the porous media. Xanthan show less adsorption than HPAM in porous media due to a reduced degree of positively charged groups in its molecular structure [88]

Mechanical entrapment of polymers arises when large polymer molecules become lodged in narrow flow channels (e.g., pore throats). Therefore, mechanical entrapment is dependent on the molecular sizes present in the polymer solution [64, 91]. Mechanical entrapment also dependent on the rocks pore size distribution and is a more likely mechanism in low-permeability formations. A consequence of mechanical entrapment is a build-up of material close to the injection well leading to pore blocking and well plugging.

Hydrodynamic retention is a less known mechanism but is believed to be the result of polymer molecules becoming temporarily trapped in stagnant zones [88] as illustrated in Figure 3.15. However, polymer retention resulting from hydrodynamic retention is more prevalent in core experiments and is thought to be of neglecting importance in field applications.

3.12. Low Salinity Polymer Flooding

As mentioned before, HPAM is more stable in low salinity brine environments compared to high salinity environments.

Ayirala et al. (2010) [94] addressed the advantages of using low salinity water for polymer flooding. They analyzed the effect of low salinity and polymer flooding applications on offshore

projects. They concluded that polymer flooding with low salinity water is more economical compared to seawater polymer flooding. A change from seawater to low salinity brine was anticipated to contribute to a 5-10 times reduction in polymer consumption due to less retention at low salinities.

Kozaki (2012) [95] investigated the effect of low salinity polymer injection in Berea sandstone cores. He reported an increase in recovery of injecting low salinity brine compared to injecting high salinity brine. The low salinity polymer floods were performed in secondary mode and tertiary mode following a high salinity flood. The result of low salinity polymer flooding showed a reduction in residual oil saturation by 5-10% over that of the secondary high salinity waterflooding. It was also noticed that the ultimate recovery was achieved with fewer pore volumes of injection than in waterfloods (≈1.5 PV).

Mohammadi et al. (2012) [96] developed a mechanistic model for low salinity polymer flooding with relative permeabilities as a function of water salinity. Simulating the effects of low salinity polymer injection in secondary and tertiary processes, they demonstrated an enhancement in oil recovery and timing by low salinity polymer flooding. This behavior was attributed to the improvement in fractional flow behavior when injecting low salinity polymer. One third or less polymer is required for polymer flood when using low salinity brine compared to high salinity brine, which reduced 5- times in chemical cost when the polymer was added to low salinity water compared to high salinity.

Shiran and Skauge (2013) [97] performed coreflooding experiments on outcrop Berea sandstone, to investigate the effect of low salinity brine and low salinity polymer solution on oil recovery. The oil recovery by polymer injection was improved significantly when the low salinity environment had been established at S_{wi} (secondary-mode) rather than S_{or} (tertiary-mode, after seawater residual oil saturation). This result is not consistent with the work done by Mohammadi et al. (2012) [96], where they claimed that behavior of combined low salinity waterflood and polymer flood process is more effective in tertiary mode than the secondary mode.

Shiran and Skauge also noticed the importance of the initial wettability, as intermediate-wet cores responded better than water-wet cores.

An analytical study that supported the work by Shiran and Skauge was performed by Khorsandi et al. (2016) [98]. They studied the behavior of low salinity waterflooding and low salinity polymer flooding in sandstones during secondary and tertiary mode, to investigate the effect on oil recovery. As illustrated in Figure 3.16 their simulation results matched the work done by Shiran and Skauge, where oil recovery was improved when the low salinity environment had been established in secondary-mode rather than tertiary-mode.

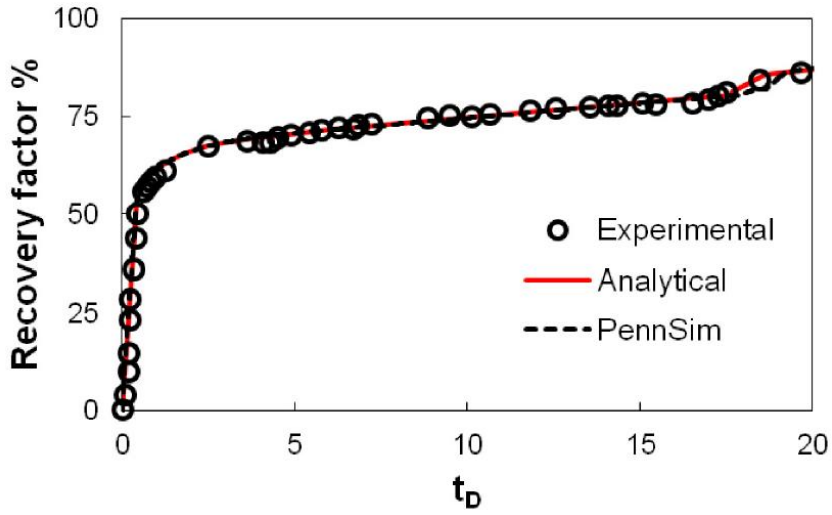

Figure 3.16: Illustration of the match between analytical solutions and experimental data for low salinity polymer flooding experiments by Shiran and Skauge (2013) [98]

Han and Lee (2014) [99] conducted a sensitivity analysis by numerical simulation to study the relationship between low salinity waterflooding and polymer flooding. The analysis included parameters such as slug size, solution salinity, and polymer viscosity, to verify which of these parameters have the most significant influence in a reservoir. The analysis indicated that efficiency of polymer flooding was significantly improved by using low salinity water in the polymer solution. The results of slug size and polymer viscosity parameters showed an increase in oil recovery obtained only with low salinity polymer flooding.

4. Experimental Procedures and Equipment

4.1. Chemicals, Fluids and Core Material

4.1.1. Fluid Properties

The composition of all three brines used in this thesis is listed in Table 4.1. Formation water (FW) was used for core saturation and connate water in all the core plugs. High salinity (HS) and low salinity (LS) brines were used during the different flooding steps. After preparation, all three brines were put on a magnetic stirrer to dissolve the salts for 24 hours before it was filtrated using a 0.45µm vacuum filter to remove unwanted particles. Then the pH measurement was performed (Table 4.2).

Table 4.1: Brine ion composition and salinity

	Concentration [ppm]		
Ion	**LS**	**HS**	**FW**
Na^+	87	13001	43732
K^+	4	468	0
Mg^{2+}	2	1574	2847
Ca^{2+}	1	493	12709
Cl^-	143	23415	97994
SO_4^{2-}	2	3282	205
HCO_3^-	2	171	142
TDS	**241**	**42404**	**157629**
I [mol/L]	**0.0042**	**0.8689**	**3.6592**

4.1.2. Crude Oil and Tagged Crude Oil

Light crude oil from the Middle East was used for aging the core plugs. After aging, the crude oil was exchanged with a tagged crude oil. The tagged oil was prepared by diluting crude oil with iodobenzene to increase the x-ray contrast between the oil phase and brines phases during flooding experiments. The tagged oil contained 80 wt% of crude oil and 20 wt% iodobenzene. The mixture was stirred on a magnetic stirrer for 24 hours before placed in a cylinder for oil exchange (chapter 4.2.9). The oil properties are given in Table 4.2

Table 4.2. Viscosity and pH properties of fluids used in experimental work

Fluid	**Viscosity [cP] at ambient temperature**	**Viscosity [cP] at 90°C**	**pH at ambient temperature**
Formation water	1.40	0.53	6.60
High Salinity	0.95	0.65	7.90
Low Salinity	0.95	0.48	7.70
Tagged crude oil	4.15	1.20	-
2000 ppm HPAM	84.40	59.1	6.70
Surfactant XOF 25S	1.68	0.40	4.80
Primol 542	250	-	-

4.1.3. Preparation of Surfactant Solution

The surfactant used in this study, are of type sodium alkyl benzene sulphonate from Huntsman. The percentage of active matter in the surfactant was 25.6%. The surfactant solution was prepared by mixing 1 wt% XOF 25S surfactant with low salinity brine (LS). The mixture was stirred on a magnetic stirrer for 2 hours before use. pH and viscosity measurement was performed, Table 4.2.

4.1.4. Preparation of Polymer Solution

The polymer used in this study are of type superpusher SAV 10 from SNF Floerger. The polymer has thermal stability up to 120°C. These are terpolymers containing N-Vinyl-Pyrrolidone that can sustain high temperatures and are efficient in high salinity brines [100]. The polymer solution was prepared, by dissolving partially hydrolyzed polyacrylamide (HPAM) in low salinity brine. First, a stock solution was prepared (mother solution had a concentration of 5000 ppm). Then the stock polymer solution was diluted to desired polymer concentrations (e.g., 2000 ppm in this study). The preparation of polymer solution took about two days. pH and viscosity measurement was performed, see Table 4.2.

The following steps summarize the preparation of the polymer stock solution.

- 500g of LS brine was added to a 800mL beaker. The beaker was placed on a magnetic stirrer, and the speed was set to create a vortex of 75% towards the bottom of the beaker.
- 2.788g of HPAM polymer weighed in a tray was added to the brine, by carefully sprinkling the polymer powder just below the vortex shoulder. This step was conducted slowly to avoid creation of any lumps in the solution.
- The mixture was stirred for three hours at that speed before the speed was reduced to lower rate where the polymer particles still float in the solution, and the beaker was covered with perforated parafilm and left for 24 hours.

The viscosity of the solution was then measured using cone and plate geometry on a Malvern Kineuxus rheometer. The solution was then placed in the fridge to slow down chemical degradation.

The activity of HPAM powder is approximately 90 %. The final concentration of ppm is, therefore.

$$C_{polymer} = 10^6 x\ W_{poly}\ x\ 0.90\ /\ (W_{poly}+W_{brine}) \quad (4.1)$$

The diluted polymer solution was prepared using the procedure below.

- A coated magnet was added to Duran flask with half of the brine. The polymer from the stock solution was added by weight to the Duran flask. The rest of the brine was added so that the concentration of the polymer matches the final concentration wanted.
- The solution was put on a magnetic stirrer at low speed < 150 rpm, sealed by parafilm and cork and left stand overnight. The solution was then filtrated using 40 μm filter and vacuum apparatus before using it for viscosity measurements and flooding process.

It is essential to consider these aspects under preparation of the polymer solution; such as unnecessary exposition to air, iron contamination, shear degradation, sample homogeneity, and creation of microgels.

4.1.5. Expansion Factor of Tagged Crude Oil and Brine

To determine the expansion factor of tagged crude oil, HS brine, and LS brine at reservoir conditions, three samples of fluids were placed in a heating cabinet for three days at 90°C. The initial volume of the three samples was 15mL. The expansion factor was calculated as the ratio between the changes in the volume of the fluids at 90°C to the volume at room conditions. The expansion factor for tagged oil was used to calculate the amount of oil produced at reservoir conditions.

Table 4.3: Fluid expansion factor at 90°C of tagged oil, HS brine, and LS brine

Fluid	**Initial Volume [±0.3mL]**	**Final Volume [±0.3mL]**	**Expansion factor [±0.04mL]**
Tagged crude oil	15	15.6	1.04
High Salinity	15	15.3	1.02
Low Salinity	15	15.4	1.03

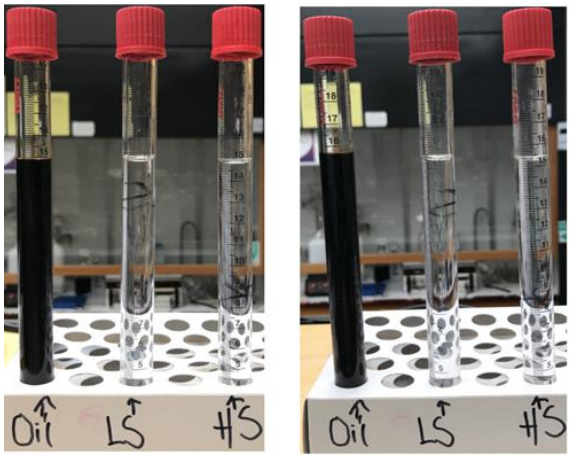

Figure 4.1: Illustration of the fluids before placed in the oven (left) and after placed in oven for three days (right)

4.1.6. Core Material

Indiana Limestone core plugs were selected in this study to perform imbibition and flooding experiments. Based on x-ray diffraction (XRD) analysis by Chrucher et al. (1991) [16], Indiana limestone contains 99% Calcite and 1% Quartz.

Four short cores (5 cm in length and 3.7 cm in diameter) designated as S1-S4 were used to perform imbibition tests to examine wettability state of the cores in aged and unaged condition. The cores S2-S4 were cut from the same batch, while core S1 and S3 selected from a different batch. The long core plugs (15 cm in length and 3.7 cm in diameter) were designated as L1-L4. L3 and L4 were from the same batch, while L1 and L2 selected from a different batch. The long cores were used in flooding experiments. The petrophysical properties of the cores used in this study are given in (Table 5.1 ,Chapter 5.1)

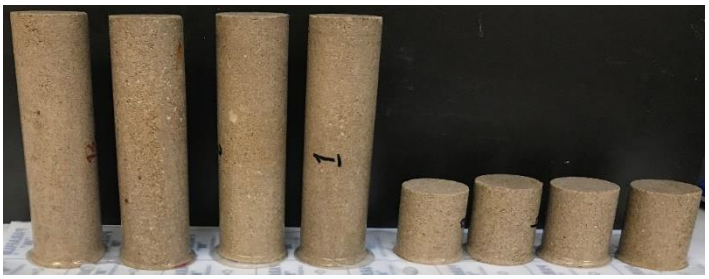

Figure 4.2: Indiana Limestone core plugs used in the experiments.

4.2. Core Preparation and Waterflooding

4.2.1. Core Preparation

The core plugs were cut from a whole core and dried in an oven at 80°C for 48 hours. The length and diameter of the cores were measured using a caliper. The cores were then weighed in dry conditions and later vacuumed until they reached low vacuum pressure (< 1.0 Torr).

4.2.2. Porosity Measurements

The cores were saturated with formation brine after they were vacuumed. The porosity of the cores was determined using the difference in weight of the cores in dry and saturated conditions. The cores were left in formation water for one week to achieve ionic equilibrium.

4.2.3. Permeability Measurements

All cores were put into Hassler-type core holders with 30 bars confining pressure. After the porosity measurements, the absolute permeability to formation water was measured. The cores were flushed with 2 PV of formation water before conducting permeability measurements. Five injection rates of formation water were applied, and the pressure drop was recorded for each injection step when a steady state condition was achieved. By plotting differential pressure versus injection rate, the slope of the curve was achieved as illustrated in Figure 4.3. By knowing the brine viscosity, length of the core and cross-sectional area the permeability can be calculated using equation (2.5) The back pressure was maintained constant at 20 bar.

The same method was also used for calculating oil permeability and water relative permeabilities later in this study.

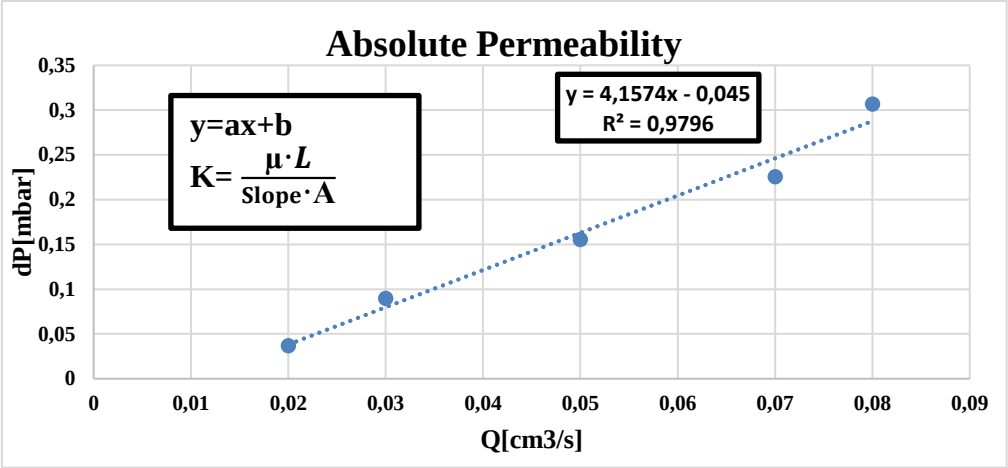

Figure 4.3: Illustration of permeability calculations

4.2.4. Dispersion Test

Dispersion is the study of effluent concentration change during a miscible displacement. The idea is to inject a tracer solution that displaces the fluid in the core and then measure the electrical conductivity of the core. The test was performed to obtain information about fluid transport properties and pore structures.

After the absolute permeability measurements, the cores were saturated with 100% FW water. A solution of 10 wt% FW was prepared by dilution of FW with distilled water to make the tracer solution. The core was placed horizontally and injected with tracer at a constant flow rate of (0.2 mL/min) to displace the FW in the core (laminar flow). The conductivity cell used for dispersion test was calibrated first with the FW representing as 100% - and the tracer representing as 0%. 2.5 pore volume (PV) tracer was injected into the cores.

A plot of brine normalized concentration (C/Co) was plotted versus pore volume injected in order- to investigate the dispersion characteristics based on measuring electrical conductivity.

4.2.5. Phase Behavior Study of Crude Oil in Contact with Brine of Different Salt Concentrations

To investigate the possibility of formation of an emulsion between oil and HS and LS brines, seven samples of oil-brine mixtures composted of 50% crude oil and 50% of brine with different concentrations were prepared and examined at room condition as well as 90˚C.

Seven samples were kept at room temperature, and seven samples were placed in an oven at 90˚C. The samples were shaken gently every day and left to equilibrate for seven days. The oil-brine mixtures did not show any sign of emulsion formation at room condition and 90˚C for the different brine concentrations (Figure 4.4). Table 4.4 summarizes the different brine solutions used for phase behavior studies.

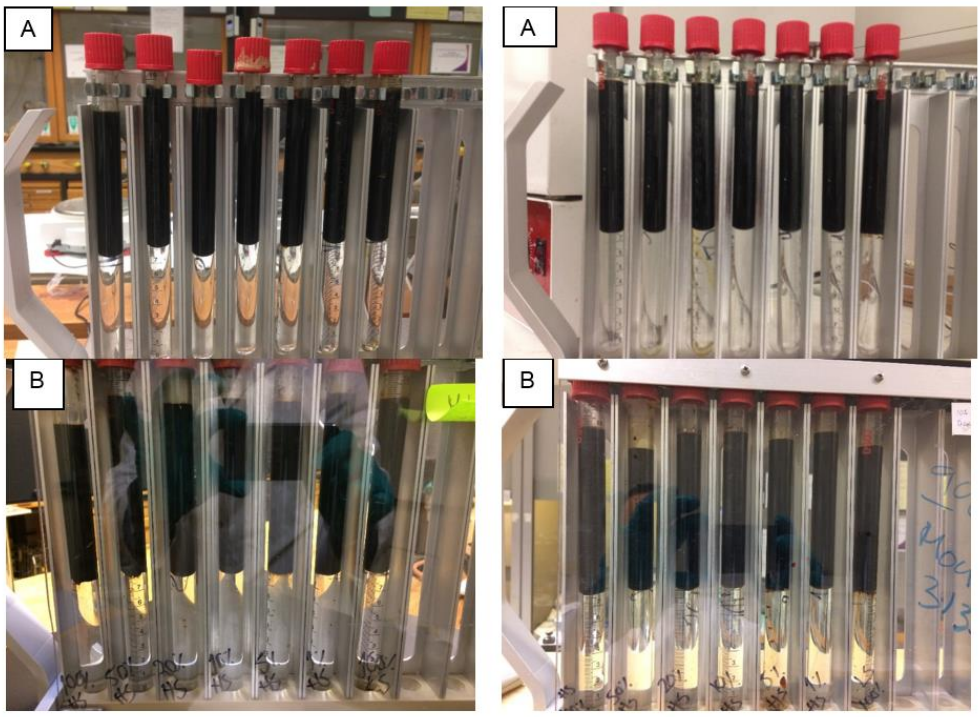

Figure 4.4: Crude oil-brine phase behavior A) from left at room temperature, and right after seven days. B) from left at 90˚C, and right after seven days

Table 4.4: Brine concentration used for phase behavior studies

Brine	wt% FW
HS	100
HS	50
HS	20
HS	10
HS	5
HS	1
LS	100

4.2.6. X-ray In-Situ Saturation Monitoring

The four long cores after each flooding sequence were placed in a 2-D X-ray cabinet to detect saturation change or possible saturation re-distribution in the cores. The 2-D x-ray cabinet consists of a generator, detector, and data acquisition system. The core samples were scanned from the top (outlet) to bottom (inlet) as shown in the figure below, generating (1D) intensity profile. A plot of x-ray count number versus core length was made to investigate the saturation change along the cores as illustrated in Figure 4.5.

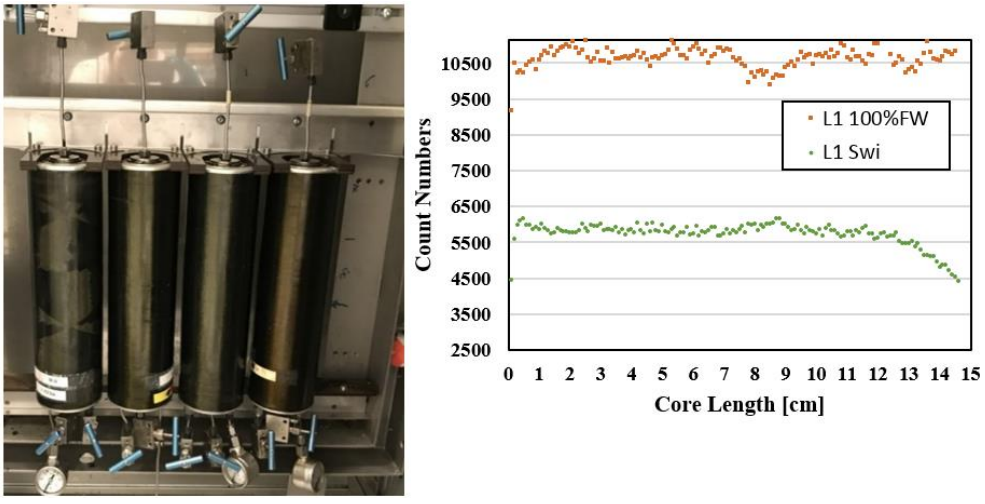

Figure 4.5: Illustration of the cores in the X-ray apparatus (left), and a plot of count numbers versus core length (right) for core L1 at 100% FW saturation and irreducible water saturation Swi.

4.2.7. Drainage

The formation water-saturated cores were flooded with Primol 542 oil to establish the irreducible water saturation. Primol 542 oil, which is highly viscous oil, was injected gravity stable from the top at a low flow rate to displace the brine efficiently. The flow rate was increased stepwise until no more water was produced, and the irreducible water saturation was achieved.

To reduce the capillary end-effects, the cores were flooded with Primol 542, one pore volume in the other direction, or until no water was produced. To calculate the oil permeability at S_{wi} the same procedure as the absolute permeability was used.

After the measurement of the oil permeability at irreducible water saturation, the primol 542 oil was exchanged with Middle East crude oil (MEo). This step was done in a heating cabinet at a temperature of 50°C to achieve better viscosity contrast between the oils and to avoid precipitation of oil components in the crude oil. MEo was flooded with very low flow rate for two PV, and then the flow rate was increased stepwise. The cores were flooded in both directions.

4.2.8. Aging and Wettability Alteration Procedure

After oil exchange, two short cores and two long cores were placed in a heating cabinet for three weeks at a temperature of 90°C. The purpose of this procedure was to achieve different wettability states other than water-wet condition. To control the overburden pressure and avoid possible damage to the core plugs due to pressure increase during the aging period, a cylinder filled with Marcol-152 at the bottom and nitrogen at the top with a pressure of 30 bars, was connected to the confining pressure port of the core holder. A back-pressure regulator of 20 bars was connected to the outlet of the set-up to ensure that no gas phase exists in the flow system and only liquid phase flows in the core and tubings.

The reason for aging the cores at high temperature is to enhance and increase the speed of reaction between crude oil components and core material. After one week of the wettability alteration period, crude oil inside the cores was replaced by fresh crude oil at a low injection rate of 0.01 mL/min and stopped before the last week of the aging period. The cores were

connected in series so that the crude oil passed all the four cores. After the aging period was completed, oil permeability after aging was measured to compare with oil permeability before aging. A reduction of 27-50% in oil permeability was observed in the aged core plugs which could indicate wettability alteration in these cores.

4.2.9. Exchanging the Crude Oil with Tagged Crude Oil

After the cores were aged, and oil permeability measured with crude oil (MEo), the MEo was exchanged with tagged crude oil. MEo was tagged with iodobenzene to increase the density of the crude oil. The purpose of this step was to improve the density contrast between the formation water and the crude oil phases to get a better X-ray measurement of the local saturation distribution in the core plugs.

The exchange of the MEo with the tagged oil was done with the cores inside the core holder. The core holder was placed vertically with an injection of tagged oil from the top with low flow rate (0.1 mL/min). The core was first flushed by one PV, and after one PV the injection rate was increased to 0.5 mL/min and up to 5 mL/min. Then the direction of injection was changed to avoid any capillary end-effects. Two PV were injected in the other direction with the same injection rate. (Total of four PV).

After the oil was exchanged, the cores were placed in a 2-d x-ray cabinet to detect saturation changes. The saturation of the cores was at irreducible water saturation (Swi).

4.2.10. Spontaneous Imbibition Test

Brine imbibition test was performed to examine wettability states of aged and unaged core plugs. Aged and unaged short cores at irreducible water saturation were individually placed in an Amott cell filled with high salinity (HS) brine. Oil production by brine imbibition was recorded for 30 days before the brine was changed to low salinity brine (LS) for another 30 days. The experiment was conducted at ambient temperature. The start time of the experiment was recorded as soon as the core was placed in the Amott cell. The produced oil by spontaneous imbibition was recorded visually at the top of the cell. The oil recovered was plotted as a function of time as a percentage of OOIP.

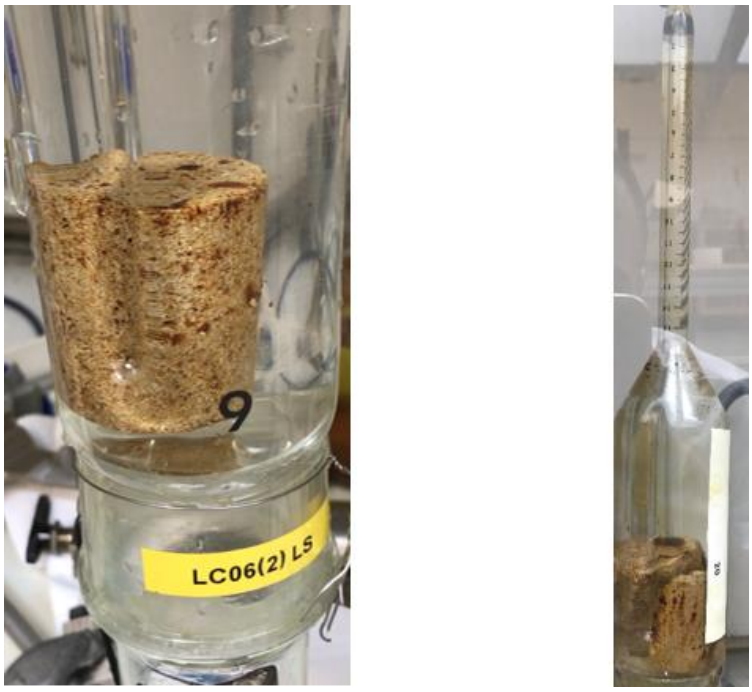

Figure 4.6: An example of spontaneous water imbibition of short cores. Notice that short core S2 was crushed (right)

4.2.11. Core Flooding Experiment (short cores)

When there was no oil production due to low salinity brine imbibition, the cores (S1, S3 and S4) were removed from imbibition cell and mounted in Exxon core holders. Waterflood experiment was conducted at ambient temperature using low salinity brine. The injection rate was 0.1→0.5→1mL/min. The LS brine was injected until WOR was very high, and produced oil was insignificant. Pressure changes were continuously monitored with FUJI pressure transducer and logged during injection. Volumetric production profile of different phases from all floods was acquired by collecting the effluents using Foxy Jr fraction collector equipped with 20x14mm test tube racks. At the end of the experiments, the effective water permeability was measured with LS brine by decreasing injection rates to not mobilize more oil. The cores were connected to a confining pressure of 30 bar and back pressure of 20 bar.

4.2.12. Core Flooding Experiment (long cores)

Four core floods including two aged and two unaged cores were performed in this study. The flooding experiments were performed in an oven at a temperature of 90°C and consisted of five flooding sequences. The experimental setup and procedure were similar for all sequences, but with different injection fluids. The flooding sequences started with an injection of high salinity brine (HS), followed by, low salinity brine (LS), low salinity surfactant (LSS), low salinity polymer (LSP) and finally a slug of low salinity brine (LS).

Before starting with the waterflood experiment, cores were flooded with tagged oil at a low flow rate (0.01mL/min) for 24 hours inside the oven at 90°C. The reason was to displace oil with fresh oil and to obtain equilibrium state in the flooding system. The cores were connected to a confining pressure of 30 bar and back pressure of 20 bar as mentioned earlier.

All experiments started with the injection of high salinity brine (HS) as secondary mode waterflood. The injection stopped when no significant oil was produced. The core flooding was continued with an injection of low salinity brine (LS) as tertiary mode followed by 0.5 PV low salinity surfactant (LSS), 2 PV low salinity polymer (LSP) and finally an injection of 3 PV low salinity brine as chase water. The injection rate was kept constant at 0.1mL/min. Pressure changes were continuously monitored with FUJI pressure transducer and logged during injection. Volumetric production profile of different phases from all floods was acquired by collecting the effluents using Foxy Jr fraction collector equipped with 20x14mm test tube racks. At the end of the experiments, the effective water permeability was measured with LS brine by decreasing injection rates to not mobilize more oil (0.1, 0.08, 0.06 and 0.04 - mL/min). The effective water permeability was measured at 90°C and ambient temperature, and the end point relative permeability was calculated.

After each sequence the heat was turned off, to reach ambient temperature. Then x-ray scan was performed to detect the saturation changes inside the core. After x-ray scan, the core was put back in the oven for 24 hours at 90°C before the next sequence of flooding.

These experiments aimed to examine the oil recovery efficiency during tertiary low salinity waterflood, low salinity surfactant, and low salinity polymer in carbonate rock samples at different wettability states. The experimental setup is as illustrated in Figure 4.7.

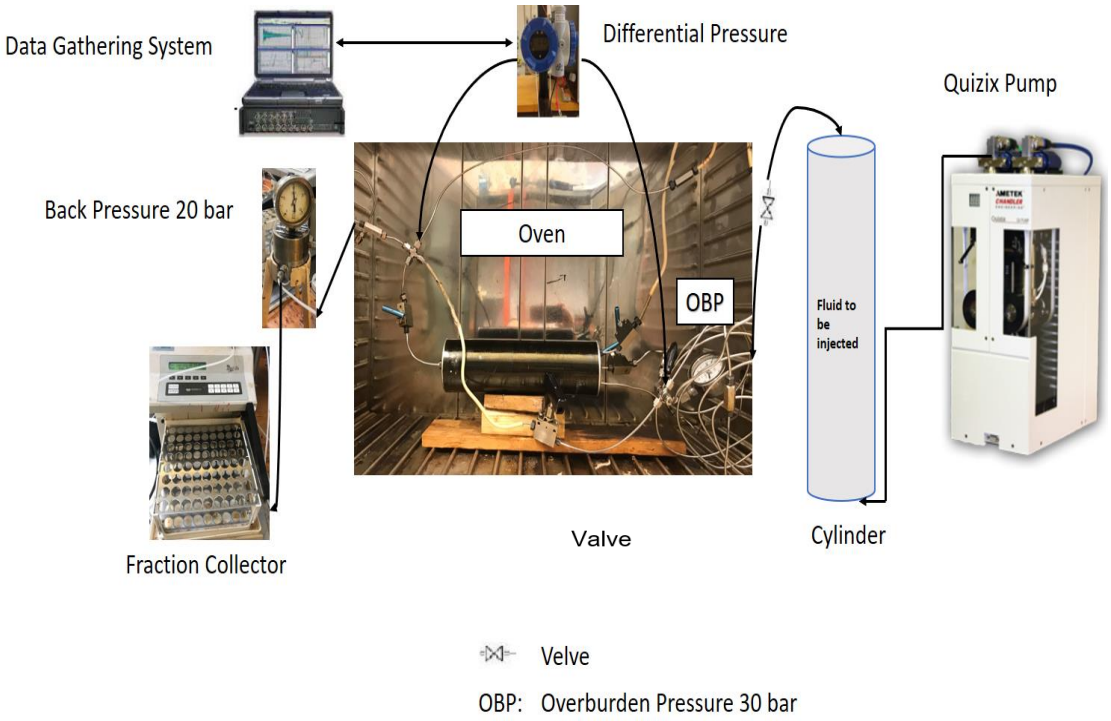

Figure 4.7: Experimental setup

4.3. Equipment

In this section, the equipment used for the experiment will be described with emphasis on setting, principles, and uncertainties.

4.3.1. Rheometer

The viscosity of the fluids was measured by using Malvern Kinexus rheometer Figure 4.8. This is a rotational rheometer that relates the force needed to turn an object in a fluid to the viscosity of the fluid. The rheometer is coupled with a software system called rSpace. The rheometer was equipped with different types of geometry. In this study, double gap geometry was used to measure the viscosity of low viscosity fluids such as brines, oil and surfactant. The measurements were conducted at a single shear rate of 10 s^{-1}.

Cone and plate geometry were used to measure the viscosity of viscous fluids such as polymer solutions. The measurements were conducted at different shear rates from 1 to 1000 s^{-1}. The rheometer temperature during viscosity measurements was controlled by a heat exchanger connected to the rheometer. The uncertainty in the measurements was estimated to be 5 % of the absolute value obtained

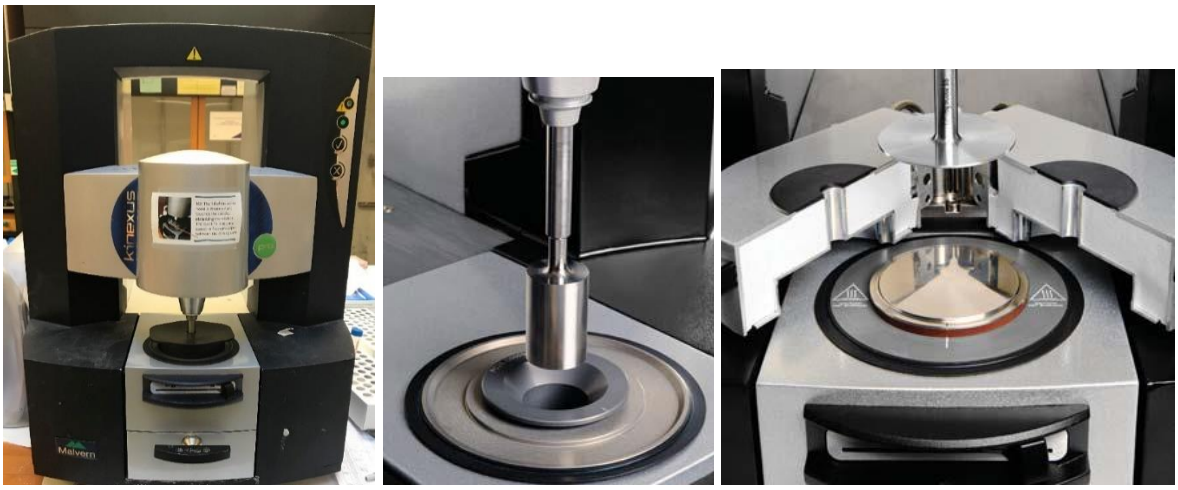

Figure 4.8: Malvern Kinexus Rheometer(left), Double gap geometry (middle) and Cone and plate geometry (right)[101]

4.3.2. pH Measurements

The pH measurements were performed using Hach Lange pH-meter with an uncertainty of ±0.01 pH. Before the pH measurements, the pH-meter was calibrated using three different fluids of pH 4, 7 and 10. The electrode was washed with distilled water and dried using paper in between every calibration.

The electrode was placed in the solution after calibration. The electrode was stirred gently, ensuring a homogeneous solution during measurements. Three pH measurements were performed, and the electrode was cleaned and dried in between each measurement. The average value was used as the absolute pH.

An electrochemical cell for pH measurements always consist of an indicating electrode, a reference electrode, and the aqueous sample to be measured. The indicating electrode is directly proportional to pH, while the reference electrode is independent of pH. If all three parts are in

contact with each other, the potential can be measured between the indicating electrode and the reference electrode, which depends on the pH of the sample and its temperature [102].

Figure 4.9: Hach Lange pH-meter

4.3.3. Fraction Collector

Foxy Jr. fraction collector from Greiner Bio-one- 14 mL tubes were used to collect effluent fluid samples. In this study, the fraction collector was set to operate by time so that for each set of time the collector will change to the next tube after 30 minutes. The uncertainty in the reading was estimated of the tubes to be 0.30 mL.

Figure 4.10: Foxy Jr. fraction collector

4.3.4. Pump

A Quizix pump was used for injecting different fluids into the core. The pump is equipped with two floating-piston transfer cylinders.

Figure 4.11: Quizix Pump

4.3.5. Dispersion, Conductivity Measurements

Pharmacia Conductivity Monitor was used for the dispersion test. The use of the device was explained in chapter 4.2.4.

Figure 4.12: Pharmacia Biotech Conductivity Monitor

4.3.6. X-ray

The InnospeXion Aps 2-D X-ray Core Scanner was used to check the saturation change of the core before the main experiment and after each fluid injection. The machine used from 15- 20 min to heat up before it started the scan.

Figure 4.13: InnospeXion Aps 2-D X-ray Core Scanner

4.3.7. Fuji Electric FCX-FKC

The apparatus was used to measure the differential pressure over the core. The maximum span limit was 5000 mbar. A voltage signal was sent from the apparatus to the computer where the signal was converted to pressure readings with LabVIEW software. The uncertainty of the readings was 1% of full range.

Figure 4.14: Fuji electric FCX-FKC

4.3.8. Core Holders

The cores were held in rubber sleeves inside the core holder, forcing the flow through the core. It was important that the sleeve was tight to the core, preventing flow going around the core as well as preventing fluid used for confining pressure to invade the core.

The short cores were mounted in Exxon core holder, and long cores were mounted in composite core holders who were suitable for X-ray scanning.

Figure 4.15: Exxon core holder (left) and composite core holder (right)

4.4. Accuracy in Measurements

This chapter will highlight the accuracy of the measurements and some of the uncertainties. There are some uncertainties regardless of this experimental work. It is difficult to predict how accurate the test results were when there were several factors which may affected the results. The accuracy of the measurements is given in the Appendix chapter. The main uncertainties are in both equipment based, accuracy in calculations and human errors.

The deviation in length and the diameter are due to the accuracy of the measurements equipment and the heterogeneity of the rocks. Porosity measurements are a function of length, difference in dry weight and saturated weight and volume of the cores. Hence the porosity uncertainty is a function of three parameters.

Permeability measurements is a function of the differential pressure (dP), the uncertainty is in the dP measurements. However, permeability calculations contained viscosity, length and cross section area, which might have affected the final values.

The produced oil by spontaneous imbibition was recorded visually at the top of the cell, which was sometimes difficult to read due to the meniscus between oil and water. This was the most significant uncertainty in the spontaneous measurements.

The differential pressure transducer had an uncertainty of 1%. However, for lower pressure the uncertainty is significant compared to higher pressure, which was observed during the experiment at lower differential pressures.

The uncertainty in the production data (long cores) was due to two reasons. The first one is the oil expansion factor, which was measured visually by reading the change in volume from the tubes. The second was due to the reading of the oil produced. When the tubes contained a small fraction of oil, they were weighted to find the mass of the oil and then convert it to volume. Thus, we may expect higher uncertainty in the volume of oil produced. For instance, a reading of ± 0.5mL oil during HS brine injection in core L2 would give a higher/lower incremental oil recovery of ≈ ± 3%, which is significant. If the uncertainties propagated for every single flood, the oil production may be over/under-estimated.

To summarize approximately errors of the measured values, a comparison between the absolute error and absolute value (relative error) are summarized in Table 4.5 for some given values in this experiment. A high relative error means less accuracy in the obtained values. The uncertainty of all the measurements are given in the Appendix chapter.

Table 4.5: Approximately errors for some of the measured values and relative error

	Values ± uncertainty	**Relative error [%]**
Absolute permeability (L2)	170 ± 3	± 2
Porosity (L2)	19.6 ± 0.3	± 2
HS brine production (L2) at 90°C	8.9 ± 0.3	± 3
pH of 2000 ppm HPAM at ambient temperature	6.70 ± 0.20	± 3
Viscosity of 2000 ppm HPAM at ambient temperature	84.4 ± 0.6	± 0.7
Ko,Swi [mD] after aging (L2)	132 ± 9	± 7

5. Results and Discussion

This thesis has investigated the effects of combining low salinity water injection with surfactant followed by a subsequent polymer flood to enhance oil recovery. Laboratory imbibition tests and flooding experiments have been conducted on both aged and unaged cores of outcrop Indiana Limestone rock material. The performance of the hybrid EOR method was evaluated by flooding experiments in tertiary recovery mode after secondary high salinity waterflooding. This chapter summarizes and discusses the primary results and observations obtained during the experimental work.

5.1. Petrophysical Properties of the Cores

Eight core samples of outcrop Indiana Limestone rock material were used in this thesis. Four long cores (~15 cm) designated as L1-L4 and four shorter cores (~5 cm) designated as S1-S4 (cf. Table 5.1)

Table 5.1: Petrophysical properties of Indiana Limestone cores.

Core ID	Length [cm]	Diameter [cm]	Bulk Volume [cm^3]	Pore volume [mL]	Porosity (φ) [%]	Abs.Permeability (K_w) [mD]	S_{wi} [%PV]	S_{oi} [%PV]	$K_o(S_{wi})$ [mD] Primol 542	$K_o(S_{wi})$ [mD] after aging
L1	14.80	3.80	166.020	28.6	17.2	160	0.36	0.64	179	-
L2*	15.20	3.71	163.80	32.2	19.6	170	0.33	0.67	215	132
L3	15.20	3.70	166.20	32.6	19.6	116	0.33	0.67	201	-
L4*	15.10	3.680	160.500	31.3	19.5	154	0.34	0.66	216	157
S1*	5.03	3.74	55.20	10.2	18.4	176	0.43	0.57	266	193
S2	5.005	3.70	53.90	9.8	18.2	285	0.06	0.94	566	-
S3	4.91	3.701	52.770	10.0	19.2	202	0.42	0.58	241	-
S4*	4.84	3.770	53.96	9.5	17.7	183	0.24	0.76	267	128

*Aged core

Table 5.1 summarizes the results with regards to core properties on the eight cores. The cores were chosen from a broader set of cores as to minimize the effects of differences in petrophysical properties. Hence, a narrow porosity range (17.2–19.6%) was obtained, with a corresponding absolute permeability of (116–285mD). The variation in porosities and permeabilities of the cores could be due to the heterogeneity of the carbonate pore structure [17, 103]. Some of the cores were cut from the same batch. However, the cores show some differences in physical properties.

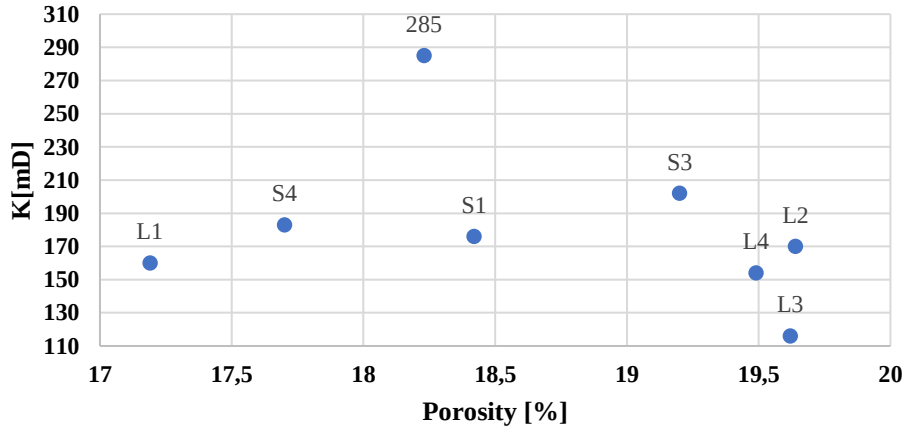

Figure 5.1: Plot of abs. Permeability (K) versus porosity (φ) for the measured values.

Figure 5.1 illustrates the relationship between absolute permeability as a function of porosity. The figure shows that there is no direct correlation between these two quantities. In carbonate reservoirs, the diversity in pore structure and fractures result in a complicated relationship between permeability and porosity [104]. The reason can be due to the complicated way of pore and throat combination and the heterogeneity of the Indiana Limestone; coordination numbers of the porous medium [20].

A Comparison of absolute permeability and oil permeability $K_{o\ (Swi)}$, after primary drainage with Primol 542, shows an increase in oil permeability. Oil occupies the largest pores in a water-wet system at irreducible water saturation, *Swi*, and therefore the oil will easily flow with minimal resistance having a high oil permeability [19].

The oil permeability (L2, L4, S1, and S4) before and after aging are listed in Table 5.1. Comparison before and after aging shows a systematic decrease in oil permeability. This likely

is related to that the wettability of the cores is reducing the flow potential for oil when the cores become more oil-wet. The oil permeability at irreducible water saturation, *Swi*, is expected to increase with increasing water wetness. As the wettability shifts toward more intermediate/oil-wet state, the oil permeability will be reduced due to the increased oil affinity on the rock surface [21]. As the wettability altered toward less water wet conditions, the flow resistance of oil will increase and lead to reduced oil permeability at irreducible water saturation.

5.2. Dispersion Test

To obtain a better understanding of the fluid flow in the core material, dispersion measurements were carried out at 100% water saturation (Formation water). Dispersion profiles for all the cores L1-L4 and S1-S4 are shown in Figure 5.2. Dispersion profiles for all the cores were obtained by measuring the effluent resistance when diluted formation water (FW) was injected, i.e., different resistance. The tracer (diluted FW profile) depends on the pore structure and the flow rate [105].

The pore space can be divided into three fractions [106]; flowing fraction (allows continuous phase flow), dendritic (dead-end, Figure 5.3) and isolated fractions. In a homogeneous porous medium displaying ideal dispersion, half of the injected concentration breaks through (BT) after one pore volume (PV) with the profile being symmetrical around this point [105]. Further, the front and the tail of the tracer pulse are distorted due to diffusion and hydraulic mixing. The tracer concentration in the effluents provides information about how well the individual pores in the core sample are connected and the number of dead-end pores. Early BT is associated with the presence of isolated pores that are not participating inflow, hence the sufficient volume of flow is less than the total pore volume.

Results, shown in Figure 5.2, reflect the variation of the pore structure and the heterogeneity of the carbonate material used in this experiment. Since early BT occurs in the porous medium (before 1 PV), that may indicate that cores are not homogenous and have some presence of isolated pores; that do not contribute to flow. An asymmetrical profile, i.e., tailing of tracer profile, indicates mass exchange with fluid in dead-end pores (pores that are connected to flow

but does not exhibit flow). The dead-end pores are bypassed by the main flow [105]. Presence of dead-end pores creates asymmetry due to concentration exchange by diffusion from the flowing volume into the dead-end pores. Diffusional exchange rather than viscous flooding displaces fluid in dead-end porosity, and hence relatively more injection time and fluid are needed to displace the initial fluid in-dead- end pores thoroughly. The concept of the dead-end pores does not only refer to single pores but could also be clusters of pores that are not a part of the flowing fraction.

Since the dispersion profiles show an asymmetrical profile, we can assume that the core has displaced by diffusional exchange from the dead-end pores. The cores have different grades of pores that are not participating in the main flow. The upper and lower fraction of dead-end pores varies from 5-23 % (1-BT) based on the fraction curves for the eight cores. The results of the tracer profiles show in somehow the same trends of BT and tailing. Comparison of short cores, S2 (abs. permeability 285mD) shows the earliest BT of the four short cores, while S4 (abs. permeability 183mD) shows the latest BT. Comparison of long cores, L3 (abs. permeability 116mD) shows the earliest BT, while L1 (abs. permeability 160mD) shows the latest BT. Since L3 and S2 had the earliest BT, it can be an indication of the highest degree of isolated pores. By dispersion measurements, S2 and L3 seem to be the most heterogeneous cores used in this study. With this in mind, the properties of the heterogeneous core may contribute to different behavior in the flooding experiment compared to the other cores.

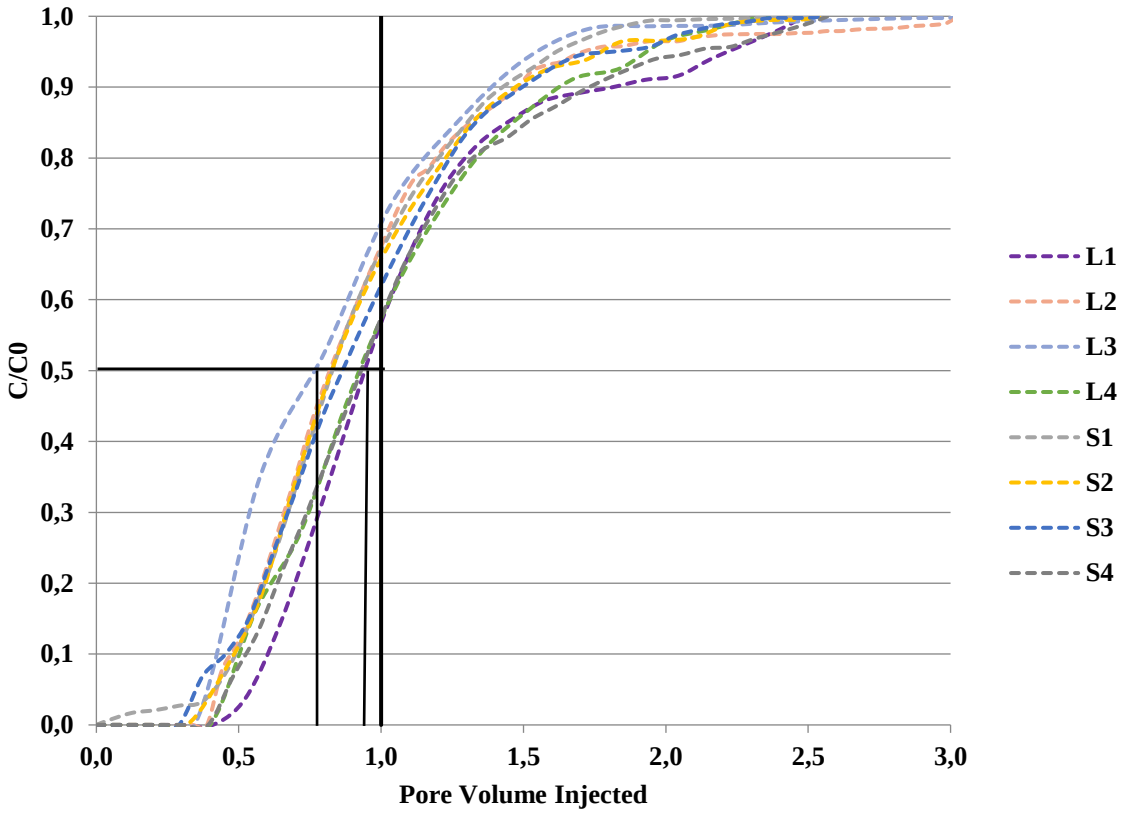

Figure 5.2: Dispersion profiles for all cores. The fractional flow of diluted FW is plotted against pore volume injected, PV.

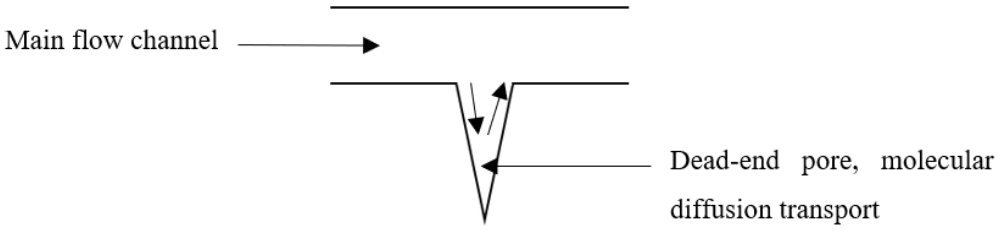

Figure 5.3:Illustrates the dead-end pores

5.3. Spontaneous Imbibition Tests

Brine imbibition test was performed to examine wettability states of aged and unaged core plugs. The brines used in this study were high salinity brine (HS) 42404 ppm for 30 days and then low salinity (LS) 241 ppm for another 30 days. The purpose of exchanging HS brine with LS brine was to investigate the effect of brine with a lower ionic concentration on oil recovery. The experiment was conducted at ambient temperature.

Table 5.2 summarizes experimental data, and Figure 5.4-Figure 5.7 shows the experimental results.

Table 5.2 Summary of spontaneous imbibition experiments

Core ID	Swi [%PV]	Soi [%PV]	$V_{o.prod.HS}$ [mL]	Recovery Factor HS [% OOIP]	$V_{o.prod.LS}$ [mL]	Recovery Factor LS [% OOIP]	Final Recovery Factor [% OOIP]	ΔSw spont. Imbibition	Final Sw spont. Imbibition	$S_{or,after\ sp.imb}$ [%PV]
S1*	0.43	0.57	0.04	0.69	0.05	0.86	1.55	0.01	0.44	0.56
S2**	0.06	0.94	1.7	18.42	0	0	18.42	0.17	0.23	0.77
S3	0.42	0.58	0.65	11.20	0	0	11.20	0.06	0.48	0.52
S4*	0.24	0.76	0.07	0.96	0.1	1.38	2.34	0.02	0.26	0.74

*Aged core

** Crushed during imbibition test

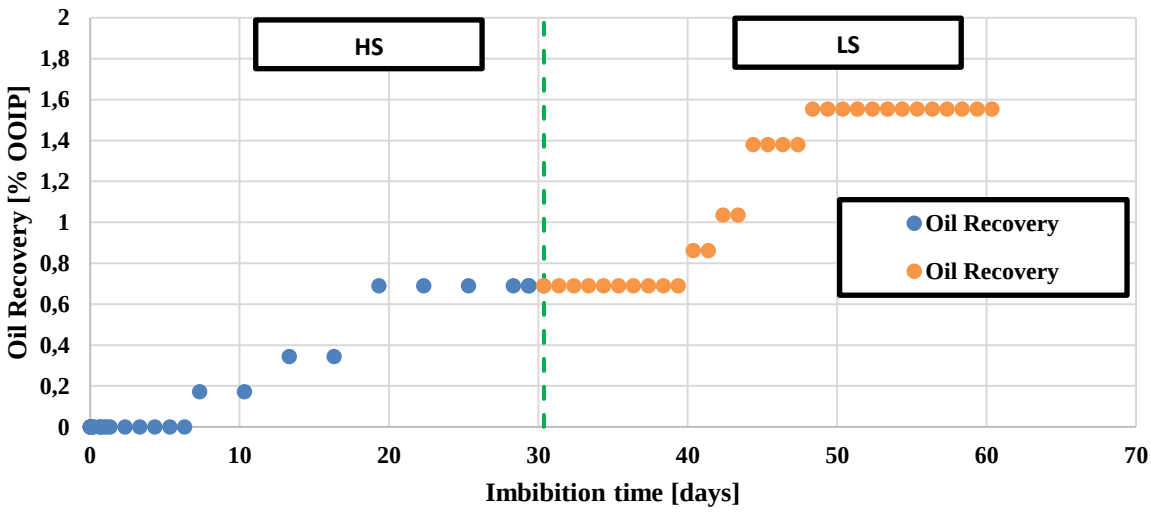

Figure 5.4: Spontaneous imbibition into the oil- saturated short core S1 (aged) using brines with different salinity. Dashed lines represent brine changeover

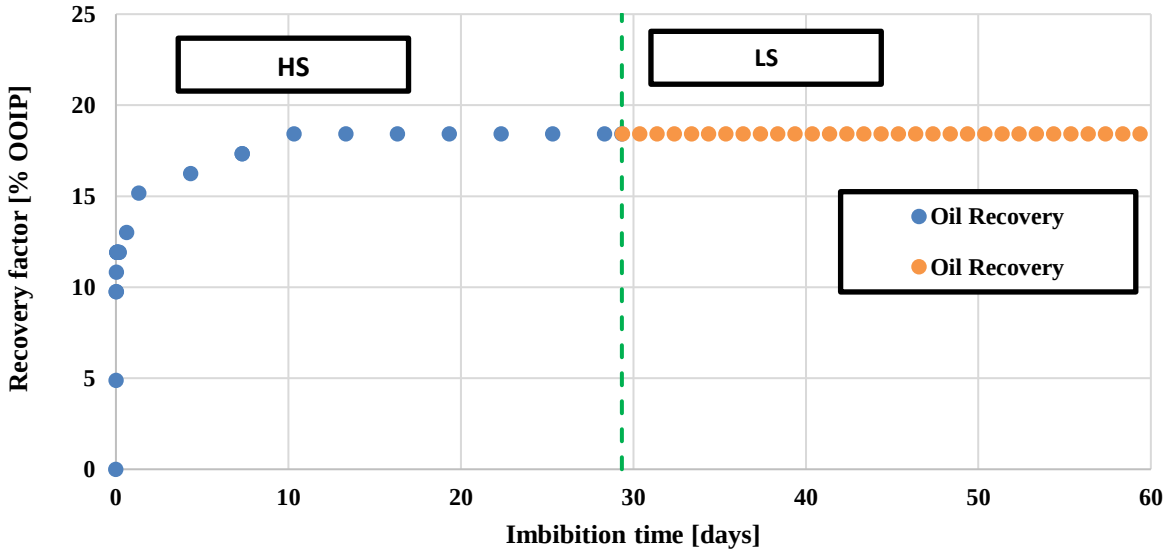

Figure 5.5: Spontaneous imbibition into the oil- saturated short core S2 (unaged) using brines with different salinity. Dashed lines represent brine changeover

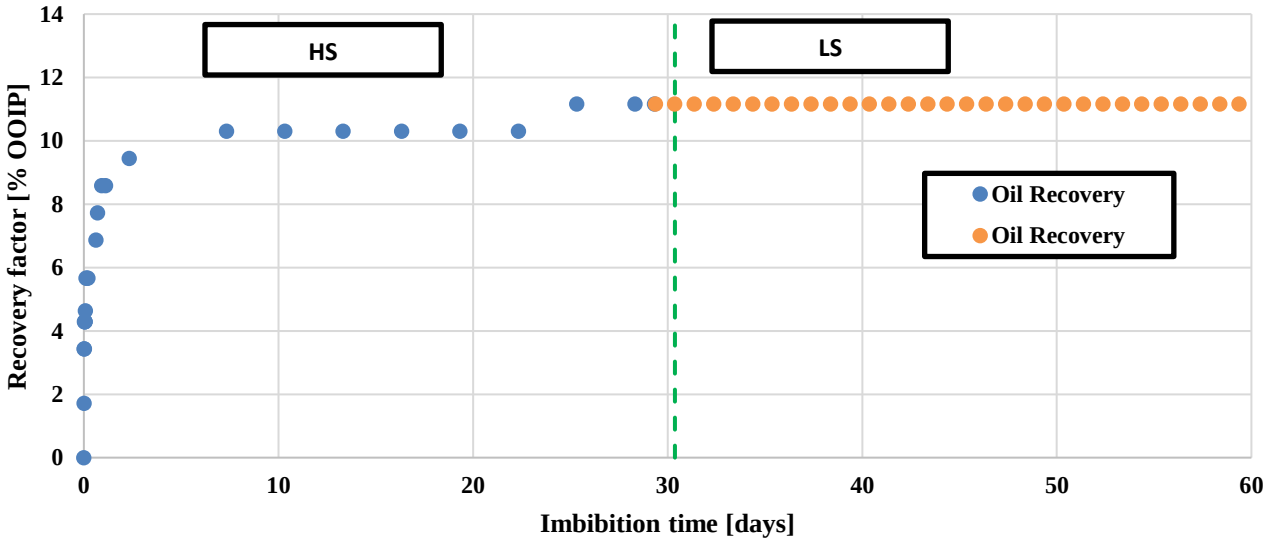

Figure 5.6: Spontaneous imbibition into the oil- saturated short core S3 (unaged) using brines with different salinity. Dashed lines represent brine changeover

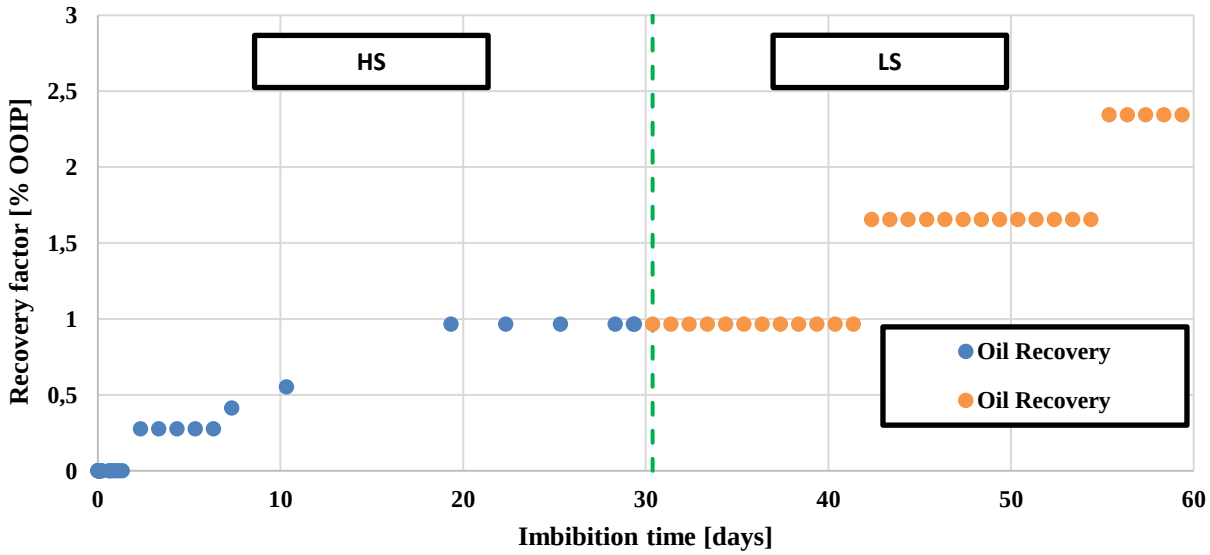

Figure 5.7: Spontaneous imbibition into the oil- saturated short core S4 (aged) using brines with different salinity. Dashed lines represent brine changeover

5.1.1 Experimental Observations- Short core S1 (aged)

Figure 5.4 shows the recovery factor as a function of imbibition time for core S1. Spontaneous imbibition of S1 placed in HS brine (30 days), resulted in a recovery factor of 0.69% OOIP. The production did not start immediately, which may indicate that aging of the core has changed the wettability to less water wet. Which is consistent with the change in oil permeability after aging (cf.Table 5.1) When no more oil production was observed (30 days), the HS brine was exchanged with LS brine. The purpose of exchanging HS brine with LS brine was to investigate the effect of the lower ionic concentration. Changing from HS brine to LS brine gave an additional recovery of 0.17% OOIP, corresponding to a recovery factor of 0.86% OOIP. The final recovery factor was 1.55% OOIP. It should be noted since the recovery factor was low during spontaneous imbibition; we may expect great potential of LS waterflooding. (cf. Production Profiles Short Cores).

5.1.2 Short core S2 (unaged)

Figure 5.5 shows the results of spontaneous imbibition of S2 placed in HS brine (30 days), resulted in a recovery factor of 18.42% OOIP. It should be noted that S2 had the highest initial oil saturation of all four short cores. This core was damaged when it was transferred to the Amott cell (Spontaneous Imbibition Test, Figure 4.6). The production started immediately, which indicating the presence of water-wet pores within the media and might be due to an increase in the surface area (damaged), where more oil might be in the fractured areas; hence increasing the imbibition of water. When no more oil production was observed (30 days), the HS brine was exchanged with LS brine. No additional oil production was observed with LS brine (30 days).

5.1.3 Short core S3 (unaged)

Figure 5.6 shows the results of the spontaneous imbibition of S3 placed in HS brine (30 days), resulted in a recovery factor of 11.2% OOIP, which is 7% lower than S2. The lower recovery factor compared to S2 may be attributed to the initial oil saturation of the core and the damage

of core S2. The production started spontaneously, which might indicate water-wet conditions [28].When no more oil production observed (30 days), the HS brine was exchanged with LS brine. The change of brine from HS brine to LS brine showed no increase in the oil production.

5.1.4 Short core S4 (aged)

Figure 5.7 shows spontaneous imbibition of S4 placed in HS brine (30 days), resulted in a recovery factor of 0.96% OOIP, which is 0.27% higher than S1. The results might be attributed to the initial oil saturation in the cores. The production did not start immediately. After almost three days the oil production started. When no more oil production observed (30 days), the HS brine was exchanged with LS brine. The oil did not produce instantly. After almost four days the oil started to produce. LS brine gave an additional recovery factor of 0.42% OOIP, corresponding to a recovery factor of 1.38% OOIP. The final recovery factor was 2.34% OOIP.

5.1.5 Comparison of S1 and S4 (aged cores)

The rate of spontaneous imbibition depends on several factors such as wettability, viscosity, interfacial tension, pore structure and initial water saturation of the porous medium [28]. S1 and S4 had initial oil volume of 5.8mL and 7.3mL (S_{oi}= 0.57 and 0.76), respectively. More oil is available in core S4, which may produce more oil due to the spontaneous imbibition. The comparison would be more accurate if both cores had the same initial oil saturation. The change of HS brine to LS brine showed an increase in the oil recovery and higher imbibition rate for S4 compared S1. The slow imbibition rate can be an indication of the cores became less water-wet; where for a water-wet system the water will imbibe rapidly into the core. Where in a neutral/oil-wet, a small amount will imbibe into the core or no water will imbibe into the core [107], which was observed in this test.

Carbonate reservoirs display variability properties, such as mineralogy and pore structure. Even if the cores were at the same initial oil saturation, they might give different results due to the heterogeneity of the porous medium. The main reason for the different recovery factors of these two cores might be due to the initial oil saturation of the cores. On the other hand, the

differences in the oil recovery factor are insignificant. S1 and S4 show a systematic approach regarding spontaneous imbibition; the two cores show a similar delay in production concerning brine change over. The low recovery factor during HS brine may be attributed to the rock oil surface, where the rock surface became more oil-wet during aging, hence water do not have access to the rock surface. The majority of oil production was observed during the brine with lower ionic strength.

This shift may be attributed to the electrical double layer (EDL) expansion triggered by salinity reduction. HS brine has greater ionic strength compared to LS brine, which means changing from HS brine to LS brine generates higher repulsion forces. This repulsion force expands the EDL and promotes a more stable water film, which gives water more accessible to the rock surface. A spontaneous imbibition test conducted at 70°C of different carbonate samples studied by Romanuka et al. (2012) [59] reported that the wettability altered towards more water-wet conditions by using a brine with lower ionic strength and higher surface interacting ions such as sulfate.

To conclude, it has been observed that lowering the ionic strength of the imbibing brine leads to increase in oil recovery. As shown in Figure 5.4 and Figure 5.7, oil recovery by spontaneous imbibition ranges from ~ 0.7 to 1% OOIP for HS brine. The LS brine imbibition gave an additional oil recovery of ~ 0.2 to 0.4% OOIP. We believe the mechanism behind the LS effect on the aged cores was due to wettability alteration. However, more investigation is needed to explain why low salinity trigged the oil recovery during LS brine.

5.1.6 Comparison of S2 and S3 (unaged)

As shown in Figure 5.5 and Figure 5.6 oil recovery by spontaneous imbibition during HS brine imbibition ranges from 11 to 18% OOIP. Higher oil production of core S2 could be the result of crushing during the experiment. No additional oil recovery was observed during LS brine imbibition. If the cores were at strong water-wet conditions, we would expect a faster imbibition rate and higher change in water saturation 40- 50 % [108] (cf.Table 5.2). The imbibition test did not show a strong water-wet behavior based on the obtained results. We bileive that the

cores wettabilty was more weak water-wet. Under water-wet conditions, residual oil is trapped as disconnected blobs (snap off) in pore bodies.

5.1.7 Comparison of Imbibition Test on Aged and Unaged Cores

Comparison of recovery factor of aged and unaged cores is shown in Figure 5.8. Unaged cores (water-wet/ weak water-wet) show significant oil production. However, there was no oil production after the brine change. It is clear from the curves that changing the wettability influence the imbibition rate and final water saturation.

As mentioned in the theory section, spontaneous imbibition is a capillary force driven process, which the wetting fluid will displace the non-wetting fluid. The positive capillary pressure, which is influenced by the wettability of the porous media, determines the production rate and oil produced by spontaneous imbibition; hence the spontaneous imbibition rate and amount of imbibed water reflect this property of the porous medium. Since core S2 and S3 are in water-wet state, water will spontaneously imbibe into the smaller pores, because the capillary pressure is highest at this point. Hence less work is necessary for water to displace the oil [28]. Since S1 and S4 became more oil-wet after the aging process, more work (capillary forces) is required to force water into the core, resulting in lower spontaneous imbibition.

Initial water saturation is one of the parameters that influence the rate of water imbibition into the core (Anderson 1986 [107]). In this case, HS brine was added to the Amott cell, instead of formation water (FW). HS brine had lower ion strength compared to FW and the highest sulfate ions (SO_4^{2-}) concentration of the three brines used in this experiment. As mentioned in the literature review, SO_4^{2-} may interact with the rock surface, thus lowers the positive surface charge at the rock surface and makes calcium ions (Ca^{2+}) react with adsorbed oil polar compound, i.e., carboxylic acids. Then calcium carboxylate can be released from the surface [71] which might affect the rock wettability, hence increase the oil recovery. The change of brine (HS to LS) showed an increase in the oil recovery (S1 and S4) with an overall slower imbibition rate.

According to a spontaneous imbibition study made by Graue et al. (2002) [109] on Rødal chalk, imbibition rate and the imbibition endpoint for water saturation decreased as the aging time increased. They also studied the Amott index, which showed that the core plugs become less

water-wet as the aging time increased. In the same study, the recovery factor decreased as the aging time increased. Graue et al. study are consistent with a study made by Zhou et al. (2000) [110] where they studied the relationship between wettability and oil recovery by spontaneous imbibition and water flooding on Berea sandstone. Their study also showed decreased recovery factor by increasing the aging time when spontaneous imbibition was conducted. The work by Graue et al. and Zhou et al. are in line with the obtained results in our study, where the aging process affected both the imbibition rate and the recovery factor. For the aged cores, the oil recovery is less than 3 % of OOIP, which might indicate that the aging process possibly shifted the wettability to less water-wet state.

After completion of spontaneous test imbibition test, the cores were placed in a core holder for a waterflood test (forced imbibition) with LS brine.

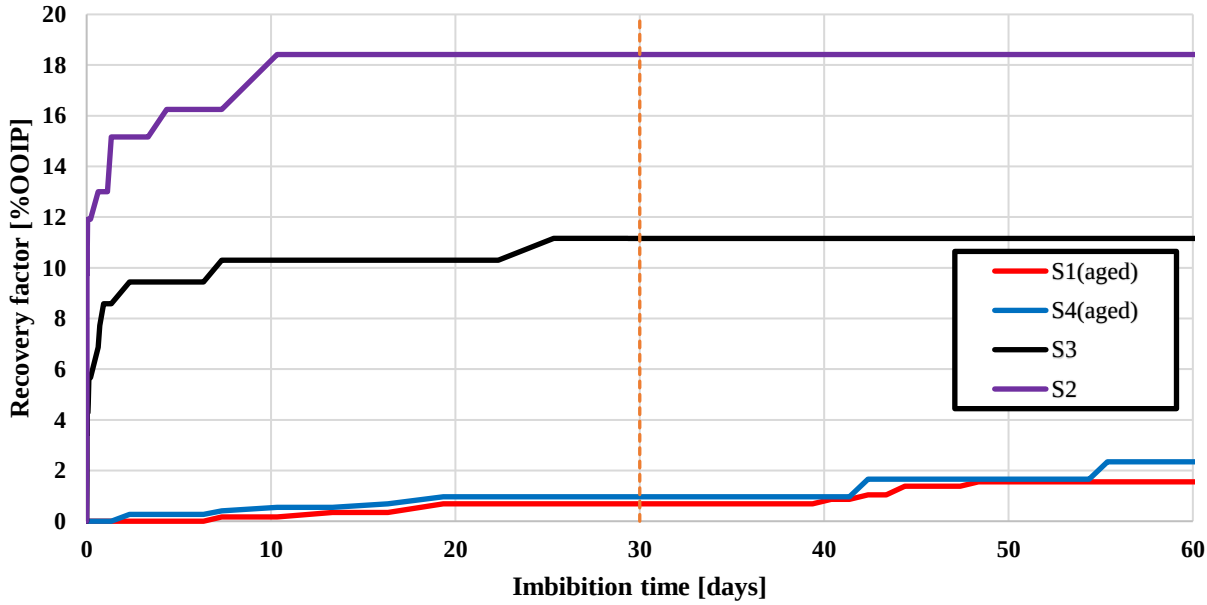

Figure 5.8: Comparison of the spontaneous imbibition experiment of the short cores. Dashed lines represent brine changeover.

5.4. Production Profiles Short Cores

The results in this section is a study of forced imbibition experiment of the three short cores. Whereas core S1 and S4 were aged cores, and S3 were unaged core. Brine used in this waterflood experiment was low salinity brine (LS) 241 ppm, to investigate the effect of lower ionic concentration on oil recovery. The composition of the LS brine listed in (Table 4.1). The experiment was conducted at ambient temperature with three injection rates of 0.1→0.5→1 mL/min. The LS brine injected until WOR was very high, and produced oil was insignificant. Table 5.3 summarizes experimental data, and Figure 5.9-Figure 5.11 shows the experimental waterflood results.

Table 5.3 Summary of waterflood test of short cores with LS

Core ID	S_{oi} **[%PV]**	$S_{or,after\ sp.imb}$ **[%PV]**	**Recovery Factor 0.1 mL/min [% OOIP]**	**Recovery Factor 0.5 mL/min [% OOIP]**	**Recovery Factor 1 mL/min [% OOIP]**	**Final Recovery Factor waterflood [% OOIP]**	**Final Recovery Factor Sp.imb + waterflood [% OOIP]**	S_{or} **[%PV]**	$K_w(S_{or;LS})$ **[mD]**	K_{rw} $(S_{or,LS})$
S1*	0.57	0.56	21.9	30.7	32.5	32.5	34.0	0.38	29	0.16
S2**	0.94	0.77	-	-	-	-	18.4	-	-	-
S3	0.58	0.52	1.90	3.80	24.5	24.5	35.7	0.37	35	0.17
S4*	0.76	0.74	17.8	20.8	34.4	34.4	36.8	0.48	34	0.19

*Aged core

** Crushed during imbibition test

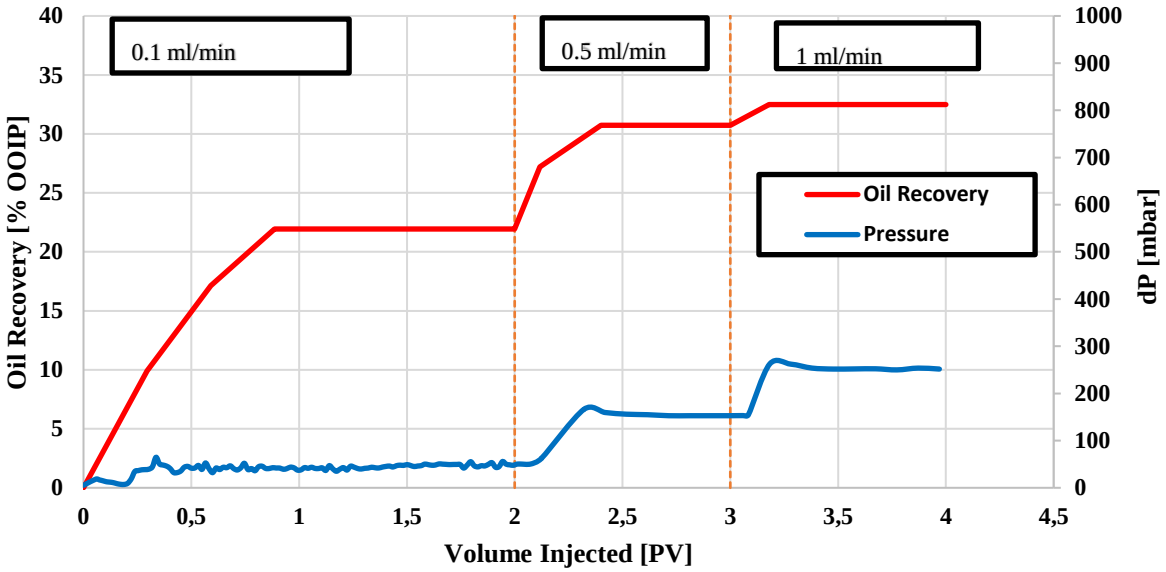

Figure 5.9: Recovery and pressure profile of short core S1(aged) during to LS waterflooding.

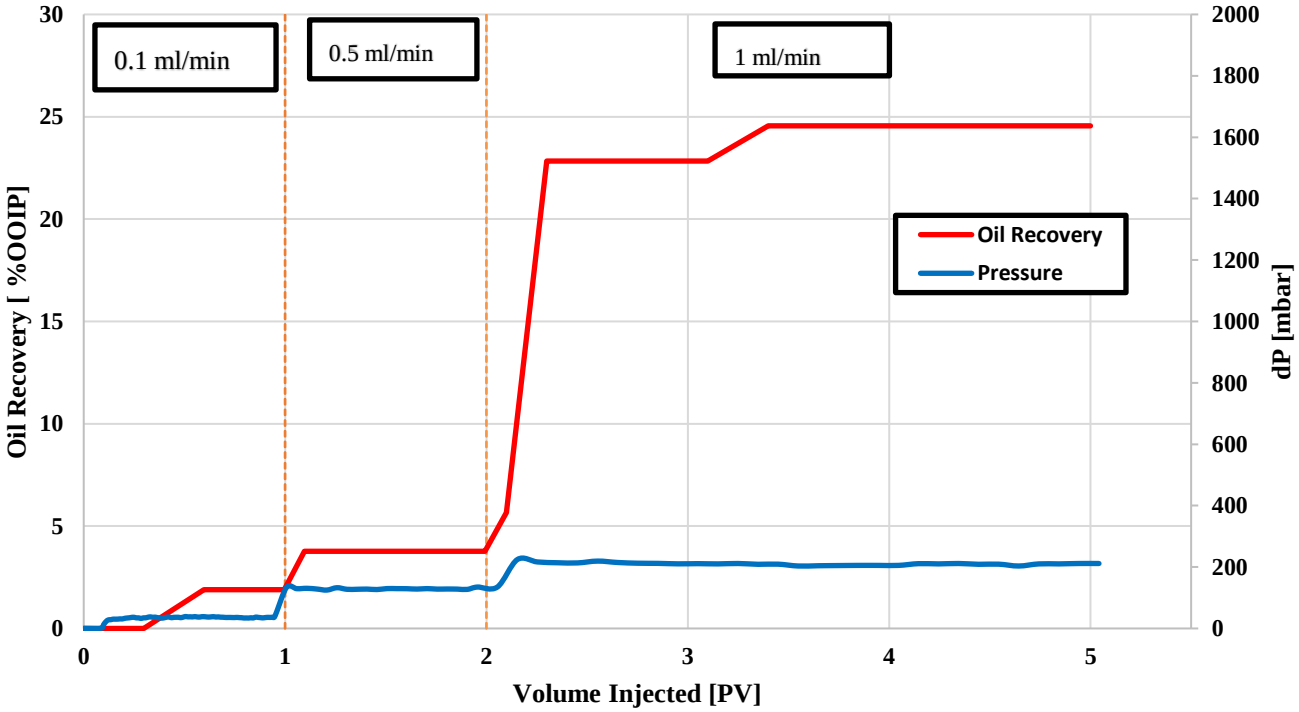

Figure 5.10: Recovery and pressure profile of short core S3 (unaged) during to LS waterflooding.

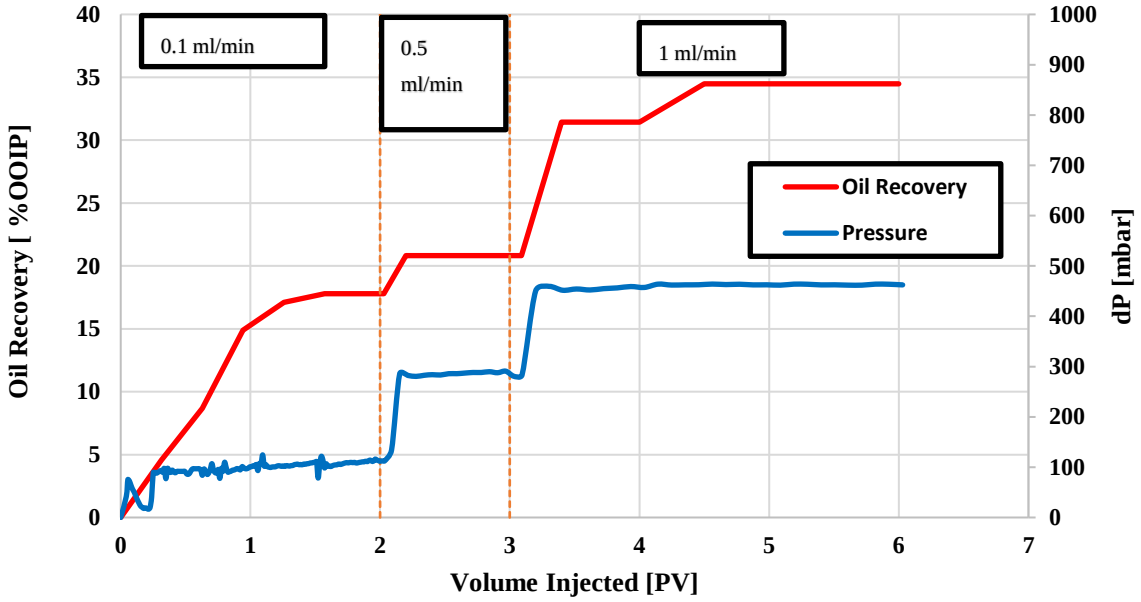

Figure 5.11: Recovery and pressure profile of short core S4 (aged) during to LS waterflooding.

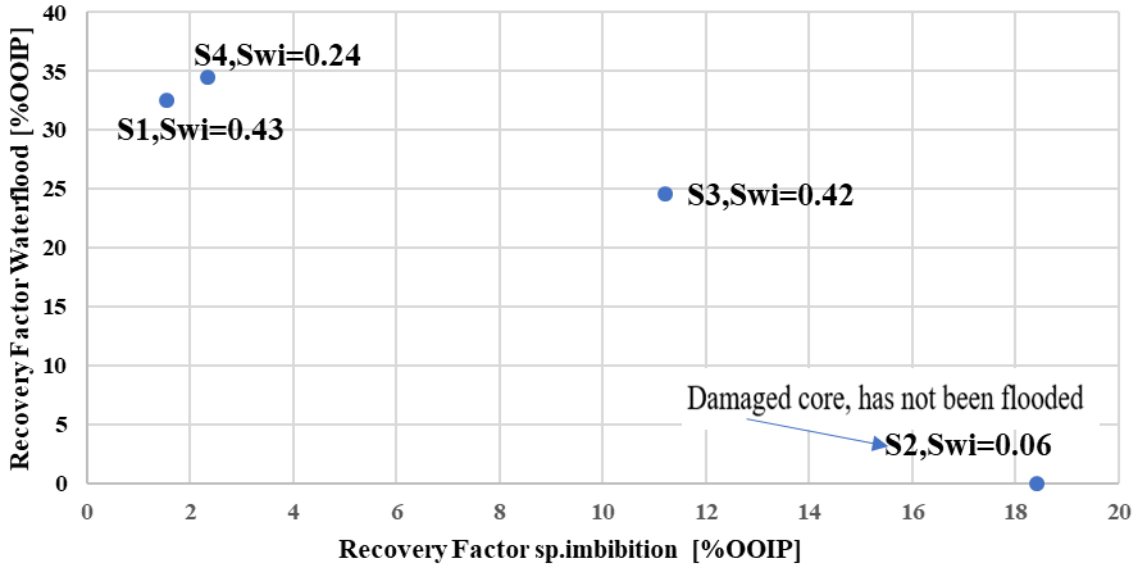

Figure 5.12:Final waterflood oil recovery versus final oil recovery by spontaneous imbibition for different initial water saturation

Observations

Figure 5.9 shows the oil recovery and differential pressure (dP) as a function of injected PV for core S1 (aged). LS injection of 0.1mL/min resulted in a recovery factor of 21.9% OOIP. The injection rate was increased at the end of each flooding sequence, for two reasons; to eliminate capillary end effects and investigate on further reduction of the residual oil saturation and oil mobilization. Injection of 0.5mL/min gave an additional recovery of 8.8% OOIP, corresponding to a recovery factor of 30.7% OOIP. Increasing the injection rate, (1mL/min) gave an additional recovery of 1.8%, corresponding to a recovery factor of 32.5% OOIP. Final recovery factor was 32.5% OOIP. The differential pressure over the core increased with each step of increased injection rate. Some fluctuating pressure gradient was observed throughout the first flood (0.1mL/min) followed by leveling off to a constant and stable differential pressure for higher injection rates.

Figure 5.10 shows the results of core S3 (unaged). Injection of 0.1mL/min resulted in a recovery factor of 1.90% OOIP. The low recovery factor may be a consequence of higher recovery factor during spontaneous imbibition (11.2% OOIP). Higher injection rate resulted in increased recovery factor of 3.80% OOIP and 24.5% OOIP, respectively (incremental oil recovery of 1.9% OOIP and 20.7%OOIP). The change in injection rates induced the jump in pressure profile. A small fluctuating pressure gradient was observed throughout the whole sequence. The lowest differential pressure was observed in S3, which may be attributed to the absolute permeability of the core (202mD).

Figure 5.11 illustrates the results obtained for core S4 (aged), LS flooding (0.1mL/min) resulted in a recovery factor of 17.8% OOIP, which is 4% lower than S1. The similar pressure profile was observed as S1 throughout the flood, but with a higher differential pressure across the core. 0.5mL/min gave an incremental oil recovery of 3% OOIP, corresponding to a recovery factor of 20.8% OOIP. Increasing the injection rate, (1mL/min) gave an additional recovery of 13.6% OOIP, corresponding to a recovery factor of 34.4% OOIP. Final recovery factor was 34.4% OOIP.

Figure 5.12 illustrates the relationship between forced waterflood oil recovery as a function of oil recovery by spontaneous imbibition. At first glance, S4 (aged) core with a lower *Swi* compared to S1 (aged) had higher imbibition recovery factor and higher recovery factor after waterflood. The difference may be explained by two reasons based on the results. The first explanation may be related to initial water saturation of the cores. S4 had lower *Swi* (0.24) compared to S1 *Swi* (0.43). Hence the lower water saturation makes S4 more responsive to spontaneous imbibition compared to S1. The second explanation may be attributed to the higher differential pressure across S4 compared to S1. S4 reached higher differential pressure when flow rate increased (~110 → 290 → 460 mbar), while S1 (~50 → 250 → 250 mbar). Thus, that might explain the higher recovery factor during LS waterflood.

S3(unaged) core responded well to spontaneous imbibition; it is reasonable to assume that S3 had a weakly water-wet condition. Therefore S3 responded better to spontaneous water imbibition. However, S3 had lower recovery factor during LS waterflood. The lower recovery factor might be explained by the lower differential pressure along the core (~35→ 130 → 200 mbar), lower than S1 and S4. Another explanation for low recovery factor of S3 might be attributed to snap- off effect, where the water flows in films at the pore surface, and snap-off occurs in pore throats and therefore resulting in trapping of oil droplets in pore bulk area.

Interestingly, the aged cores showed higher differential pressure, which was surprising, since we expected that the unaged core would give higher differential pressure due to lower endpoints relative permeability at water-wet states according to the literature review. However, water relative permeability showed that all of the three cores had a water relative permeability in weak water-wet conditions.

Irregular differential pressure across the core may indicate dissolution or precipitation (i.e., $CaSO_4$) [111]. The differential pressure was in somehow stable during the waterflood for the three cores. Therefore precipitation and plugging during the LS brine injection can be excluded. The fluctuation during 0.1mL/min injected may be attributed to instability in pressure transducer at low pressures. Hence it gives unstable recordings. For the higher injection rates, viscous forces will dominate and therefore give a more accurate differential pressure reading

along the core. Some fluctuation in the differential pressure was observed at higher injection rates, that may be attributed to the difference in petrophysical parameters such as permeability, heterogeneity of the cores and varying oil saturation distribution along the cores.

As presented in Table 5.3, water relative permeability ranges from 0.16-0.19. At first glance, it is a possibility to assume that the cores are in weak water-wet states since water relative permeability reflects the wettability state in the porous medium. Water permeability for strongly water-wet states at S_{or} should be low, since water remains in the smallest portions of the pore space, giving very low water relative permeability and significant trapping of oil in the larger pores at the end of waterflooding, due to snap-off [19]. On the other hand, at an oil-wet state, water relative permeability can rise to higher values since the water fills the centers of the larger regions of the pore space, which improve water flow. However, more investigations need to be done in detail to confirm if the wettability have changed during these tests, e.g. investigation of capillary pressure curves or wettability indexes.

5.5. Core Flooding Results

This chapter summarizes the main results obtained from high salinity brine (HS), low salinity brine (LS), low salinity surfactant (LSS) and low salinity polymer (LSP) flooding experiments in secondary and tertiary injection modes.

The production data for secondary water injection and tertiary low salinity water injection are summarized in Table 5.4- Table 5.5. The experiment was conducted at an elevated temperature of the 90°C, confining pressure of 30 bar and back pressure of 20 bar and one single rate was used in all flooding sequences of 0.1mL/min. The pressure was measured continuously. Abrupt changes in the production and pressure profiles are due to change of the fluid injected. The pressure data has been averaged to simplify the input in the curves. The average has been done using the add-on TDMS Reader in MATLAB Computer Runtime.

After each flooding sequence, the cores were placed in a 2-D X-ray cabinet to detect saturation changes or possible saturation re-distribution of the phases along the cores.

This section is organized as follows:

- Main observations
- Secondary high salinity waterflood
- Tertiary mode LS, LSS and LSP flooding
- Pressure profiles
- Endpoint relative permeability
- Polymer effluent results
- X-ray in-situ saturation monitoring

Table 5.4 Experimental results from secondary high salinity (HS) waterflooding

Core ID	PV [mL]	S_{wi} [%PV]	S_{oi} [%PV]	WBT [Fraction PV]	RF @WBT [%OOIP]	Final Recovery Factor HS [% OOIP]	$S_{or,HS}$ [% PV]
L1	28.6	0.36	0.64	0.29	52.5	79.1	0.12
L2*	32.2	0.33	0.67	0.17	28.8	43.5	0.36
L3	32.6	0.33	0.67	0.16	31.7	53.2	0.29
L4*	32.3	0.34	0.66	0.23	36.7	48.3	0.32

*Aged core

Table 5.5 Experimental results from tertiary mode

Core ID	LS RF [% OOIP]	$S_{or,LS}$ [% PV]	Δ $RF_{HS\rightarrow LS}$ [% OOIP]	LSS RF [% OOIP]	$S_{or,LSS}$ [% PV]	Δ $RF_{LS\rightarrow LSS}$ [% OOIP]	LSP RF [% OOIP]	$S_{or,LSP}$ [% PV]	Δ $RF_{LSS\rightarrow LSP}$ [% OOIP]	Final Recovery Factor LS [% OOIP]	$S_{or,LS}$ [% PV]	Δ $RF_{LSP\rightarrow LS}$ [% OOIP]	$K_{rw}S_{or,LS}$ @90℃	$K_{rw}S_{or,LS}$ @22℃
L1	79.1	0.12	0	79.1	0.12	0	80.4	0.11	1.3	80.4	0.11	0	0.23	0.17
L2*	45.1	0.34	1.6	45.1	0.34	0	52.0	0.30	6.9	54.4	0.29	2.4	0.49	0.30
L3	55.7	0.28	2.5	58.7	0.26	3	69.4	0.19	10.7	69.4	0.19	0	-	-
L4*	54.4	0.29	6.1	56.8	0.27	2.4	64.5	0.22	7.7	66.4	0.21	1.9	0.16	0.19

*Aged core

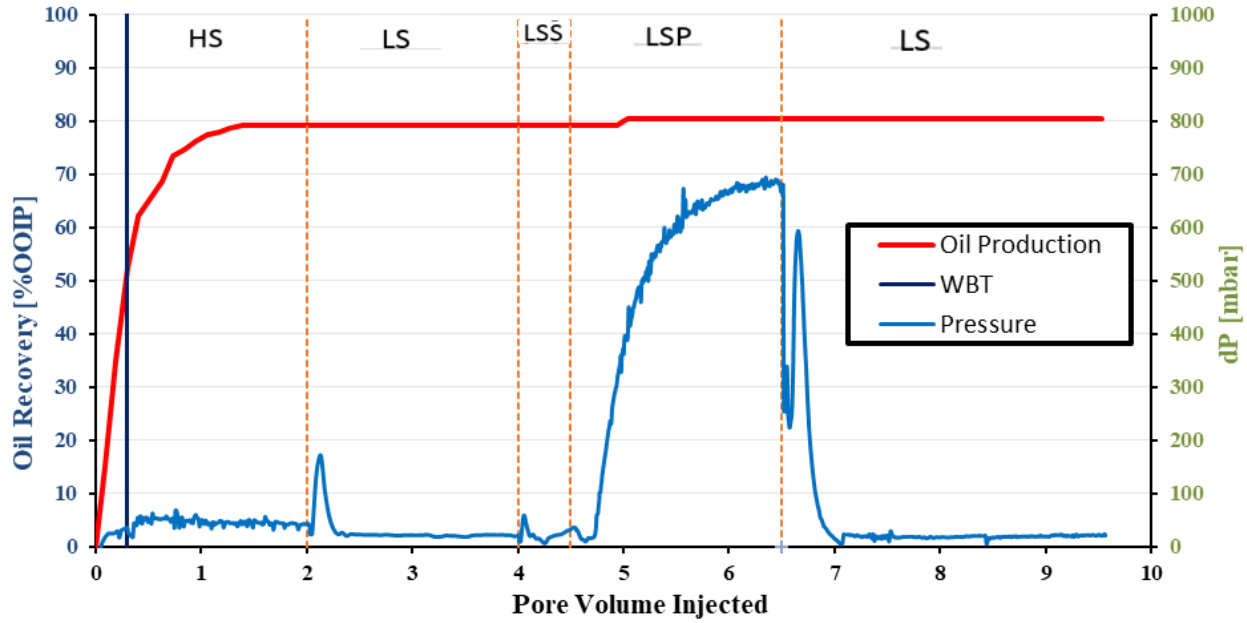

Figure 5.13: Recovery and pressure profile of L1(unaged) of the whole flooding sequences. Dashed lines represent fluid changeover.

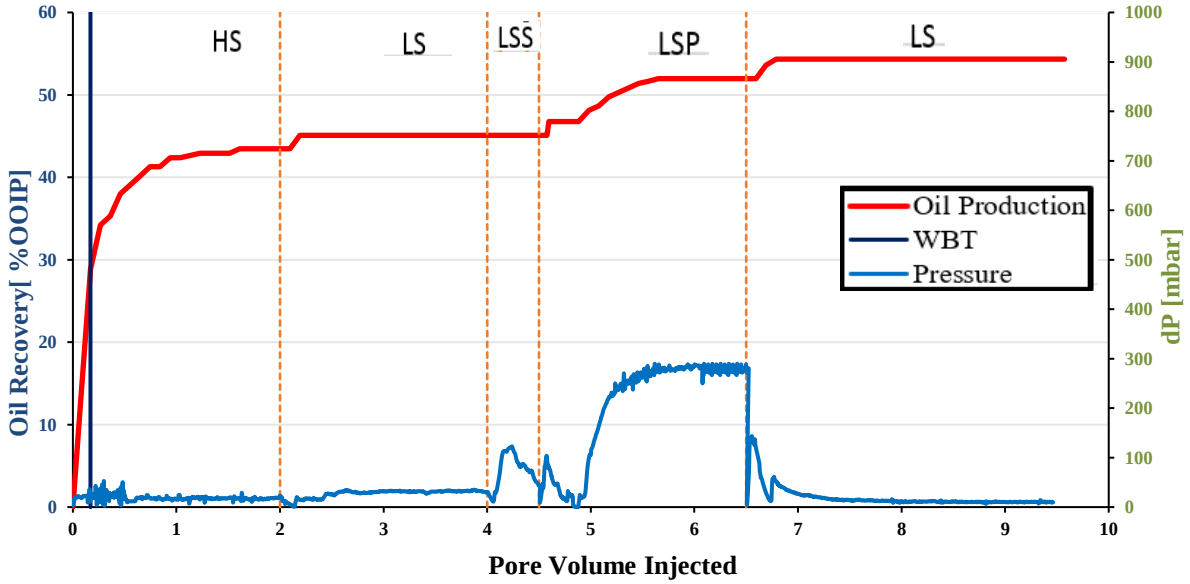

Figure 5.14: Recovery and pressure profile of L2 (aged) of the whole flooding sequences. Dashed lines represent fluid changeover

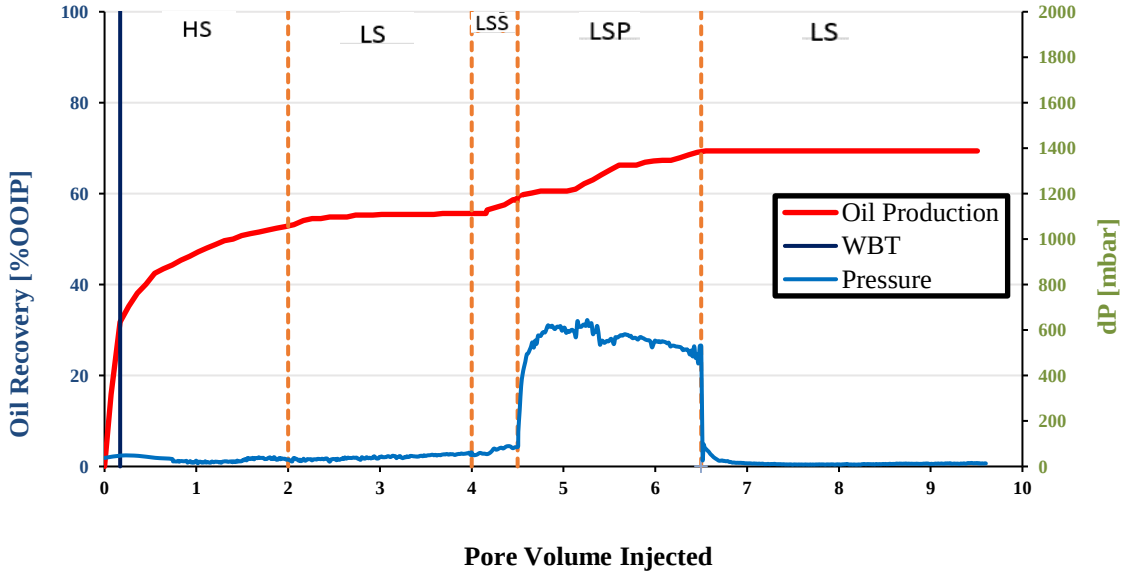

Figure 5.15: Recovery and pressure profile of L3 (unaged) of the whole flooding sequences. Dashed lines represent fluid changeover.

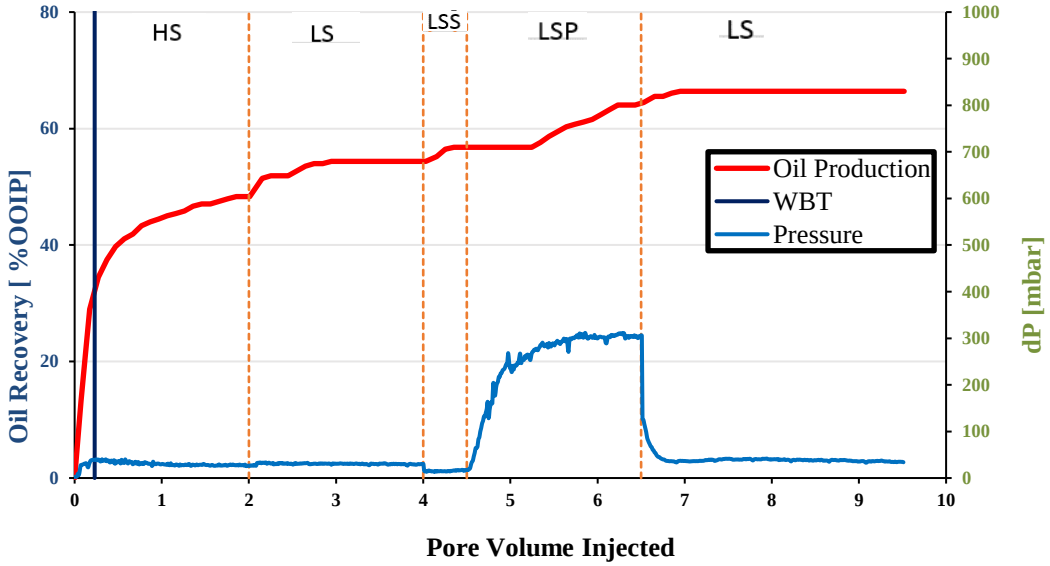

Figure 5.16: Recovery and pressure profile of L4 (aged) of the whole flooding sequences. Dashed lines represent fluid changeover.

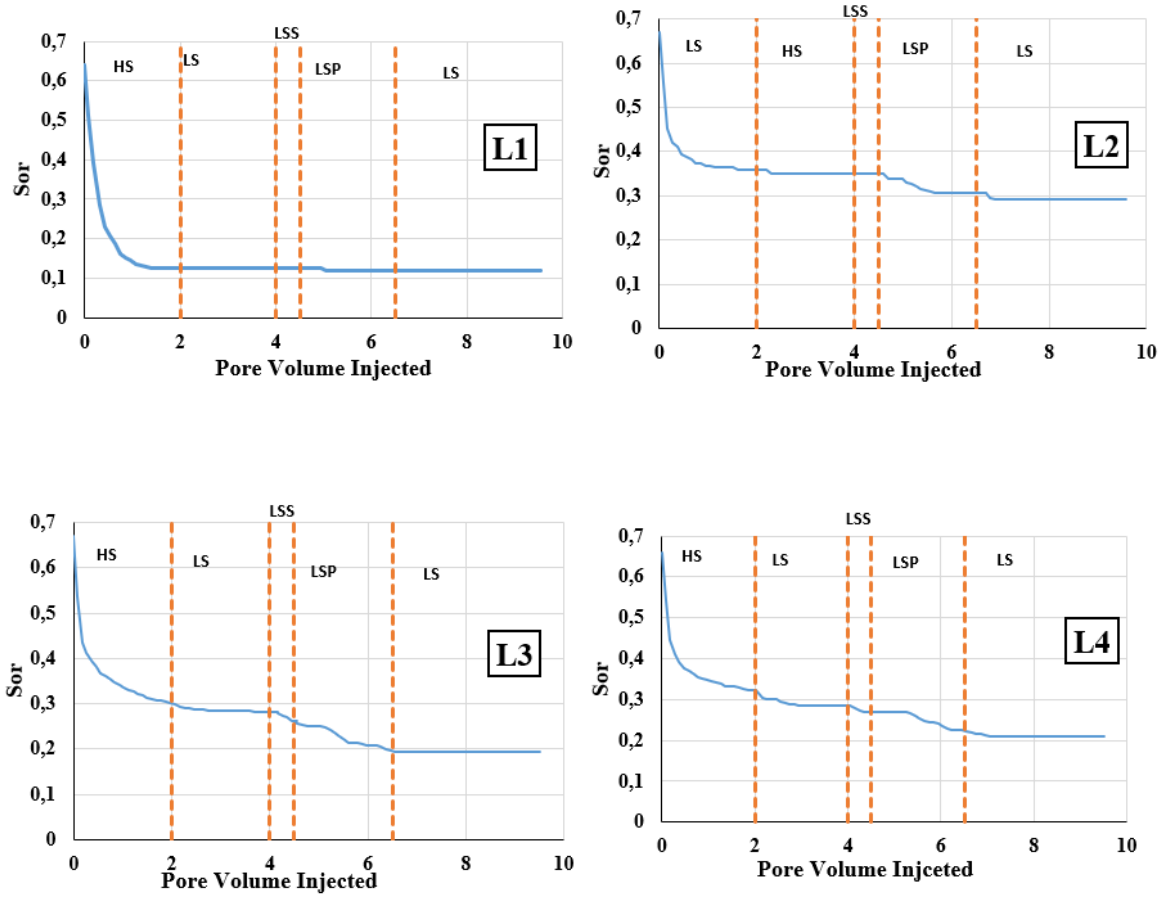

Figure 5.17: Residual oil saturation for the whole flooding sequences of the cores; unaged (L1 and L3) and, aged (L2 and L4)

5.6. Secondary and Tertiary Mode Flooding

5.6.1. Secondary High Salinity (HS) Waterflooding

Firstly, all the long cores (L1-L4) were flooded with high salinity (HS) brine (42404 ppm). The composition of the HS brine listed in Table 4.1.Whereas core L1 and L3 were unaged cores, and L2 and L4 were aged cores. The water flood took place at an elevated temperature of 90°C with an injection rate of 0.1mL/min. The purpose of this step was to recover the oil at secondary oil recovery mode. The HS brine injected until WOR was very high after 2 PV injection, and produced oil volume was insignificant. The results obtained from this step for all the cores are summarized in Table 5.4

5.6.2. Combined Low Salinity, LSS and LSP Flooding

The displacement experiment in the tertiary mode was performed on cores (L1-L4) with low salinity (LS) brine with a salinity of 241ppm, followed by low salinity surfactant (LSS), low salinity polymer (LSP) and finally low salinity(LS) brine as a chase water. The properties of the fluids used are listed in Table 4.2. The displacement experiment took place at 90°C with an injection rate of 0.1mL/min. The aim was to investigate the combined effect of LS, LSS and LSP flooding on further reduction of the residual oil saturation and oil mobilization. The results obtained from this step for all the cores are summarized in Table 5.5

The primary postulation was that the combination of LS, LSS and LSP flooding might have a synergistic effect on oil recovery, i.e., higher oil recovery than injection of just low salinity brine. The reason for this postulation is the fact that the EOR processes such as surfactant flooding and polymer flooding often favor being implemented in low salinity environment[15, 88]. At low salinity condition the retention of polymer or surfactant is decreased, and therefore the bulk injection solution could maintain its initial properties long enough during the flooding process [82, 88].

Observations

Figure 5.13 shows the oil recovery and differential pressure (dP) as a function of pore volume injected PV for core L1 (unaged). HS brine flooding resulted in a recovery factor of 79.1% OOIP. Thus, a significant part of the total volume in place was recovered in this step. Two-phase production continued after WBT (0.29 PV). It should be noted that since the HS brine recovery factor was high, it may not see the full potential of LS in this experiment. Injection of LS brine and LSS gave no additional recovery. Injection of LSP gave a small oil bank coressponding to an additional recovery of 1.3 % OOIP, higher increase in differential pressure was observed during LSP. This gave a recovery factor of 80.4 % OOIP. Injection of 3 PV LS gave no additional oil recovery.

Figure 5.14 shows the results obtained from L2 (aged) core. HS brine resulted in a recovery factor of 43.5% OOIP. Two-phase productions continued after WBT (0.17 PV). Since the recovery factor was low, we expect potential of LS brine injection. Injection of LS brine gave an additional recovery of 1.6% OOIP, thus a recovery factor of 45.1% OOIP. LSS injection did not recover more oil, even if the differential pressure along the core increased. Injection of LSP increased the differential pressure over the core and gave an incremental oil recovery of 6.9% OOIP, corresponding to a recovery factor of 51.9% OOIP. LS injection gave an additional recovery of 2.4% OOIP, resulting in a final recovery of 54.3% OOIP.

Figure 5.15 shows the results obtained from L3 (unaged) core. Note that the pressure for core L3 before 1 PV injected was not measured since the computer restarted while conducting the measurement, all pressure data below one PV injected was lost. HS brine resulted in a recovery factor of 53.2% OOIP, which is ~26% lower than after injection of HS brine for L1. Two-phase productions continued after WBT (0.16 PV). Injection of LS brine and LSS gave an additional recovery of 2.5% OOIP and 3% OOIP, respectively. Corresponding to a recovery factor of 55.7% and 58.7% OOIP respectively. LSP increased the differential pressure, and more oil was recovered in this step; with an additional incremental recovery of 10.7%, corresponding to a recovery factor of 69.4% OOIP. It should be noted that the LSP in core L3 had the highest LSP

recovery factor of all cores. LS injection gave no additional recovery, resulting in a final recovery of 69.4% OOIP.

Figure 5.16 shows the results obtained from L4 (aged) core. HS brine resulted in a recovery factor of 48.3% OOIP, which is ~ 5% higher than L2 during HS brine injection. Since the recovery factor was low, we expect potential of LS brine injection. Two-phase productions continued after WBT (0.23 PV). Injection of LS brine gave an additional recovery of 6.1% OOIP, even if the differential pressure of the core was decreasing; corresponding to a recovery factor of 54.4% OOIP. LSS injection increased both the differential pressure and recovery factor, which gave an additional recovery of 2.4% OOIP, corresponding to a recovery factor of 56.8% OOIP. Injection of LSP increased the differential pressure over the core and gave an additional recovery of 7.7% OOIP, corresponding to a recovery factor of 64.5% OOIP. The second LS brine injection gave an additional recovery of 1.9% OOIP, resulting in a final recovery of 66.4% OOIP.

Based on the waterfloods done in secondary mode, indications of wettability preferences in the cores may be observed. Studies of waterflood characteristic such as oil/water production profiles, water breakthrough (WBT) and endpoint permeability to water may indicate in to which degree the wettability has been altered [84]. This characteristic may serve as qualitative indicators of wettability states.

The aged cores L2- L4, shows early WBT at 0.17 PV and 0.23 respectively. Both cores had significant tail production after WBT; this can be an indication of wettability have been altered to more intermediate/oil-wet during the aging process. According to Figure 5.2, dispersion profiles, L2 had earlier BT compared to L4, which might indicate that the porous medium have isolated pores reducing the PV of interconnected pores that are not participating in flow, which mean that the efficient PV during flow is less than the total PV. From the literature; oil-wet systems have earlier water breakthrough (WBT) with significant oil production continuing for some pore volumes and more extended tail production compared to water-wet systems [37], which was observed in the aged cores. However, comparison of absolute permeability and oil permeability after aging of these two cores shows that L2 responded well to the aging process

than L4. Absolute permeability for L2 was initially 170mD, and after aging it reduced to132mD. Thus a significant change in the permanently was observed. The L4 core had an absolute permeability of initially 154mD and 157mD oil permeability after aging. Thus a small change in the permeability occurred during the aging process.

Unaged core L1 and L3 during HS brine injection show early WBT for L3 at 0.16 PV and L1 0.29 PV. After WBT both cores had significant oil production and tailing production curves. This type of production indicates that the core have less water-wet conditions [25, 39] Another explanation may be that the cores being more heterogeneous, or due to the channeling in the porous medium (Figure 5.2). Dispersion results illustrated in Figure 5.2, shows the earliest BT occurred in L3, and the latest was for core L1. From the literature, WBT for water-wet states should be close to ~ 50 % PV with no two-phase production after WBT.

Observation of the in-situ x-ray saturation monitoring Figure 5.20-Figure 5.26 (X-ray In-Situ Saturation Monitoring), shows that the highest oil produced was during HS brine injection. This can be explained as the cores are at S_{wi} and were conducted to waterflood for the first time.

5.7. Summary of Tertiary Flooding Sequences

5.7.1. Oil Recovery during LS Brine Injection

Observations

Several studies have shown that lowering the brine salinity and ionic strength may give higher oil recovery [49, 57, 111-113]. In a water-wet system, the water occupies the smallest pores and covers the surface of the largest pores, while oil occupies the biggest pores. After establishing S_{orHS}, the trapped oil is trapped by either capillary forces in the largest pores or bypassed as explained in the literature review.

During injection of LS brine in L1(unaged), which will imply that the LS brine mobilizes the trapped oil from the largest pores or bypassed oil, LS brine did not affect the trapped oil in L1. As illustrated in Figure 5.20, higher counting numbers were observed during LS brine injection,

which indicates that some oil has mobilized internally and along the core, without being produced.

For the unaged core (L3), incremental oil recovery was observed during LS brine injection; this may be attributed to the residual oil saturation after HS brine injection S_{orHS} =0.29. As shown in Figure 2.24 higher counting numbers were observed during LS brine injection. Hence, the saturation of the core has changed during LS brine injection.

The explanation behind the incremental oil recovery during LS brine injection of L2 and L4 (aged) may be due to the residual oil saturation after HS brine injection (S_{orHS}= 0.36 PV for L2 and S_{orHS} = 0.32 for L4). The second reason may due to the wettability alteration which may increase the water wetness of the rock surface, and more water can reach the rock surface. As several studies have shown that lowering the ionic strength or changing the brine salinity of the injected brine, may alter the wettability of the carbonate rocks to more water-wet conditions; Alotabibi et al. (2010) [7], Yousef et al. (2011) [49], Al-Attar et al. (2013) [62].

Tang & Morrow (1997) [55] reported that both aging time and temperature influence the oil recovery. The authors reported that during low salinity waterflooding, the oil recovery increased as the aging time and temperature increased. As illustrated in and Figure 5.24 and Figure 5.26 higher counting numbers were observed during LS brine injection, which may indicate that some oil has mobilized internally and along the cores and being produced.

However, some of the literature showed that low salinity effect was not observed in tertiary mode [114]. Jiang et al. (2014) conducted waterflood test with synthetic formation brine SFB (29888 ppm) on three Phosphoria cores (low permeability rock 2mD). Their results showed oil recovery from 38-64 %OOIP in secondary mode. Tertiary low salinity waterflooding (10 times diluted SFB) did not have any effect on oil recovery. They stated their results might be due to the heterogeneity of the reservoir rock which controls the waterflooding.

To reduce the trapped oil by capillary forces, two mechanisms can be used; either reduce the interfacial tension between oil and water or increase the viscous forces. Step one implies adding a surfactant to the injection water, while step two is either increasing the injection rate or increasing the viscosity of the injection water (adding polymer).

5.7.2. Oil Recovery during LSS and LSP Flood

Following the LS injection, the cores were injected with low salinity surfactant (LSS) and low salinity polymer (LSP). The procedure was similar for all cores. The purpose of combined (LSS) and (LSP) flooding was to investigate the effect on oil recovery after establishing low salinity environments in the cores. The experiment was carried out by injecting an LSS slug of 0.5 PV, followed by a 2 PV LSP slug. The production curves are given in Figure 5.13- Figure 5.16 and production results are given in Table 5.5.

Ass illustrated in Table 5.5, additional oil production during LSS injection resulted in incremental recovery of 2.4-3% OOIP. The decrease in interfacial tension may influence the oil production by mobilizing oil that has been trapped, or by invading the smaller uncontacted pores due to more favorable capillary pressure. The LSS injection did not affect the oil recovery of core L1(unaged) and L2 (aged), however incremental recovery for L3 was obtained (unaged) and L4 (aged) of 3% OOIP and 2.4% OOIP, respectively. For core L2 this is not consistent with the work done by Alagic et al. (2011) [84] where aged cores showed a better response to LSS flooding compared to unaged cores. However, this variance may be attributed to the residual oil saturation after LS brine and the rock properties.

As illustrated in Figure 5.24 and Figure 5.26 higher counting numbers was observed during LSS injection in core L3 and L4, which is consistent with the incremental oil recovery. On the other hand, insignificant change in the counting numbers was observed in core L1 and L2, which may indicate that some oil has mobilized internally and along the cores.

Table 5.5 shows the additional oil production during injection LSP, which results in incremental recovery of 1.3– 10.7%. This may be due to the increase of the viscous forces which improve the volumetric sweep efficiency and the favorable mobility ratio.

The primary use of the polymer slug was to maintain stable displacement and mobilize the bypassed oil. Higher differential pressure resulted in oil production in all the cores. The cores

that had the greatest responded to LSP, was L3 (unaged), L4 and L2 (aged). For core L4 and L2 (aged), it is consistent with less retention/adsorption mechanism since oil coat the rock surface and gives less retention of polymer molecules to the rock surface. However, L3 was expected to be more affected by polymer adsorption/retention mechanism (explained more in the pressure profile LSP below) since it is in a water-wet state. An explanation of the incremental oil recovery of L3 might be due to the higher differential pressure, which could attribute to higher oil recovery. On the other hand, the pressure-build up can also due to permeability reduction (explained more in the pressure profile LSP below). Another explanation might be due to the residual oil saturation (0.26 PV) in the core, which was bypassed in the previous flooding. Hence injecting LSP, it mobilizes the trapped oil in the big pores.

As illustrated in Figure 5.20-Figure 5.26, higher counting numbers were observed for L1 and L3, however insignificant change in counting numbers was observed for core L2 and L4 during LSP injection; even if the latter cores decreased the oil saturation along the core. That may designate that some oil had mobilized internally and along the cores.

5.7.3. Oil Recovery during the Second LS Brine Injection

Following the LSP injection, the cores were injected with 3 PV (LS) brine for the second time. The purpose of LS brine injection was to investigate the efficiency as a tertiary injection mode after LSS and LSP. The production curves are given in Figure 5.13- Figure 5.16, and the production results are given in Table 5.5. Since L2 had the highest $S_{or,\ LSP}$ =0.30 after LSP injection, we might expect significant potential of LS brine injection on this core.

L1 (unaged) did not produce more oil during LS brine injection. It can be explained either by capillary forces which are responsible for trapping of oil or perhaps due to the efficient oil recovery by previous floods ($S_{or,\ LSP}$ = 0.11). Notice the lower differential pressure along the core (discussed in detail in the chapter below). However, in-situ saturation monitoring (Figure 5.20) indicated that counting numbers increased significantly during LS injection; this indicates that oil has been mobilized along the core, without being produced.

L2 gave an incremental oil recovery of 2.4% OOIP, which was the highest incremental recovery of all the four cores during the second LS brine injection. As mentioned above, we expected full potential of LS brine on L2 since the core had the highest residual oil saturation at the end of LSP injection. The x-ray in-situ saturation monitoring (Figure 5.22) shows some changes in counting numbers during the second LS injection.

L3 did not produce more oil during the last sequence, note the low differential pressure along the core. However, a small change in counting numbers was detected as illustrated in Figure 5.24.

L4 had $S_{or,\ LSP}$ =0.22 at the beginning of the second LS flood. Hence we may expect some potential for oil recovery during LS brine injection. Figure 5.26 shows an insignificant change in counting numbers along the core, even if the core produced oil. The additional oil recovery in the aged cores (L2 and L4) during the second LS brine was believed to be the mobilized oil during polymer flood, which is a combined effect of low salinity polymer flood.

5.7.4. Pressure Profile

Figure 5.13-Figure 5.16 illustrates the differential pressure along the cores, L1-L4, for each fluid injection. The most common pressure trend for all cores was the jumps induced by changing the injected fluid at the end of each slug. The lowest absolute permeability of the four cores was for the unaged core, L3, (116mD) and the highest was for L2, aged (170mD), we may expect the highest differential pressure from the core with the lowest permeability, and lowest for the core with the highest permeability.

The highest differential pressure observed during HS brine injection was for the core L1 and L3 (unaged). These results may be attributed to the relative permeability (K_{rw}) to water in a water-wet system. In a water-wet system, K_{rw} is much lower compared to K_{rw} in an oil-wet system, due to the water moves through films along the pore walls. Since we assume L1 and L3 are in water-wet/weak water-wet state, the explanation behind the higher differential pressure may be due to the lower relative permeability to water in a water-wet system, which will result in a higher differential pressure along the core.

L1 had the highest oil recovery of all cores during HS brine injection, and the highest differential pressure observed from Figure 5.13. The only core that showed a classical pressure build-up before water breakthrough (WBT), followed by leveling off to a constant and stable differential pressure was L4 (aged). The three other cores showed pressure build up after WBT and irregular pressure gradient profiles during the HS brine injections.

Differential pressure along core L1 during LS injection reached higher differential pressure, before leveling off to a constant pressure; that may be explained by the unstable reading from the pressure apparatus before leveling off. The similar trend was observed for core L2 (aged) during LS injection. Differential pressure increased for L2 continuously before it reached a stable pressure, which may explain the 1.6 % OOIP incremental oil recovery. L3 showed steady differential pressure and increased continuously without leveling off, that may explain the increase in recovery factor during LS injection.

L4 showed increasing differential pressure during LS injection, before reaching a stable pressure. L4 had the highest incremental oil recovery during LS injection (6.1% OOIP). According to a study reported by Yousef et al. 2011 [49] on aged carbonates with low salinity water injection (explained in the literature review section), they observed a constant reduction of pressure profile with an injection of different diluted salinity brine. They reported that reduction in differential pressure is an indication of alternation of brine/oil/ rock interactions. They confirmed their experiment by contact angle measurements. Yousef et al. observation of pressure decrease with lower salinity brine injection are not in line with what obtained in this experiment on aged cores. This can be due to the difference in the petrophysical properties of the cores.

L1 and L2 shows an irregular pressure gradient during LSS injection. L1 shows a fluctuating pressure gradient throughout the LSS flood. L2 shows a pressure build-up, followed by an abrupt pressure; which may indicate remobilization of blockage in pore constrictions and mobilization of fluid. No oil production was observed during LSS for L1 and L2. However, the

results of the x-ray in-situ saturation monitoring Figure 5.20 and Figure 5.22 shows that oil redistributed along the cores.

L3 shows continuously pressure build up throughout the LSS flood. The pressure build up may explain the highest incremental oil recovery during of L3 (3%OOIP) during LSS injection. Note that L3 had the highest continuously pressure build during LSS injection, this may be due to the formation of an oil bank induced by the decreased interfacial tension between oil and water.

L4 shows the lowest differential pressure of all four cores. L4 had lower differential pressure during LSS compared to LS. However, incremental oil recovery was observed (2.4% OOIP).

Interestingly, L4 produced oil even if the pressure was constant compared to L1 and L2, which might be due to the formation of an oil bank induced by a decrease in interfacial tension between oil and water. Another factor that may explain the pressure behavior is adsorption/ retention of the surfactant molecules on the rock surface. When aging the cores, rock wettability may have changed, and the rock surface may develop more oil-wet state. At these conditions, oil occupying adsorptions sited on the rock surface and thus making the fewer sites available for surfactant adsorption. When there is less retention in a porous medium, the differential pressure along the porous medium decreases, due to higher flow paths.

The highest differential pressure observed in this experiment was for the cores L1 and L3 (unaged) during LSP injection. L1, L2, and L4 show similar pressure build-up tendency during LSP injection. L1 shows increasing in differential pressure throughout LSP injection and gave an incremental oil recovery of 1.3%OOIP. Interestingly, L3 (unaged) had the similar pressure build up with fluctuating pressure gradient and gave an incremental oil recovery of 10.7% OOIP. However, this may be attributed to the low recovery factor of L3 compared to L1 after earlier slugs.

L2 and L4 (aged) showed the same pressure build-up tendency and gave an incremental oil recovery of 6.9% and 7.7% OOIP, respectively. Note that neither of L1 nor L2 did produce any oil during LSS injection. However, higher pressure build up for L2 was observed during LSS.

Hence that may explain the high production of oil during LSP. The oil may have been mobilized along L1 and L2, during LSS (Figure 5.20 and Figure 5.22) and produced oil during LSP.

The observed pressure build up might be a result of either viscous effect of the fluid or pore blocking and permeability reduction [64]. Interestingly, the dP was more than twice as for unaged cores L1 and L3 (i.e., 600 ~700 mbar) compared to aged cores L2 and L4 (i.e., ~300mbar). The higher pressure build up might be attributed to the higher retention/adsorption of polymer on unaged cores (water-wet rock surface) compared to aged cores (oil-wet/ intermediate rock surface). The adsorption retention mechanism of the polymer is lower for aged material compared to unaged materials [115]. After aging the cores, oil "coat" the rock surface, which might reduce the polymer molecules to interact with the rock surface, hence reduce polymer adsorption. On the other hand, water-wet rock surface has higher polymer adsorption and may results in poor sweep efficiency as a result of polymer molecule losing their viscosifying effect [88].

Another explanation of pressure build up is the permeability reduction, due to polymer retention which leads to a lower permeability and may result in a pressure build up. The permeability reduction effect is most significant for a porous medium with low permeability [88]. L1 and L3 had an absolute permeability of 160mD and 116mD, respectively. L2 and L4 had a permeability of 170mD and 154mD. From the absolute permeability quantities, pore blocking/permeability reduction should be highest of L3. Hence we expected higher differential pressure for L3.

L3 showed high and irregular differential pressure throughout the LSP injection. An effluent sample of the polymer solution was investigated (after 1.8 PV injected), for comparison of the viscosity before and after injection to examine if retention has occurred in core L3. The viscosity measurement showed 88% reduction in viscosity. Which may be explained by adsorption of the bulk polymer solution on the rock surface, hence increasing the differential pressure in core L3 (Explained in detail in the Polymer Effluent Results, chapter 5.7.6). Chippa et al. (1999) [115] postulated in their paper that the permeability reduction observed after a polymer flood was caused by an adsorbed polymer layer that reduces pore throat radii.

L1 did not produce a significant amount of oil, on the other hand, L3 had almost the same differential pressure and gave an incremental recovery of 10.7% OOIP. It can be explained by, L1 produced a significant amount of oil during HS brine injection, while L3 still had a significant volume of oil before the LSP injection.

As illustrated in Figure 5.13-Figure 5.16 the pressure build up at the start of second LS injection shows similar behavior for all cores; this can be related to change from LSP to LS brine. After 0.5 PV LS injection in core L1, the pressure stabilized and reached similar values as the first LS injection, hence pore blocking /permeability reduction could perhaps not occurred during LSP injection. L2 shows the similar behavior as L1, pressure decreased and stabilized after 0.5 PV (lower than first LS injection) during LS injection. Note that incremental oil recovery (2.4% OOIP) occurred throughout the first 0.5 PV injected, that could relate the pressure build up to the incremental oil recovery as well as possible mobile oil in the system.

L3 had the lowest pressure build of all the cores during LS injection and did not produce more oil during LS injection. This could be related to the low Sor (0.19 PV) during the previous floods. L4 had higher pressure build compared to LS during the first injection, and 1.9% OOIP incremental oil recovery was observed.

To conclude, L3 had the lowest absolute permeability of all cores, which reflected in high pressure during LSP. L2 had the highest absolute permeability and showed the lowest differential pressure during LSP.

As mentioned in the literature review using low salinity water for polymer/surfactant flooding is more economical compared to high salinity polymer flooding. The economic benefits are attributed to less retention mechanism of polymer/surfactant at low salinity environments. Thus, less polymer/surfactant are required to enhance oil production.

5.7.5. Effective/ Water Relative Permeability

Table 5.6 Experimental permeabilities results

Core ID	Abs.Permeability (Kw) [mD]	$K_o(S_{wi})$ [mD] Primol 542	$K_o(S_{wi})$ [mD] After aging	$K_w(S_{or,LS})$ [mD] @90℃	$K_w(S_{or,LS})$ [mD] @22℃	$K_{rwS_{or,LS}}$ @90℃	$K_{rwS_{or,LS}}$ @22℃
L1	160	179	-	36	26	0.23	0.17
L2*	170	215	132	83	51	0.49	0.30
L3	116	201	-	138	88	-	-
L4*	154	216	157	25	29	0.16	0.19

*Aged core

Table 5.6 shows the experimental results of the effective permeability after the last LS flood at S_{or} and the corresponding water relative permeability at different temperatures. Note that water relative permeability was calculated based on the absolute permeability. The water relative permeability for core L1 (unaged) at the end of LS injection was 0.23 and 0.17 (at S_{or} = 0.11). As illustrated in Table 5.6, water effective permeability shows a systematic decrease (36mD and 26 md) for L1. The water relative permeability for core L2 (aged) at the end of LS injection was 0.49 and 0.30 (at S_{or} = 0.29). A similar trend to L1 was observed, where water effective permeability decreased (83mD and 51mdD). L4 (aged) core shows an increase in the water relative permeability, 0.16 to 0.19 (at S_{or} = 0.21) at ambient temperatures compared to 90˚C. The explanation behind the water relative permeability for L4 may be due to the uncertainty of the viscosity measurements, where the uncertainty is ± 5 % of the absolute viscosity value measured.

Comparison of differential pressure during the second LS brine injection with water endpoint relative permeability may give indicators of wettability states. The average differential pressure of core L1, L2 and L4 during LS brine second injection was ~ 17mbar, ~ 11mbar, and ~ 39 mbar respectively. For a water-wet porous medium, the endpoint relative permeability is low and affect differential pressure along the core by increasing differential pressure. As illustrated in Table 5.6, L1 and L4 had lower endpoint relative permeability compared to L2 and had higher differential pressure compared to L2. However, more investigation need to be done to conclude our observations regarding endpoint relative permeability.

The polymer can reduce the permeability due to the retention mechanism; polymer adsorption/ or trapped within the small pores. The adsorbed polymer layer changes the flow properties of the rock and may reduce the water permeability [115].

The temperature affects relative permeability by, lowering the residual oil saturation and increase the irreducible water saturation [18]; as stated, at higher temperatures interfacial tension between oil and water decrease, as well as contact angle between COBR system, thus at higher temperatures the rock becomes more water-wet. Relative permeability to oil increase while relative permeability to water decreases at any given saturation. This was observed in the results above, except L4, where *krw* decreased when it was measured at ambient temperature, which perhaps may be explained as accuracy in the viscosity at higher temperatures.

Some conclusion can be made from the results obtained in this experiment. The results of water endpoint relative permeability $k_{rw,\,LS2}$ to core L1 was consistent with the initial wettability state of the core. L1 showed a tendency to be in a less water-wet state, referring to the time of WBT and the higher $k_{rw,\,LS2}$ at the end of the second LS brine injection. L2 (unaged) resulted in higher water endpoint permeability and early WBT. Thus, the wettability may have altered during the aging process. Another reason that may strengthen this conclusion was due to the significant change in the absolute permeability compared to oil permeability after aging. Comparison of the absolute permeability compared to oil permeability after aging for L4 shows an insignificant change in these two quantities. Thus, a small change in wettability occurred during the aging procedure, which can be reflected in WBT and endpoint effective permeability. Another explanation for the low $k_{rw,\,LS2}$ might be due to the lower salinity brines, which might alterd the wettability back to the core initial wettability state.

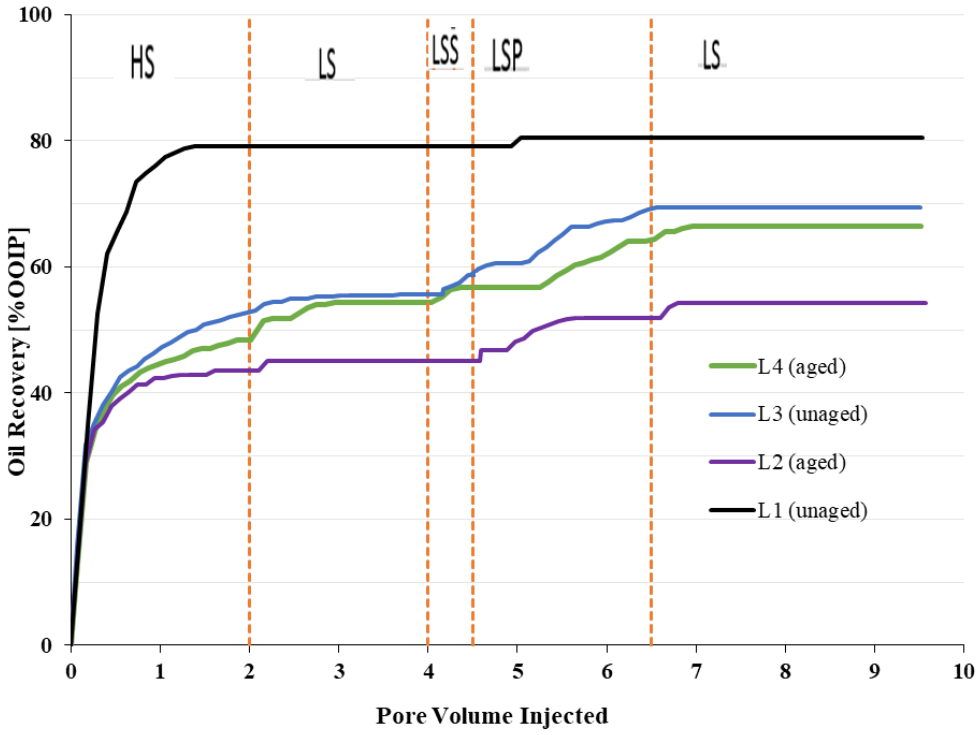

Figure 5.18: Oil recovery profile of the different flooding sequences in core L1-L4

5.7.6. Polymer Effluent Results

As mentioned in the literature review polymer flow in porous media is complicated as it travels through variation of pores and pore throats. As illustrated in Figure 5.19 comparison of apparent viscosity (10cP) and rheometer viscosity (84cP) at a shear rate of $10s^{-1}$, corresponds to 88% reduction in viscosity after 1.8 pore volume polymer injected in core L3 (unaged). This could be attributed to three factors. Polymer solution is exposed to shearing (mechanical degradation) in the porous medium, which tends to make the polymer molecules to lose their viscosity effect. However, it is not possible that this was the main factor since the flow rate was low (0.1 mL/min), hence shear rate was low in this experiment and it is not enough to reduce the viscosity. The second explanation is the retention/adsorption (polymer adhesion to pore walls), thus lowering the viscosity. The third and main effect could be that polymer has been exposed to higher temperatures (90°C) (hydrolysis will be rapid [88], as the effect of temperature and oil present at higher temperatures) which may decrease the viscosity of the polymer solution.

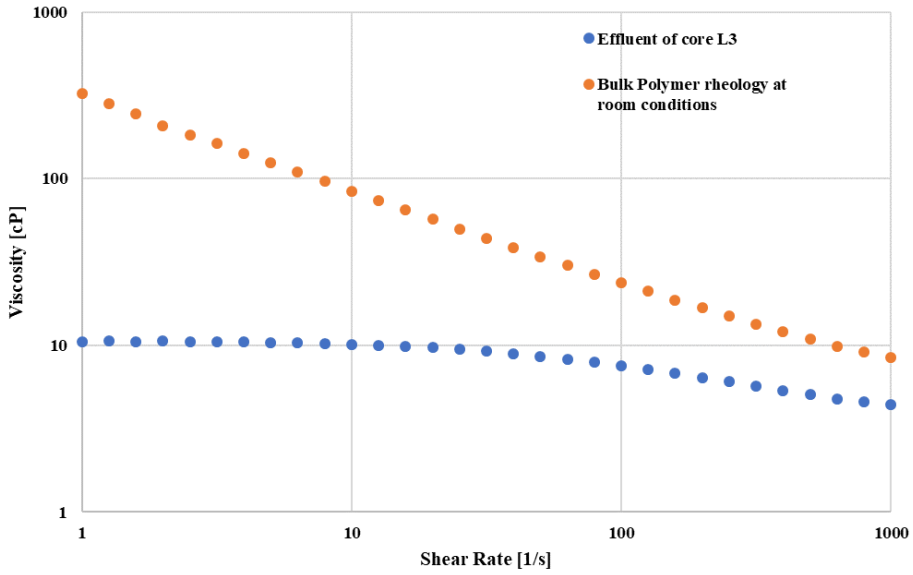

Figure 5.19: Illustrates the bulk polymer rheology at room conditions and the polymer effluent solution after 1.8 pore volume injected in core L3 (unaged) measured at room conditions.

5.8. X-ray In-Situ Saturation Monitoring

The x-ray count numbers as a function of core length for the x-ray in-situ saturation monitoring of cores L1-L4 are illustrated in (Figure 5.20, Figure 5.22, Figure 5.24, and Figure 5.26). The maximum points represent the saturation at 100% formation water saturation and the minimum points, represent the core at irreducible water saturation S_{wi}. Note that the S_{wi} x-ray saturation monitoring was conducted with tagged crude oil for L1-L4 (L2 and L4 after aging). The x-ray in-situ saturation monitoring gives information about the possible in-situ redistribution of the fluids in the core. Moreover, it also could provide if the oil recovery is influenced by capillary end-effect, as well as the source of extra oil recovered by low salinity injection. The first observation to make is that the x-ray count numbers decrease with increase in oil saturation. L1-L4 showed similar saturation change along the cores when HS brine was injected, which is consistent with the results obtained above (flooding experiment).

Based on Figure 5.20 of L1 (unaged), two observations can be made. The first one is the observed heterogeneity of the porous medium (circled) in the figure. The change in the x-ray count number at the same position for the different fluids, which indicates characteristics of the porous medium. Observation two was due to the similar relative change in x-ray count numbers during each fluid injection. As illustrated in the figure (circled) the same change occurs at the same position. The same level of counting numbers is shifted downwards (from FW to the other fluids) at the same position. That means that it was no shift from single phase to two-phase. Which indicates no capillary end-effects and a homogeneous saturation change along the core.

Figure 5.22 illustrates the x-ray counting numbers for core L2 (aged). Three observations can be made. The first one is, no observation of a slope towards Swi. Instead, it is observed a stable x-ray count number with the same level, similar to L1 at S_{wi}. The second observation is the slopes in FW and the injected fluids (first circle). A systematic change observed from the figure in all the displacement between FW and S_{wi}, which indicate more heterogenic saturation with length. The third observation was the peak in the injected fluids (circle two), which was not the same as FW. If the system were homogenous, we would expect the same pattern throughout the injected fluids. The two-phase saturation is different than L1, more heterogeneous saturation changes along core L2. Note the counting numbers, decreased during LSS injection, especially

from the middle of the core towards the outlet. This may be coupled to oil bank formation during LSS flooding. This is consistent with oil production during polymer flooding as illustrated in Figure 5.14

L3 (unaged) and L4 (aged) were cut from the same batch. However, they differ from another in x-ray count numbers at 100 % FW and Swi (Figure 5.24 and Figure 5.26). In the case of L3, it shows more unstable x-ray count numbers at S_{wi} and different pattern than the other saturation, which may be explained by the heterogeneity of the porous medium. However, for the FW and the saturation between it shows the same pattern throughout the core (circled in the figure), which indicates homogenous saturation along the core with two-phase. The heterogeneity is visualized in the count numbers, moreover in the two-phase as illustrated in the figure.

L4 shows somehow insignificant change in x-ray counting numbers; this is inconsistent with oil bank produced during polymer flooding, Figure 5.16. Probably, the accuracy in x-ray counts limits detection of the oil bank.

The consequence of the homogenous saturation observed in the figures above within the uncertainty in the x-ray measurements indicate that there were no capillary end-effects phenomena. Thus, we believe that the additional oil production was due to the low salinity effect. However, further investigation is needed to explain the mechanism(s) behind the low salinity effect. For instance, wettability measurements such as wettability indexes would have strengthened our conclusion if the wettability altered due to the low salinity injection. Capillary pressure curves could be used as a wettability indicator to identify the possible wettability shift and its direction during low salinity injection.

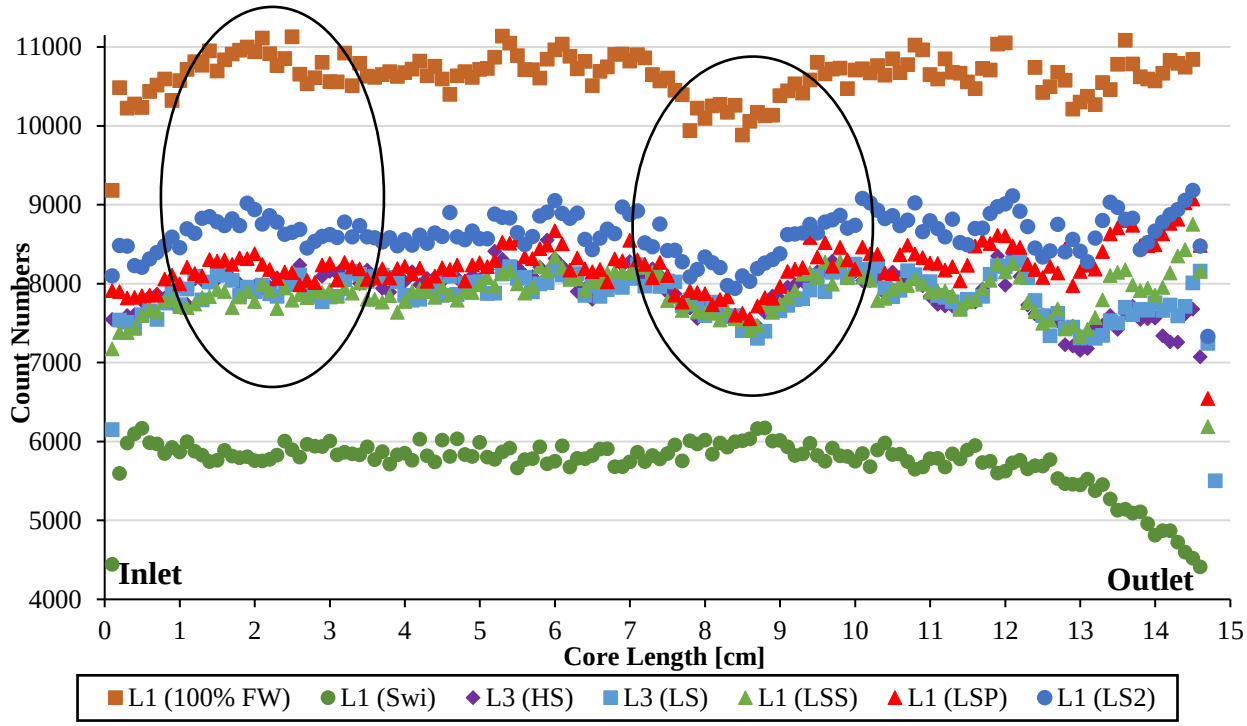

Figure 5.20: X-ray in-situ saturation monitoring after each flooding process in core L1 (unaged). The circles indicate the heterogeneity of the material

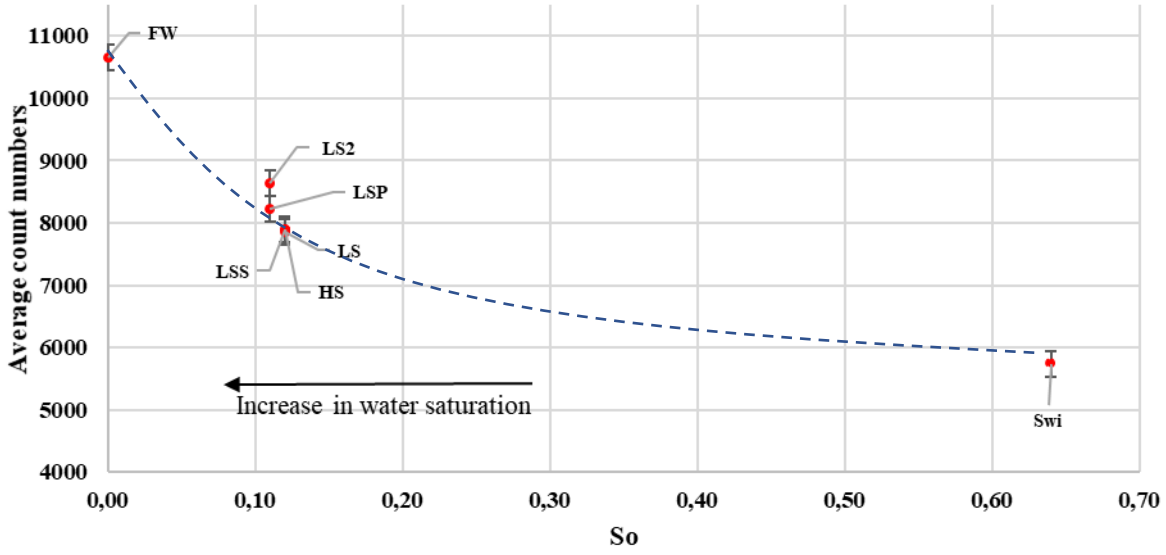

Figure 5.21 : Illustrate the average count numbers versus oil saturation and the different flooding sequences for L1 (unaged). Assuming linear count numbers

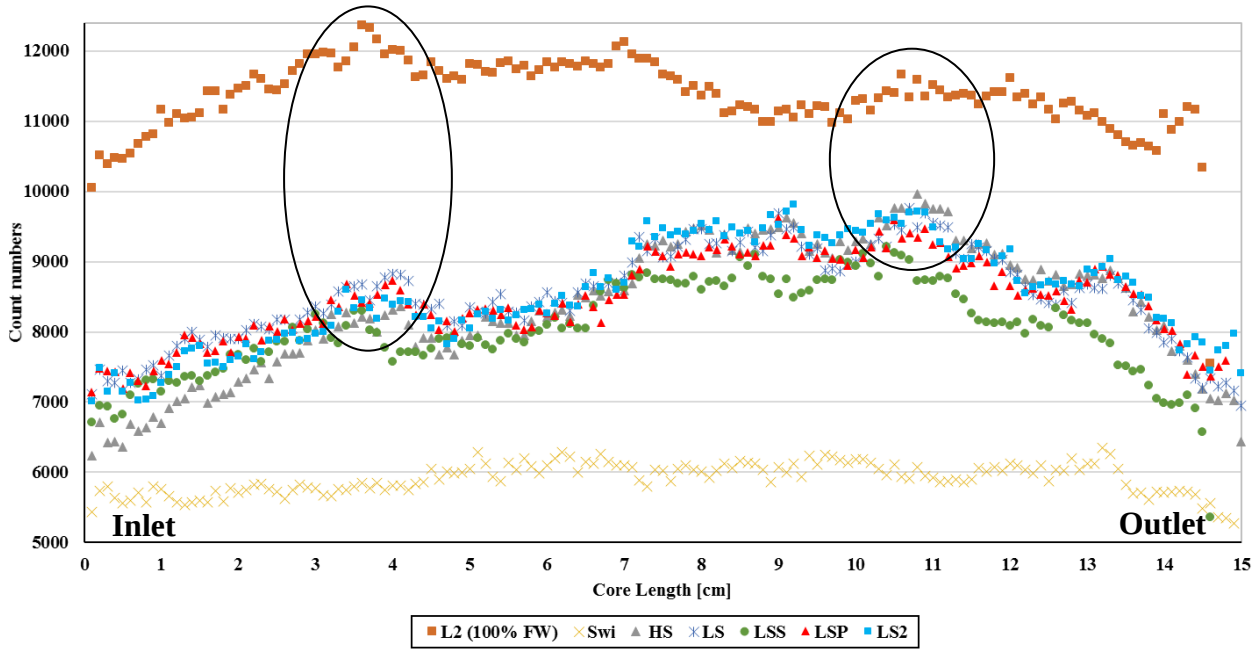

Figure 5.22: X-ray in-situ saturation monitoring after each flooding process in core L2 (aged). The circles indicate the heterogeneity of the material

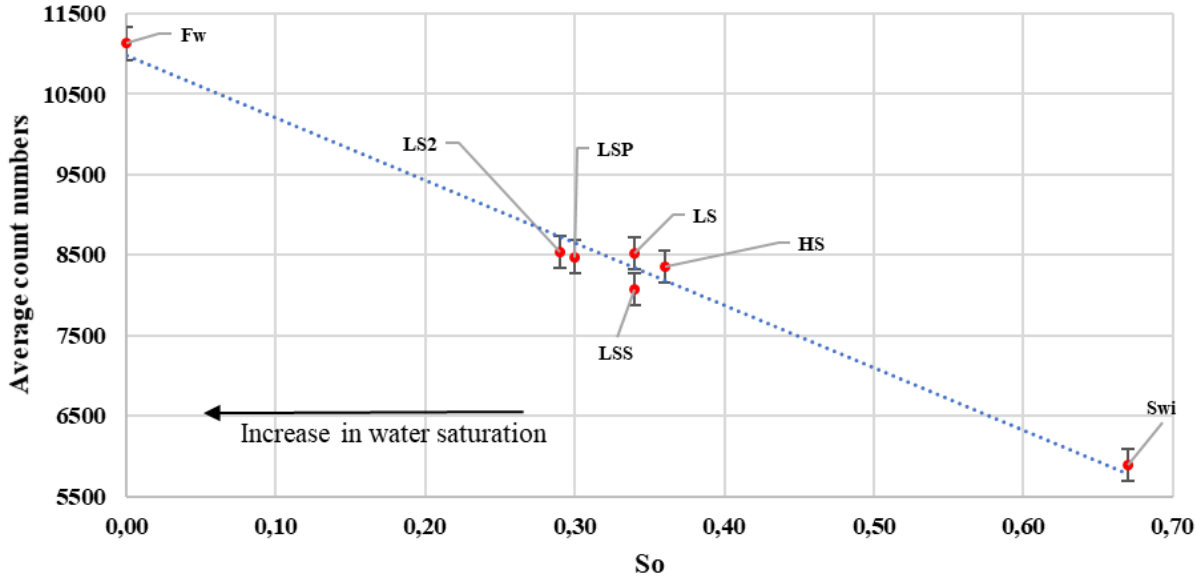

Figure 5.23: Illustrate the average count numbers versus oil saturation and the different flooding sequences for L2 (aged). Assuming linear count numbers

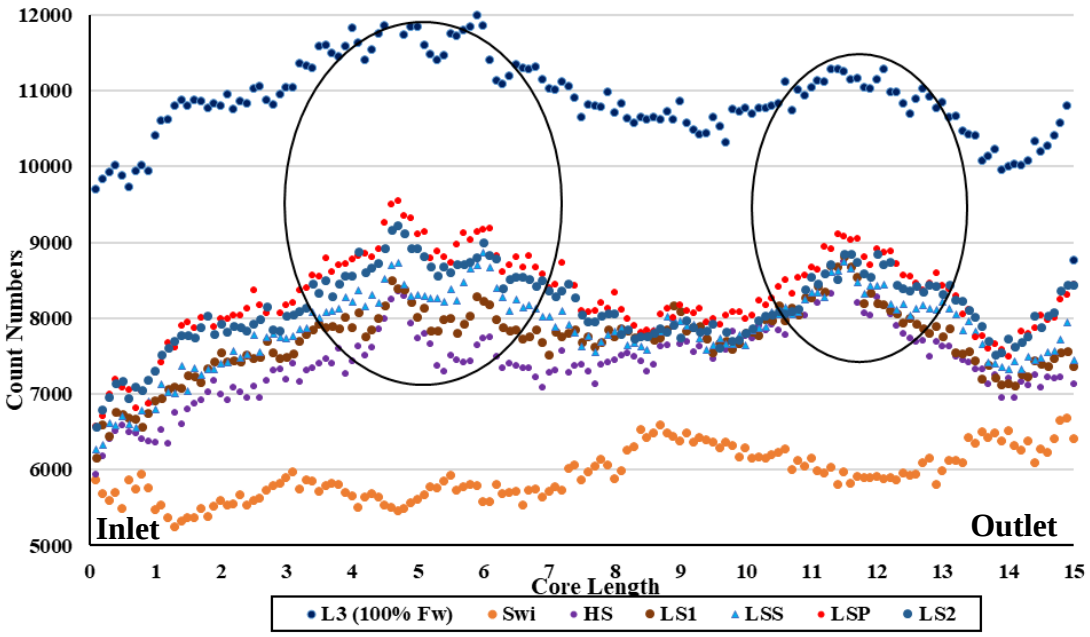

Figure 5.24: X-ray in-situ saturation monitoring after each flooding process in core L3 (unaged). The circles indicate the heterogeneity of the material

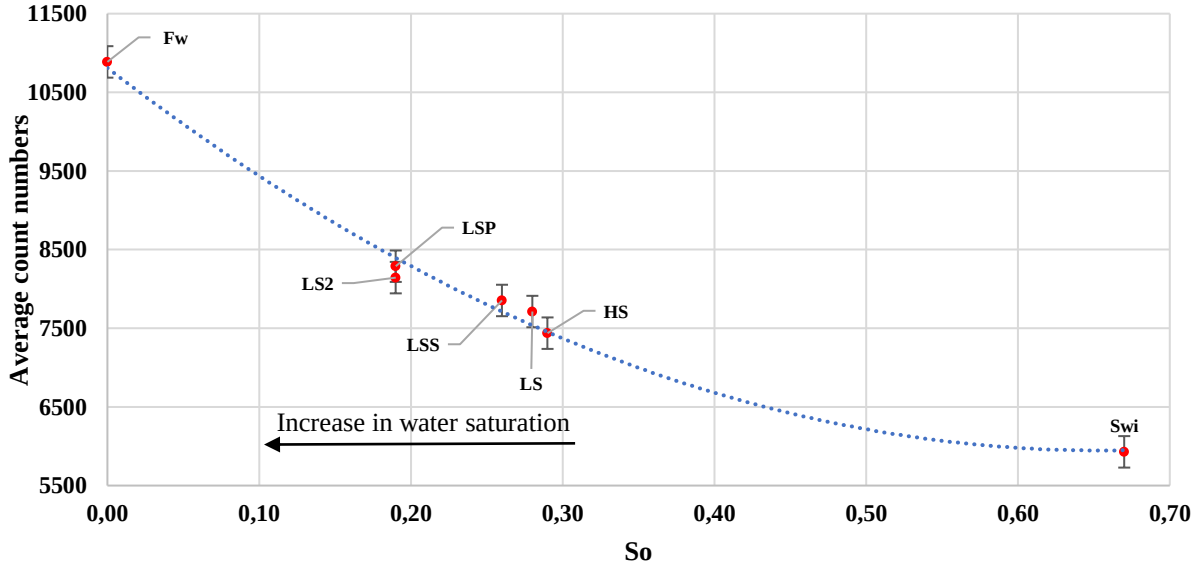

Figure 5.25: Illustrate the average count numbers versus oil saturation and the different flooding sequences for L3 (unaged). Assuming linear count numbers

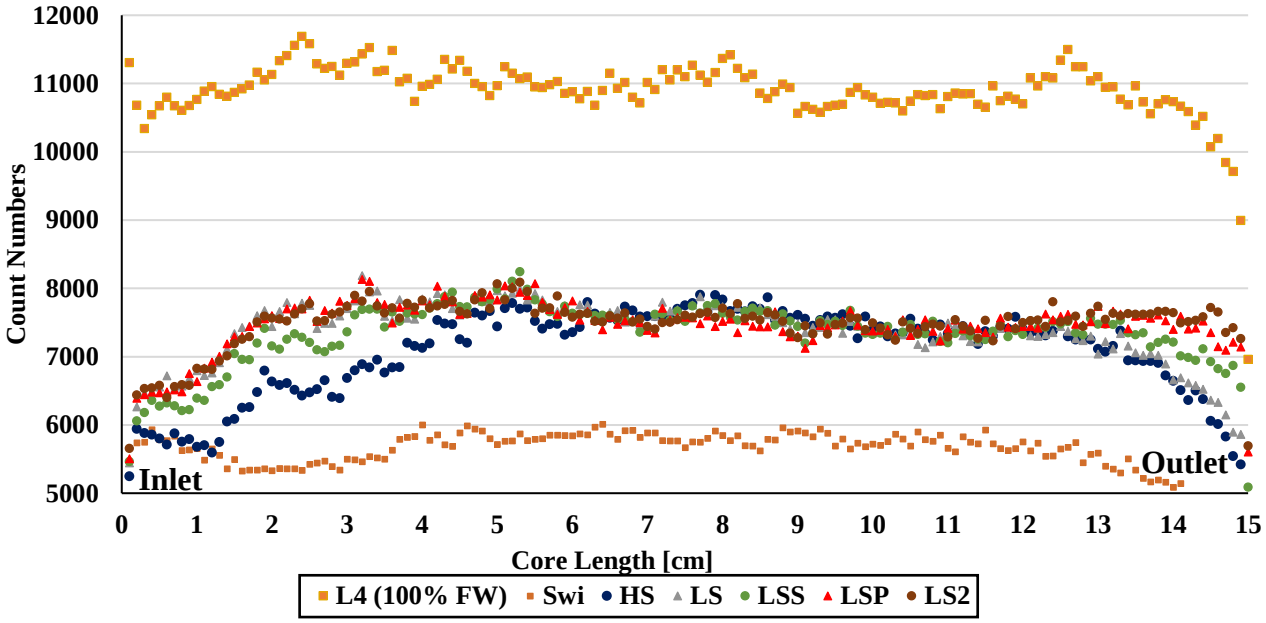

Figure 5.26: X-ray in-situ saturation monitoring after each flooding process in core L4 (aged)

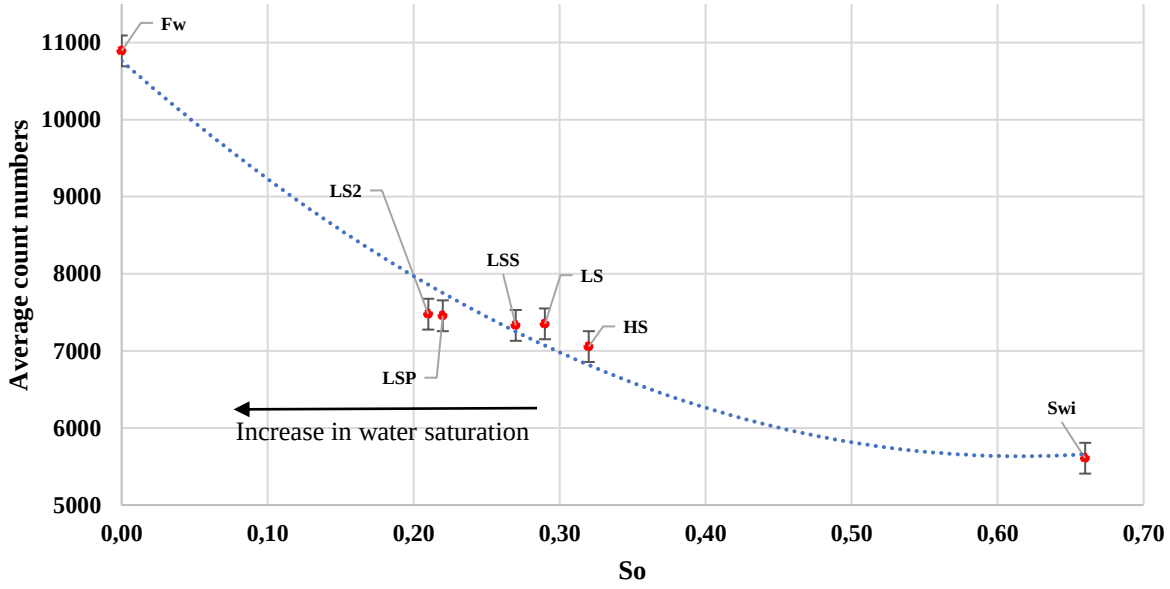

Figure 5.27: Illustrate the average count numbers versus oil saturation and the different flooding sequences for L4 (aged). Assuming linear count numbers

Table 5.7: Comparison of estimiated change in x-ray saturation units LSP-HS versus change in saturation units of Sor (material balance)

Core ID	Δ in Count number Sw=1-Swi	Soi [%]	Saturation* units Fw-Swi	Uncertainty in saturation units [± %] from x-ray	Δ in Count number from LSP-HS	Saturation units LSP-HS Count numbers [%]	Saturation** units LSP-HS Sor [%]
L1	4918	64	77	3	332	4	1
L2	5243	67	78	3	128	2	6
L3	4958	67	74	3	851	12	10
L4	5284	68	78	3	400	5	10

*Assuming linear count number versus saturation

** Material balance calculations (Change in Sor from LSP to LS1)

Table 5.7 represents a comparison of the change of saturation units of 100% water saturation (Fw) to S_{wi} and LSP to HS brine. We assume that our model is linear (Figure 5.21, Figure 5.23, Figure 5.25 and Figure 5.27) and have an uncertainty in the count numbers (averaged) of ± 200 count numbers. The x-ray count numbers below may be not visual in x-ray saturation monitoring.

The purpose of these calculations was to compare the change in saturation units of x-ray count numbers LSP- HS versus the change in saturation units obtained from S_{or} (material balance). The uncertainty was ± 3% saturation units correspond to ± 200 count numbers. Based on the x-ray count numbers we get saturation changes during the different floodings. As illustrated in the table, small changes in saturation units of LSP-HS; L1 (4%), L2 (2%), and L4 (5%) was obtained based on x-ray counting numbers. Therefore it is difficult to see these changes in the x-ray count numbers plots. However, L3 shows the highest deviation in saturation units (12%) which is out of the range of the uncertainty, and it was observed in Figure 5.24 (HS and LSP).

6. Conclusions

The potential for enhanced oil recovery by combined low salinity, low salinity surfactant and low salinity polymer flooding in aged/unaged four long Indiana Limestone rock material have been investigated through laboratory measurements. Also, laboratory water imbibition tests were conducted on four short aged/unaged Indiana Limestone outcrop to examine how aging process influence oil recovery during brine with low ionic strength.

- Imbibition test on aged short cores using low salinity brine shows limited potential. Incremental oil recovery of 0.2 to 0.4% OOIP was observed during brine change over from HS to LS brine. The mechanism behind the incremental oil production was believed to be due to wettability alteration.
- Imbibition tests on unaged short cores using low salinity brine gave no incremental oil recovery.
- High salinity injection into the long cores in a secondary mode resulted in a recovery factor of 43% to 79% OOIP.
- Low salinity injection resulted in an incremental recovery of 1.6% to 6.1% OOIP, whereas the highest incremental oil recovery was (6.1% OOIP) observed in L4 (aged). Thus, indicating the potential of low salinity effect. This could be attributed to wettability alteration mechanism as reported in the literature. However, indicators other than endpoint relative permeabilities are required to detect the direction of the wettability shift.
- Low salinity surfactant (LSS) injection gave an incremental recovery of 2.4% to 3% OOIP in L4 (aged) and L3 (unaged), respectively.
- Significant oil production in aged cores was achieved during LSP flooding, even though the differential pressure was considerably lower than the differential pressure in unaged cores.
- Higher oil recovery is achieved by low salinity surfactant/polymer flooding with less need to surfactant/polymer, due to less adsorption/retention in low salinity environments, which have economic advantages.
- It was observed that aged cores responded better to the second low salinity brine injection compared to the unaged core. The additional oil recovery in the aged cores was believed to be the mobilized oil during polymer flood.

- X-ray in-situ saturation monitoring showed a change in recovery below the detection limit for x-ray in most experiments. Within the accuracy of x-ray count numbers, it was observed that there were no capillary end-effects in the cores, which indicates that the additional oil recovery by combining of low salinity, LSS and LSP flooding is not affected by capillary end-effect but is due to low salinity effect.

7. Further Work

Despite the growing interest in low salinity waterflooding, there are still many aspects which need to be further investigated.

- An effluent analysis should be carried out to give a better understanding of how the low salinity waterflooding works and the mechanisms behind it that lead to improving oil recovery. These analyses are effluent pH, and the concentration of the ion composition presents in the effluent compared to the injected brine.

- Investigation of LS effect in a secondary mode, to study if it would be beneficial to oil recovery. This could be further extended to study the effects of LS brine on different wettability systems in secondary mode.

- Further investigation is needed to explain why low salinity brine had a positive response to the long cores flooding sequence. For instance, wettability measurements such as wettability indexes would have strengthened our conclusion if the wettability altered due to the low salinity. Moreover, investigate how low salinity influenced the capillary pressure curves.

- A simulation study of combined low salinity brine, low salinity surfactant and polymer flooding in secondary and tertiary modes is recommended to confirm the results from displacement experiments and to get a better understanding of the mechanisms controlling the increased oil recovery by this hybrid method.

8. References

1. Flügel, E., *Microfacies of carbonate rocks : analysis, interpretation and application*, A. Munnecke, Editor. 2010, Springer: New York.
2. Morrow, N. and J. Buckley, *Improved Oil Recovery by Low-Salinity Waterflooding.* Journal of Petroleum Technology, 2011. **63**(5): p. 106-112.
3. Akbar, M., et al., *A snapshot of carbonate reservoir evaluation.* Oilfield Review, 2000. **12**(4): p. 20-41.
4. Chilingar, G.V. and T.F. Yen, *Some Notes on Wettability and Relative Permeabilities of Carbonate Reservoir Rocks, II.* Energy Sources, 1983. **7**(1): p. 67-75.
5. Treiber, L.E. and W.W. Owens, *A Laboratory Evaluation of the Wettability of Fifty Oil-Producing Reservoirs.* Society of Petroleum Engineers Journal, 1972. **12**(06): p. 531-540.
6. Kuchuk, F., M. Sengul, and M. Zeybek, *Oilfield Water: A Vital Resource.* Middle East Well Evaluation Review, Number 22, 1999: p. 4-13.
7. Alotaibi, M.B., R. Azmy, and H.A. Nasr-El-Din, *Wettability Challenges in Carbonate Reservoirs*, in *SPE Improved Oil Recovery* 2010, Society of Petroleum Engineers: Tusla, Oklahoma, USA 24-28 April 2010.
8. Manrique, E.J., et al., *EOR: Current Status and Opportunities*, in *SPE Improved Oil Recovery Symposium*. 2010, Society of Petroleum Engineers: Tulsa, Oklahoma, USA.
9. Gupta, R., B. Adibhatla, and K.K. Mohanty, *Parametric Study to Enhance Oil Recovery Rate from Fractured Oil Wet Carbonate Reservoirs*, in *SPE Annual Technical Conference and Exhibition*. 2008, Society of Petroleum Engineers: Denver, Colorado, USA.
10. Seethepalli, A., B. Adibhatla, and K.K. Mohanty, *Wettability Alteration During Surfactant Flooding of Carbonate Reservoirs*, in *SPE/DOE Symposium on Improved Oil Recovery*. 2004, Society of Petroleum Engineers: Tulsa, Oklahoma.
11. Zolotuchin, A.B. and J.-R. Ursin, *Introduction to petroleum reservoir engineering*. 2000, Kristiansand: Høyskoleforlaget.
12. Stephan, B. *Porosity Explained*. PetroProphet 2016 [cited 2017 19.06.2017]; Available from: https://www.petroprophet.com/porosity-explained/.
13. Hook, J.R., *An introduction to porosity.* Petrophysics (Houston, Tex.), 2003. **44**(3): p. 205-212.
14. Skarestad, M. and A. Skauge *Reservoarteknikk 2, PTEK 213, fluid propeties and recovery methods, UIB 2009.* 2009.
15. Lake, L.W. and E. Society of Petroleum, *Enhanced oil recovery*. 2010, Richardson, Tex: Society of Petroleum Engineers. 550.
16. Churcher, P.L., et al., *Rock Properties of Berea Sandstone, Baker Dolomite, and Indiana Limestone*, in *SPE International Symposium on Oilfield Chemistry*. 1991, Society of Petroleum Engineers: Anaheim, California, 20-22 February.
17. Freire-Gormaly, M., et al., *Pore Structure Characterization of Indiana Limestone and Pink Dolomite from Pore Network Reconstructions.* Oil & Gas Science and Technology, 2016. **71**(3): p. 33.
18. Donaldson, E.C., G.V. Chilingarian, and T.F. Yen, *Enhanced oil recovery: 1: Fundamentals and analyses*. Vol. 1. 1985, Amsterdam: Elsevier.
19. Anderson, W.G., *Wettability Literature Survey Part 5: The Effects of Wettability on Relative Permeability.* Journal of Petroleum Technology, 1987. **39**(11): p. 1453 - 1468.

20. Gharbi, O. and M.J. Blunt, *The impact of wettability and connectivity on relative permeability in carbonates: A pore network modeling analysis.* Water Resources Research, 2012. **48**(12): p. 1-14.
21. Anderson, W., *Wettability Literature Survey- Part 1: Rock/Oil/Brine Interactions and the Effects of Core Handling on Wettability.* Journal of Petroleum Technology, 1986. **38**(10): p. 1125-1144.
22. Lien, J.R., *PTEK212 Reservoarteknikk 1, Institutt for Fysikk og Teknologi, Universitet i Bergen.* 2011.
23. Skauge, A., et al., *Theoretical and experimental evidence of different wettability classes.* Journal of Petroleum Science and Engineering, 2007. **57**(3): p. 321-333.
24. Høiland, L., K. Spildo, and A. Skauge, *Fluid flow properties for different classes of intermediate wettability as studied by network modelling.* Transport in Porous Media, 2007. **70**(1): p. 127-146.
25. Salathiel, R.A., *Oil Recovery by Surface Film Drainage In Mixed-Wettability Rocks.* Journal of Petroleum Technology, 1973. **25**(10): p. 1216-1224.
26. Golsanami, N., A. Kadkhodaie-Ilkhchi, and A. Erfani, *Synthesis of capillary pressure curves from post-stack seismic data with the use of intelligent estimators: A case study from the Iranian part of the South Pars gas field, Persian Gulf Basin.* Journal of Applied Geophysics, 2015. **112**(Supplement C): p. 215-225.
27. Lien, J.R., M. Jakobsen, and A. Skauge, *PTEK100 Introduksjon til petroleums- og prosessteknologi.* University of Bergen, 2007.
28. Anderson, W.G., *Wettability Literature Survey- Part 4: Effects of Wettability on Capillary Pressure.* Journal of Petroleum Technology, 1987. **39**(10): p. 1283-1300.
29. Chatzis, I., N.R. Morrow, and H.T. Lim, *Magnitude and Detailed Structure of Residual Oil Saturation.* Society of Petroleum Engineers Journal, 1983. **23**(03): p. 311-326.
30. Stegemeier, G.L., *Relationship of Trapped Oil Saturation to Petrophysical Properties of Porous Media*, in *SPE Improved Oil Recovery* Society of Petroleum Engineers: Tulsa, Oklahoma, 22-24 April, .
31. Oh, S.G. and J.C. Slattery, *Interfacial Tension Required for Significant Displacement of Residual Oil.* Society of Petroleum Engineers Journal, 1979. **19**(02): p. 83-96.
32. Garnes, J.M., et al., *Capillary Number Relations for Some North, Sea Reservoir Sandstones*, in *SPE/DOE Enhanced Oil Recovery Symposium*. Society of Petroleum Engineers: Tulsa, Oklahoma, 22-25 April.
33. Lake, L.W., et al., *Isothermal, multiphase, multicomponent fluid flow in permeable media.* In Situ; (United States), 1984: p. Medium: X; Size: Pages: 1-40.
34. Sheng, J.J., *Chapter 7 - Surfactant Flooding*, in *Modern Chemical Enhanced Oil Recovery*. 2011, Gulf Professional Publishing: Boston. p. 239-335.
35. Agbalaka, C.C., et al., *The Effect Of Wettability On Oil Recovery: A Review*, in *SPE Asia Pacific Oil and Gas Conference and Exhibition*. 2008, Society of Petroleum Engineers: Perth, Australia.
36. Morrow, N.R., *Wettability and Its Effect on Oil Recovery.* Journal of Petroleum Technology, 1990. **42**(12): p. 1476-1484.
37. Anderson, W.G., *Wettability Literature Survey-Part 6: The Effects of Wettability on Waterflooding.* Journal of Petroleum Technology, 1987. **39**(12): p. 1605-1622.
38. Raza, S.H., L.E. Treiber, and D.L. Archer, *Wettability of reservoir rocks and its evaluation.* Prod. Mon.; (United States), 1968. **32:4**: p. Pages: 2-4, 6-7.
39. Jadhunandan, P.P. and N.R. Morrow, *Effect of wettability on waterflood recovery for crude-oil/brine/rock systems.* SPE Reservoir Engineering, 1995. **10**(1): p. 40-46.

40. Skauge, A. and B. Ottensen, *A Summary of Experimentally derived Relative Permeability and Residual Saturation on North Sea Reservoir Cores*, in *International Symposium of the SCA*. 2002: Monterery, California, USA.
41. Skauge, A., B. Vik, and B. Ottensen, *Variation Of Special Core Analysis Properties For Intermediate Wet Sandstone Material* in *International Symposium of the Society of Core Analysts (SCA),Pau, France*. 2003: Pau, France, 21-24 September 2003.
42. Schlumberger. *Carbonate Reservoirs*. 2017 [cited 2017 25 Nov]; Available from: http://www.slb.com/services/technical_challenges/carbonates.aspx.
43. Siffert, D. and P. Fimbel, *Parameters affecting the sign and magnitude of the eletrokinetic potential of calcite.* Colloids and Surfaces, 1984. **11**(3): p. 377-389.
44. Alotaibi, M.B., H.A. Nasr-El-Din, and J.J. Fletcher, *Electrokinetics of Limestone and Dolomite Rock Particles.* SPE Reservoir Evaluation & Engineering, 2011. **14**(05): p. 594 - 603.
45. Morrow, N.R., H.T. Lim, and J.S. Ward, *Effect of Crude-Oil-Induced Wettability Changes on Oil Recovery.* SPE Formation Evaluation, 1986. **1**(01): p. 89-103.
46. Hite, J.R., et al., *IOR and EOR: Effective Communication Requires a Definition of Terms.* Journal of Petroleum Technology, 2003. **55**(06): p. 16-16.
47. Buckley, J.S., Y. Liu, and S. Monsterleet, *Mechanisms of Wetting Alteration by Crude Oils.* SPE International Symposium on Oilfiled Chemisrty, 1998. **3**(01): p. 54-61.
48. Austad, T., et al., *Conditions for a Low-Salinity Enhanced Oil Recovery (EOR) Effect in Carbonate Oil Reservoirs.* Energy & Fuels, 2011. **26**(1): p. 569-575.
49. Yousef, A.A., et al., *Laboratory Investigation of the Impact of Injection-Water Salinity and Ionic Content on Oil Recovery From Carbonate Reservoirs.* Canadian Unconventional Resources and International Petroleum Conference, 19-21 October, Calgary, Alberta, Canad, 2011. **14**(05): p. 578 - 593.
50. RezaeiDoust, A., et al., *Smart Water as Wettability Modifier in Carbonate and Sandstone: A Discussion of Similarities/Differences in the Chemical Mechanisms.* Energy & Fuels, 2009. **23**(9): p. 4479-4485.
51. Ligthelm, D.J., et al., *Novel Waterflooding Strategy By Manipulation Of Injection Brine Composition*, in *EUROPEC/EAGE Conference and Exhibition, 8-11 June, Amsterdam, The Netherlands*. 2009, Society of Petroleum Engineers.
52. Tang, G.-Q. and N.R. Morrow, *Influence of brine composition and fines migration on crude oil/brine/rock interactions and oil recovery.* Journal of Petroleum Science and Engineering, 1999. **24**(2): p. 99-111.
53. McGuire, P.L., et al., *Low Salinity Oil Recovery: An Exciting New EOR Opportunity for Alaska's North Slope*, in *SPE Western Regional Meeting*. 2005, Society of Petroleum Engineers: Irvine, California, 30 March-1 April.
54. Lager, A., et al., *Low Salinity Oil Recovery - An Experimental Investigation1*. Petrophysics, 2008. **49**(01): p. 8.
55. Tang, G.Q. and N.R. Morrow, *Salinity, Temperature, Oil Composition, and Oil Recovery by Waterflooding.* SPE Reservoir Engineering, 1997. **12**(04): p. 269-276.
56. Strand, S., E.J. Høgnesen, and T. Austad, *Wettability alteration of carbonates—Effects of potential determining ions (Ca2+ and SO42−) and temperature.* Colloids and Surfaces A: Physicochemical and Engineering Aspects, 2006. **275**(1-3): p. 1-10.
57. Mohanty, K.K. and S. Chandrasekhar, *Wettability Alteration with Brine Composition in High Temperature Carbonate Reservoirs*, in *SPE Annual Technical Conference and Exhibition*. 2013, Society of Petroleum Engineers: New Orleans, Louisiana, USA.
58. Gupta, R., et al., *Enhanced Waterflood for Carbonate Reservoirs - Impact of Injection Water Composition*, in *SPE Middle East Oil and Gas Show and Conference*. 2011, Society of Petroleum Engineers: Manama, Bahrain, 25-28 September.

59. Romanuka, J., et al., *Low Salinity EOR in Carbonates*, in *SPE Improved Oil Recovery Symposium*. 2012, Society of Petroleum Engineers: Tulsa, Oklahoma, USA, 14-18 April.
60. Hiorth, A., C. Lawrence, and M.V. Madland, *The impact of pore water chemistry on carbonate surface charge and oil wettability.* Transport in Porous media 85 (1), 2010: p. 1-21.
61. Austad, T., et al., *Seawater as IOR Fluid in Fractured Chalk*, in *SPE International Symposium on Oilfield Chemistry*. 2005, Society of Petroleum Engineers: The Woodlands, Texas.
62. Al-Attar, H., et al., *Low-salinity flooding in a selected carbonate reservoir: experimental approach.* Journal of Petroleum Exploration and Production Technology, 2013. **3**(2): p. 139-149.
63. Al-Shalabi, E., et al., *Geochemical Interpretation of Low-Salinity-Water Injection in Carbonate Oil Reservoirs.* SPE Journal, 2014. **20**(6): p. 1212-1226.
64. Zhang, Y., X. Xie, and N.R. Morrow, *Waterflood Performance By Injection Of Brine With Different Salinity For Reservoir Cores*, in *SPE Annual Technical Conference and Exhibition*. 2007a, Society of Petroleum Engineers: Anaheim, California, U.S.A. 11-14 November.
65. Agbalaka, C., et al., *Coreflooding Studies to Evaluate the Impact of Salinity and Wettability on Oil Recovery Efficiency.* Transport in Porous Media, 2009. **76**(1): p. 77-94.
66. Hognesen, E.J., S. Strand, and T. Austad, *Waterflooding of preferential oil-wet carbonates: Oil recovery related to reservoir temperature and brine composition*, in *SPE Europec/EAGE Annual Conference*. 2005, Society of Petroleum Engineers: Madrid, Spain, 13-16 June.
67. Webb, K.J., C.J.J. Black, and G. Tjetland, *A Laboratory Study Investigating Methods for Improving Oil Recovery in Carbonates*, in *International Petroleum Technology Conference*. 2005, International Petroleum Technology Conference: Doha, Qatar, 21-23 November.
68. Zhang, P., M.T. Tweheyo, and T. Austad, *Wettability Alteration and Improved Oil Recovery in Chalk: The Effect of Calcium in the Presence of Sulfate.* Energy & Fuels, 2006a. **20**(5): p. 2056-2062.
69. Zhang, P., M.T. Tweheyo, and T. Austad, *Wettability alteration and improved oil recovery by spontaneous imbibition of seawater into chalk: Impact of the potential determining ions Ca 2+, Mg 2+, and SO 4 2−.* Colloids and Surfaces A: Physicochemical and Engineering Aspects, 2007b. **301**(1): p. 199-208.
70. Strand, S., et al., *"Smart Water" for Oil Recovery from Fractured Limestone: A Preliminary Study.* Energy & Fuels, 2008. **22**(5): p. 3126-3133.
71. Zhang, P. and T. Austad, *Wettability and oil recovery from carbonates: Effects of temperature and potential determining ions.* Colloids and Surfaces A: Physicochemical and Engineering Aspects, 2006. **279**(1 3): p. 179.
72. Bagci, S., M.V. Kok, and U. Turksoy, *Effect Of Brine Composition On Oil Recovery By Waterflooding* Petroleum Science and Technology, 2001. **19**(3-4): p. 359-372.
73. Al-Shalabi, E.W. and K. Sepehrnoori, *A comprehensive review of low salinity/engineered water injections and their applications in sandstone and carbonate rocks.* Journal of Petroleum Science and Engineering, 2015. **139**: p. 137-161.
74. Zahid, A., A.A. Shapiro, and A. Skauge, *Experimental Studies of Low Salinity Water Flooding Carbonate: A New Promising Approach*, in *SPE EOR Conference at Oil and Gas West Asia*. 2012, Society of Petroleum Engineers: Muscat, Oman, 16-18 April.

75. Sari, A., et al., *Drivers of Low Salinity Effect in Carbonate Reservoirs.* Energy & Fuels, 2017. **31**(9): p. 8951-8958.
76. Shehata, A., M.B. Alotaibi, and H. Nasr-El-Din, *Waterflooding in Carbonate Reservoirs: Does the Salinity Matter?* SPE Reserv. Eval. Eng., 2014. **17**(3): p. 304-313.
77. Awolayo, A., H. Sarma, and A.M. AlSumaiti, *A Laboratory Study of Ionic Effect of Smart Water for Enhancing Oil Recovery in Carbonate Reservoirs*, in *SPE EOR Conference at Oil and Gas West Asia*. 2014, Society of Petroleum Engineers: Muscat, Oman, 31 March-2 April.
78. Strand, S., D.C. Standnes, and T. Austad, *Spontaneous Imbibition of Aqueous Surfactant Solutions into Neutral to Oil-Wet Carbonate Cores: Effects of Brine Salinity and Composition.* Energy & Fuels, 2003. **17**(5): p. 1133-1144.
79. Rezaei Gomari, K.A., O. Karoussi, and A.A. Hamouda, *Mechanistic Study of Interaction between Water and Carbonate Rocks for Enhancing Oil Recovery*, in *SPE Europec/EAGE Annual Conference and Exhibition*. 2006, Society of Petroleum Engineers: Vienna, Austria.
80. Mahani, H., et al., *Insights into the Mechanism of Wettability Alteration by Low-Salinity Flooding (LSF) in Carbonates.* Energy and Fuels, 2015. **29**(3): p. 1352-1367.
81. Winsor, P.A., *Solvent Properties of Amphiphilic Compounds*. 1954, London: Butterworths Scinetific Publications. 504.
82. Alagic, E. and A. Skauge, *Combined Low Salinity Brine Injection and Surfactant Flooding in Mixed−Wet Sandstone Cores.* Energy & Fuels, 2010. **24**(6): p. 3551-3559.
83. Tavassoli, S., et al., *Low Salinity Surfactant Flooding – A Multi-Mechanistic Enhanced Oil Recovery Method*, in *SPE International Symposium on Oilfield Chemistry*. 2015, Society of Petroleum Engineers: The Woodlands, Texas, USA, 13-15 April.
84. Alagic, E., et al., *Effect of crude oil ageing on low salinity and low salinity surfactant flooding.* Journal of Petroleum Science and Engineering, 2011. **78**(2): p. 220-227.
85. Spildo, K., A.M. Johannessen, and A. Skauge, *Low Salinity Waterflood at Reduced Capillarity*, in *SPE Improved Oil Recovery Symposium*. 2012, Society of Petroleum Engineers: Tulsa, Oklahoma, USA, 14-18 April.
86. Johannessen, A.M. and K. Spildo, *Enhanced Oil Recovery (EOR) by Combining Surfactant with Low Salinity Injection.* Energy & Fuels, 2013. **27**(10): p. 5738-5749.
87. Khanamiri, H.H., O. Torsæter, and J.Å. Stensen, *Experimental Study of Low Salinity and Optimal Salinity Surfactant Injection*, in *EUROPEC 2015*. 2015, Society of Petroleum Engineers: Madrid, Spain, 1-4 June.
88. Sorbie, K.S., *Polymer- Improved Oil Recovery*. 1991, Boca Raton, Florida: CRC Press. 359.
89. Green, D.W. and G.P. Willhite, *Enhanced oil recovery*. SPE textbook series. Vol. 6. 1998, Richardson, Tex: Henry L. Doherty Memorial Fund of AIME, Society of Petroleum Engineers.
90. Shupe, R., *Chemical Stability of Polyacrylamide Polymers.* Journal of Petroleum Technology, 1981. **33**(8): p. 1513-1529.
91. Holstein, E.D., et al., *Petroleum engineering handbook : Reservoir engineering and petrophysics*. 2007, Society of Petroleum Engineers: Richardson, TX. p. 498.
92. Stavland, A., et al., *Polymer Flooding - Flow Properties in Porous Media versus Rheological Parameters*, in *SPE EUROPEC/EAGE Annual Conference and Exhibition*. 2010, Society of Petroleum Engineers: Barcelona, Spain,14-17 June.
93. Chauveteau, G. and N. Kohler, *Influence of Microgels in Polysaccharide Solutions on Their Flow Behavior Through Porous Media.* Society of Petroleum Engineers Journal, 1984. **24**(03): p. 361-368.

94. Ayirala, S.C., et al., *A Designer Water Process for Offshore Low Salinity and Polymer Flooding Applications*, in *SPE Improved Oil Recovery Symposium*. 2010, Society of Petroleum Engineers: Tulsa, Oklahoma, USA, 24-28 April.
95. Kozaki, C., *Efficiency of low salinity polymer flooding in sandstone cores*, in *Faculty of the Graduate School of The University of Texas at Austin*. 2012, The University of Texas at Austin: Texas at Austin.
96. Mohammadi, H. and G. Jerauld, *Mechanistic Modeling of the Benefit of Combining Polymer with Low Salinity Water for Enhanced Oil Recovery*, in *SPE Improved Oil Recovery Symposium*. 2012, Society of Petroleum Engineers: Tulsa, Oklahoma, USA, 14-18 April.
97. Shiran, B.S. and A. Skauge, *Enhanced Oil Recovery (EOR) by Combined Low Salinity Water/Polymer Flooding.* Energy Fuels, 2013. **27**(3): p. 1223-1235.
98. Khorsandi, S., C. Qiao, and R.T. Johns, *Displacement Efficiency for Low Salinity Polymer Flooding Including Wettability Alteration*, in *SPE Improved Oil Recovery Conference*. 2016, Society of Petroleum Engineers: Tulsa, Oklahoma, USA, 11-13 April.
99. Han, B. and J. Lee, *Sensitivity Analysis on the Design Parameters of Enhanced Oil Recovery by Polymer Flooding with Low Salinity Waterflooding*, in *The Twenty-fourth International Ocean and Polar Engineering Conference*. 2014, International Society of Offshore and Polar Engineers: Busan, Korea, 15-20 June.
100. User, S. *New Technologies - SNF*. Snf-oil.com 2013 [cited 2018 30.jan]; Available from: http://www.snf-oil.com/en/innovation/new-technologies.
101. Malvern. *Measuring systems for Kinexus rheometer*. 2013 [cited 2018 12.jan]; Available from: https://www.malvern.com/en/products/product-range/kinexus-range/kinexus-lab-plus/accessories/measuring-systems/
102. Bier, A. *Electrochemistry: Theoery and Practice*. Hach Company 2010 [cited 2018 13 february]; Available from: https://www.wateronline.com/doc/electrochemistry-theory-practice-0001.
103. Ji, Y., et al., *Characterization of Pore Geometry of Indiana Limestone in Relation to Mechanical Compaction Caractérisation de la géométrie des pores dans le calcaire de l'Indiana (États-Unis) en relation avec la compaction mécanique.* Oil & Gas Science and Technology, 2012. **67**(5): p. 753-775.
104. He, L., et al., *Complex relationship between porosity and permeability of carbonate reservoirs and its controlling factors: A case study of platform facies in Pre-Caspian Basin.* Petroleum Exploration and Development, 2014. **41**(2): p. 225-234.
105. Coats, K.H. and B.D. Smith, *Dead-End Pore Volume and Dispersion in Porous Media.* Society of Petroleum Engineers Journal, 1963. **4**(1): p. 73-84.
106. Salter, S.J. and K.K. Mohanty, *Multiphase Flow in Porous Media: I. Macroscopic Observations and Modeling*, in *SPE Annual Technical Conference and Exhibition*. 1982, Society of Petroleum Engineers: New Orleans, Louisiana, 26-29 September.
107. Anderson, W., *Wettability Literature Survey- Part 2: Wettability Measurement.* Journal of Petroleum Technology, 1986. **38**(11): p. 1246-1262.
108. Shaker Shiran, B. and A. Skauge, *Wettability and Oil Recovery by Low Salinity Injection*, in *SPE EOR Conference at Oil and Gas West Asia*. 2012, Society of Petroleum Engineers: Muscat, Oman.
109. Graue, A., et al., *Alteration of wettability and wettability heterogeneity.* J. Pet. Sci. Eng., 2002. **33**(1-3): p. 3-17.
110. Zhou, X., N.R. Morrow, and S. Ma, *Interrelationship of Wettability, Initial Water Saturation, Aging Time, and Oil Recovery by Spontaneous Imbibition and Waterflooding.* SPE Journal, 2000. **5**(02): p. 199-207.

111. Shehata, A.M., M.B. Alotaibi, and H.A. Nasr-El-Din, *Waterflooding in Carbonate Reservoirs: Does the Salinity Matter?* SPE Reservoir Evaluation & Engineering, 2014. **17**(03): p. 304-313.
112. Yousef, A.A. and S.C. Ayirala, *A Novel Water Ionic Composition Optimization Technology for Smartwater Flooding Application in Carbonate Reservoirs*, in *SPE Improved Oil Recovery Symposium*. 2014, Society of Petroleum Engineers: Tulsa, Oklahoma, USA,12-16 April.
113. Alotaibi, M.B. and A.A. Yousef, *The Impact of Dissolved Species on the Reservoir Fluids and Rock Interactions in Carbonates*, in *SPE Saudi Arabia Section Annual Technical Symposium and Exhibition*. 2015, Society of Petroleum Engineers: Al-Khobar, Saudi Arabia,21-23 April.
114. Jiang, H., et al., *Lab Observation Of Low Salinity Waterflooding For A Phosphoria Reservoir Rock*, in *SPE Western North American and Rocky Mountain Joint Meeting*. 2014, Society of Petroleum Engineers: Denver, Colorado.
115. Chiappa, L., et al., *Polymer adsorption at the brine/rock interface: the role of electrostatic interactions and wettability.* Journal of Petroleum Science and Engineering, 1999. **24**(2-4): p. 113-122.

9. Appendix

9.1. Measured Rock Properties

Table 9.1: Measured length and diameters of the cores

Core ID	Length [± 0.001cm]	Average Length [cm]	Diameter [± 0.001cm]	Average diameter [cm]
S1	5.025	5.03 ± 0.01	3.745	3.74 ± 0.03
	5.035		3.695	
	5.015		3.775	
S2	5.005	5.005 ± 0.001	3.701	3.70 ± 0.04
	5.005		3.660	
	5.004		3.745	
S3	4.901	4.91 ± 0.01	3.701	3.701 ± 0.001
	4.901		3.701	
	4.915		3.701	
S4	4.805	4.84 ± 0.05	3.770	3.770 ± 0.002
	4.805		3.770	
	4.905		3.765	

Core ID	Length [± 0.01 cm]	Average Length [cm]	Diameter [± 0.001cm]	Average diameter [cm]
L1	14.80	14.80 ± 0.02	3.765	3.80 ± 0.01
	14.85		3.775	
	14.85		3.785	
L2	15.20	15.20 ± 0.05	3.645	3.71 ± 0.1
	15.20		3.765	
	15.10		3.715	
L3	15.20	15.20 ± 0.01	3.775	3.70 ± 0.1
	15.20		3.785	
	15.20		3.635	
L4	15.10	15.10 ± 0.05	3.685	3.680 ± 0.005
	15.00		3.675	
	15.10		3.675	

Table 9.2: Petrophysical properties

Core ID	Bulk Volume [cm^3]	Pore volume [mL]	Porosity (φ) [%]	Abs.Permeability (Kw) [mD]
S1	55.20 ± 0.01	10.2 ± 0.1	18.4 ± 0.2	176 ± 10
S2	53.90 ± 0.01	9.8 ± 0.1	18.2 ± 0.3	285 ± 26
S3	52.770 ± 0.001	10.0 ± 0.1	19.2 ± 0.2	202 ± 14
S4	53.96 ± 0.01	9.5 ± 0.1	17.7 ± 0.2	183 ± 12
L1	166.020 ± 0.003	28.6 ± 0.1	17.2 ± 0.1	160 ± 3
L2	163.80 ± 0.02	32.2 ± 0.5	19.6 ± 0.3	170 ± 3
L3	166.20 ± 0.02	32.6 ± 0.6	19.6 ± 0.4	116 ± 1
L4	160.500 ± 0.003	31.3 ± 0.1	19.5 ± 0.1	154 ± 2

Table 9.3: Oil permeability and end water relative permeability

Core ID	$K_o(S_{wi})$ [mD] Primol 542	$K_o(S_{wi})$ [mD] after aging	K_{rw} @90℃ ($S_{or,LS}$)	K_{rw} @22℃ ($S_{or,LS}$)
S1*	266 ± 2	193 ± 1	-	0.16 ± 0.01
S2**	566 ± 7		-	-
S3	241 ± 2		-	0.17 ± 0.01
S4*	267 ± 2	128 ± 1	-	0.19 ±0.01
L1	179.0 ± 0.3		0.23 ± 0.10	0.170 ± 0.002
L2*	215.0 ± 0.3	132 ± 9	0.49 ± 0.10	0.3 ± 0.10
L3	201.0 ± 0.3		-	-
L4*	216.0 ± 0.3	157 ± 4	0.16 ± 0.10	0.19 ± 0.01

*Aged core

** Crushed during imbibition

9.2. Salts

Table 9.4: Salt manufacturers

Salt	Manufacturer
NaCl	Sigma-Aldrich
CaCl2×2H2O	Sigma-Aldrich
MgCl2×6H2O	Sigma-Aldrich
NaHCO3	Sigma-Aldrich
Na2SO4	Sigma-Aldrich
KCl	Sigma-Aldrich

9.3. Fluid Properties

Table 9.5: Summary of fluid properties

Fluid	pH at ambient temperature	Average pH at ambient temperature	Viscosity [cP] at ambient temperature	Viscosity [cP] at 90°C
LS	7.70	7.70 ± 0.03	0.95 ± 0.04	0.50 ± 0.20
	7.69			
	7.63			
HS	7.88	7.90 ± 0.01	0.95 ± 0.04	0.65 ± 0.10
	7.90			
	7.91			
FW	6.56	6.60 ± 0.04	1.40 ± 0.03	0.50 ± 0.1
	6.66			
	6.65			
Surfactant XOF 25S	4.66	4.80 ± 0.10	1.68 ± 0.05	0.40 ± 0.1
	4.88			
	4.70			
2000 ppm HPAM	6.94	6.70 ± 0.20	84.40 ± 0.60	59.1 ± 0.7
	6.57			
	6.53			
Tagged crude oil	-	-	4.15 ± 0.10	1.20 ± 0.10

9.4. Viscosity Data

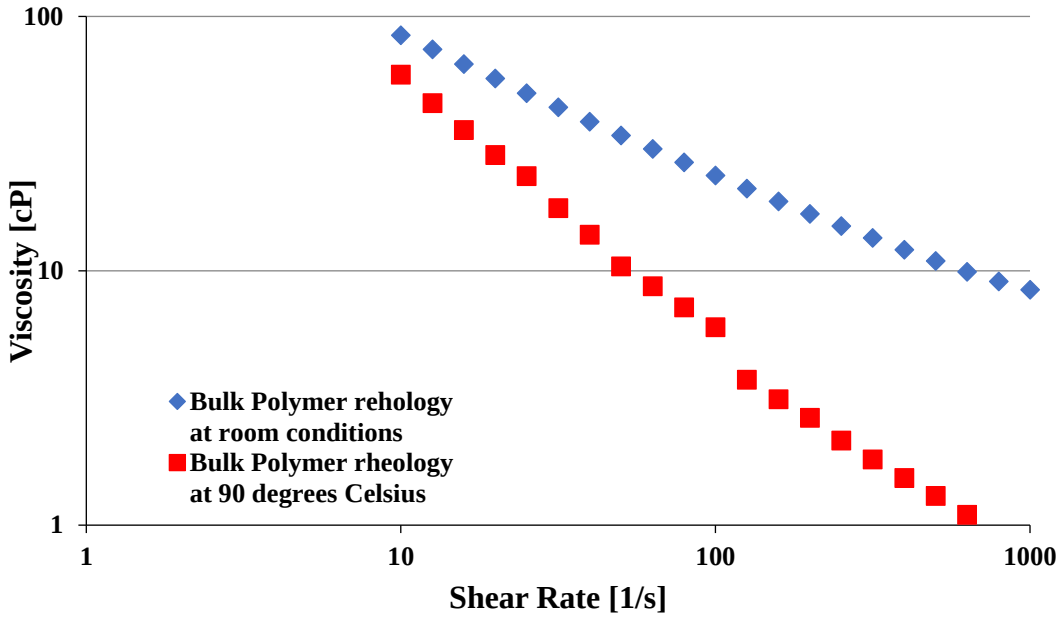

Figure 9.1: Viscosity of HPAM 2000 ppm polymer bulk solution at room conditions and 90°C

Table 9.6: Viscosity of HPAM solution at different shear rates and temperature

HPAM Concentration 2000 ppm	Shear rate [s^{-1}]			
	1	10	100	1000
Room conditions [cP]	322 ± 3	84.40 ± 0.60	23.7 ± 0.1	8.4 ± 0.1
90°C [cp]	523 ± 5	59.1 ± 0.7	6.0 ± 0.2	0.3 ± 0.1

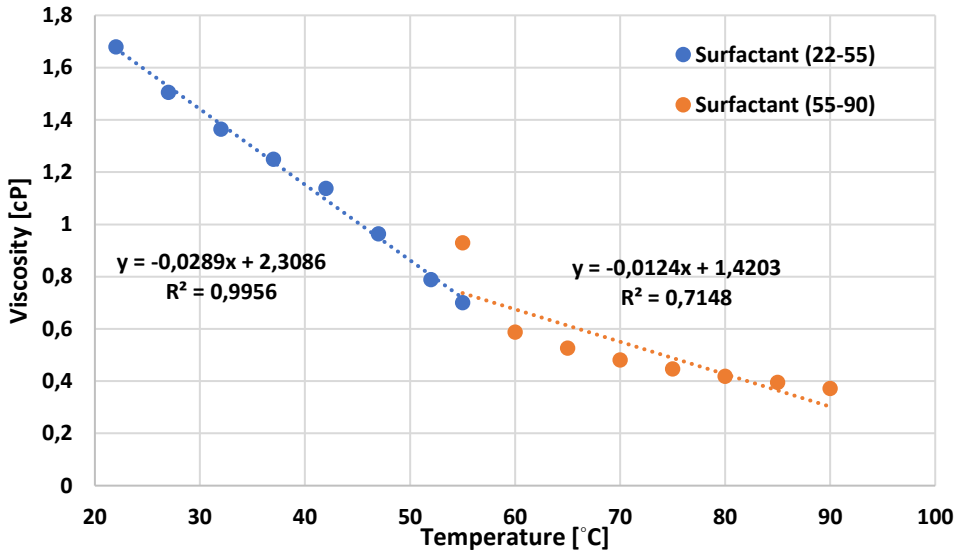

Figure 9.2: Relationship between viscosity and temperature of the surfactant, where the blue dots represent measurement conducted at 22 to 55˚C. Orange dots represent the measurements at 55 to 90˚C

9.5. Experimental Production Data of the Short Cores

Table 9.7: Experimental data obtained during spontaneous imbibition for core S1

Fluid	Imbibition time [days]	Produced oil volumes from core [mL]	Recovery factor [%OOIP]
HS	30	0.04	0.69
LS	30	0.05	1.55

Table 9.8: Experimental data obtained during spontaneous imbibition for core S2

Fluid	Imbibition time [days]	Produced oil volumes from core [mL]	Recovery factor [%OOIP]
HS	30	1.7	18.41
LS	30	0	18.41

Table 9.9: Experimental data obtained during spontaneous imbibition for core S3

Fluid	Imbibition time [days]	Produced oil volumes from core [mL]	Recovery factor [%OOIP]
HS	30	0.65	11.16
LS	30	0	11.16

Table 9.10: Experimental data obtained during spontaneous imbibition for core S4

Fluid	Imbibition time [days]	Produced oil volumes from core [mL]	Recovery factor [%OOIP]
HS	30	0.07	0.96
LS	30	0.1	2.34

Table 9.11: Experimental data obtained during low salinity brine injection for core S1

Rate [mL/min]	Total injected fluid [PV]	Produced oil volumes from core [± 0.30 mL]	Recovery factor [%OOIP]
0.1	2	1.27	21.92
0.5	1	1.77	30.73
1	1	1.88	32.50

Table 9.12: Experimental data obtained during low salinity brine injection for core S3

Rate [mL/min]	Total injected fluid [PV]	Produced oil volumes from core [± 0.30 mL]	Recovery factor [%OOIP]
0.1	1	0.11	1.88
0.5	1	0.22	1.99
1	3	1.43	24.55

Table 9.13: Experimental data obtained during low salinity brine injection for core S4

Rate [mL/min]	Total injected fluid [PV]	Produced oil volumes from core [± 0.30 mL]	Recovery factor [%OOIP]
0.1	2	1.29	17.80
0.5	1	1.51	20.82
1	3	2.50	34.48

9.6. Experimental Production Data for the Long Cores

Table 9.14: Experimental data obtained during waterfloods of L1

Fluid	Total injected fluid [PV]	Produced oil volumes from core at 90°C [± 0.30 mL]	Produced oil volumes from core at room conditions [± 0.30 mL]	Recovery factor [%OOIP]
HS	2	13.64	12.40	79.11
LS	2	0	0	79.11
LSS	0.5	0	0	79.11
LSP	2	13.87	12.61	80.41
LS	3	0	0	80.41

Table 9.15: Experimental data obtained during waterfloods of L2

Fluid	Total injected fluid [PV]	Produced oil volumes from core at 90°C [± 0.30 mL]	Produced oil volumes from core at room conditions [± 0.30 mL]	Recovery factor [%OOIP]
HS	2	8.91	8.10	43.46
LS	2	9.24	8.40	45.10
LSS	0.5	0	0	45.10
LSP	2	10.65	9.68	51.95
LS	3	11.14	10.12	54.37

Table 9.16: Experimental data obtained during waterfloods of L3

Fluid	Total injected fluid [PV]	Produced oil volumes from core at 90°C [± 0.30 mL]	Produced oil volumes from core at room conditions [± 0.30 mL]	Recovery factor [%OOIP]
HS	2	11.05	10.04	53.15
LS	2	11.65	10.51	55.65
LSS	0.5	12.19	11.09	58.70
LSP	2	14.42	13.11	69.39
LS	3	0	0	69.39

Table 9.17: Experimental data obtained during waterfloods of L4

Fluid	Total injected fluid [PV]	Produced oil volumes from core at 90°C [± 0.30 mL]	Produced oil volumes from core at room conditions [± 0.30 mL]	Recovery factor [%OOIP]
HS	2	9.46	8.60	48.33
LS	2	10.65	9.68	54.37
LSS	0.5	11.11	10.10	56.77
LSP	2	12.63	11.47	64.47
LS	3	13.00	11.82	66.40